

**Transport of nonlinearly
biodegradable contaminants in
aquifers**

Promotor:

prof. dr. ir. S. E. A. T. M. van der Zee,
persoonlijk hoogleraar bij de leerstoelgroep
Bodemscheikunde en Chemische Bodemkwaliteit

Samenstelling promotiecommissie:

prof. dr. ir. J. Grasman (Wageningen Universiteit)
prof. dr. ir. A. Leijnse (Wageningen Universiteit)
dr. ir. S. M. Hassanizadeh (Technische Universiteit Delft)
prof. dr. ir. W. H. Rulkens (Wageningen Universiteit)

VII

Reizen in derde wereldlanden zorgt voor een herijking van zaken die er toe doen.

VIII

Fotografie is veel te subjectief om een betrouwbaar beeld van de werkelijkheid te geven.

STELLINGEN

I

De balans tussen niet-lineaire afbraak en dispersie leidt in een homogene aquifer altijd tot lopende golven.

Dit proefschrift

II

In fysisch sterk heterogene aquifers wordt de frontvorm enkel bepaald door de mate van heterogeniteit.

Dit proefschrift

III

De initiële condities en randvoorwaarden bepalen of er een retardatiefactor is waarbij de biodegradatiesnelheid maximaal is.

Oya and Valocchi 1997, Water Resources Research 33, 1117-1127, Chiang et al. 1991, Transp. Porous Media 6, 33-43, en MacQuarrie and Sudicky 1990, Water Resources Research 26, 223-239.

IV

Zonder gezonde achterdocht resulteert het gebruik van modelresultaten in twijfelachtige besluitvorming.

V

‘Hoewel formules, vergelijkingen en berekeningen een essentiële rol in de wiskunde spelen, zijn zij eigenlijk niet zo belangrijk als de wiskundige ideeën en structuren waarvan zij een uitdrukking horen te zijn.’

John Allen Paulos (Wiskunde en humor)

VI

‘We zoeken onophoudelijk, en aan het eind van onze zoektocht zijn we terug bij het beginpunt dat we dan pas echt zullen ontdekken.’

T.S. Eliot, Lola rennt

NN08201,2925.

Transport of nonlinearly biodegradable contaminants in aquifers

Henriëtte Keijzer

Proefschrift
ter verkrijging van de graad van doctor
op gezag van de rector magnificus
van Wageningen Universiteit,
prof. dr. ir. L. Speelman,
in het openbaar te verdedigen
op dinsdag 16 januari 2001
des namiddags te vier uur in de Aula.

1602472

The research presented in this thesis was partly funded by Directorate General Science, Research and Development of the Commission of the European Communities, via the EC program ENVIRONMENT, under contract number EV5V-CT94-0536.

CIP-DATA KONINKLIJKE BIBLIOTHEEK, DEN HAAG

Keijzer, H.

Transport of nonlinearly biodegradable contaminants in aquifers/

Henriëtte Keijzer. - [S.l. : s.n.]

Thesis Wageningen University. - With ref. - With summary in Dutch.

ISBN 90-5808-339-X

Subject headings: solute transport / nonlinear biodegradation /
bioremediation.

Cover design: René Nieuwenburg

Printing: Ponsen & Looijen, Wageningen

ABSTRACT

Keijzer, H. 2000. **Transport of nonlinearly biodegradable contaminants in porous aquifers - Numerical, analytical and stochastic modeling.** Doctoral Thesis, Wageningen University, Wageningen. The Netherlands, 144 pages.

This thesis deals with the transport behavior of nonlinearly biodegradable contaminants in aquifers. Such transport occurs during *in situ* bioremediation which is based on the injection of an electron acceptor or electron donor. The main interests in this thesis are the mutual influences of underlying processes, i.e. transport, adsorption and biodegradation, and their influence on *in situ* bioremediation performance. To gain insight in these influences, the processes in a homogeneous aquifer are studied. Subsequently, the effect of physical heterogeneity of an aquifer on the displacement of the biodegradable contaminant is examined.

Considering a homogeneous aquifer, numerical simulations are performed to ascertain the effect of transport, adsorption and biodegradation on the displacement of the contaminant and of the electron acceptor or electron donor. In the initial phase, the developed numerical results are successfully described by first order degradation. In the final phase, the numerical results show a traveling wave behavior; the developed concentration fronts have constant front shapes and 'travel' with a constant velocity through the aquifer. This behavior is due to the balance between the steepening effect of nonlinear biodegradation and the spreading effect of dispersion. Because of this traveling wave behavior, semi-analytical solutions have been derived that satisfactorily approximate the numerical results. These semi-analytical solutions are used to assess the performance of the *in situ* bioremediation. If *in situ* bioremediation is applied to a polluted site, the electron acceptor injection concentration and the injection velocity will be the only manipulative properties. By varying these two properties, the *in situ* bioremediation performance can be influenced and optimized.

To study a physical heterogeneous aquifer, the hydraulic conductivity is considered spatially variable and it is assumed to be a random space function. The effect of physical heterogeneity is determined using a Lagrangian stochastic approach. Results show that incorporation of physical heterogeneity leads to a spreading of the breakthrough curve of both the contaminant and the electron acceptor or electron donor. In case of a large degree of heterogeneity, i.e. a strongly heterogeneous aquifer, it is the heterogeneity which determines the shape of the breakthrough curve and not the dispersion or nonlinear biodegradation.

Keywords: *in situ* bioremediation, nonlinear biodegradation, Monod kinetics, modeling, traveling wave, semi-analytical solution, stochastic approach, aquifer, porous media.

Contents

Chapter 1	General introduction	1
Chapter 2	Characteristic regimes for in-situ bioremediation of aquifers by injecting water containing an electron acceptor	11
Chapter 3	Analytical approximation to characterize the performance of in-situ aquifer bioremediation	37
Chapter 4	Semi-analytical traveling wave solution of one-dimensional aquifer bioremediation	63
Chapter 5	Effect of physical, chemical and biochemical processes on the performance of in situ aquifer bioremediation	83
Chapter 6	Stochastic analysis of nonlinear biodegradation and transport in heterogeneous aquifers	103
Chapter 7	General conclusions	125
	Samenvatting	127
	Nawoord	133
	Curriculum Vitae	135

General introduction

BACKGROUND

Around 1980, residential areas, e.g. 'Lekkerkerk', were discovered to be highly contaminated in the Netherlands. After this discovery, the government made an inventory of possibly polluted sites. The inventory showed that more than 4000 sites were polluted, of which 1000 sites would need further investigation and around 350 sites would have to be remediated immediately. The government was forced to deal with soil pollution at short notice and developed temporary regulations: de Interimwet bodemsanering (IBS), 1983. Because of the concern of the people living at or nearby the contaminated sites, the government started cleaning the most hazardous sites even before the regulations were developed. The remediation was done in a rather rigorous manner because *in situ* soil remediation techniques were unavailable. The contaminated soil was removed and replaced by unpolluted soil. The contaminated soil was either cleaned off site or transported to storage areas, e.g. the Papegaaibek or the Slufter. The costs involved were extremely high and cleaning all the contaminated sites this way was financially not feasible. Therefore, the government started to subsidize the scientific research to improve soil remediation techniques.

Soil remediation originally involved two strategies. The first is the recovery of the multifunctional application of the soil, e.g. by excavation of the soil followed by treatment [36] or storage if treatment is impossible. The second one is the isolation of the contaminant if recovery is not feasible. The isolation of the contaminant should reduce its spreading to the environment. Possible isolation techniques are placing vertical and horizontal fences in the soil, extraction of the groundwater, or physical or chemical fixation techniques [36].

Excavation is a complete but rather labor intensive and expensive remediation technique. In case of constructions on the site, excavation is not well feasible without tearing down the buildings. Therefore new recovery techniques are being developed, so called *in situ* remediation techniques, which make it possible to treat the soil at relatively low cost and without interrupting business. Nowadays, experience has been gained for the

improvement of excavation techniques but also new *in situ* remediation techniques are still being developed.

In situ REMEDIATION TECHNIQUES

In situ remediation techniques have been developed to treat contaminated soils, surfacewater and groundwater. Hamby [18] provides a comprehensive overview of these remediation techniques. In the following, some *in situ* remediation techniques are discussed that are applicable for aquifers since the main interest of this thesis concerns contaminated aquifers. The treatment of aquifers is based on the removal of the contaminant, the transformation of the contaminant into harmless compounds or both. If the contaminant is removed, it is still present in the environment, though in a smaller volume outside the aquifer, and it still has to be treated or transformed. The removal of the contaminant is a physical process, whereas the transformation can be achieved by chemical or biological processes.

One of the earliest *in situ* remediation techniques is the pump and treat technique [3, 24, 27, 25] where contaminated groundwater is extracted from the aquifer and treated above ground. This treatment can either be based on physical processes, e.g. air stripping to remove volatile contaminants [34, 36], chemical processes, e.g. activated carbon treatment to remove heavy metals [17, 36], or biological processes, e.g. bioreactors to remove organic contaminants [25, 36]. To enhance the removal of the contaminant during the pump and treat technique, the treated groundwater can be enriched with an extraction solute, e.g. surfactants for organic contaminants [6, 15, 32] or acids for heavy metals [20, 35], and injected into the aquifer so that the contaminant becomes more mobile. Furthermore, the pump and treat technique can be used to enhance biodegradation by which part of the contaminant is transformed into harmless compounds. If the contaminated groundwater is enriched with an electron acceptor or electron donor, nutrients or both, the biodegradation of the contaminant is stimulated. I will refer to this technique as *in situ* bioremediation [37, 45]. A similar *in situ* remediation technique is air sparging [19, 22, 41]. In this technique air is injected through a well to an area beneath the water table. The process aerates the groundwater and removes volatile contaminants. The air sparging process can also be used in conjunction with biodegradation to provide increased oxygen for groundwater remediation [19, 41].

Nowadays a new insight has become very popular. In principle, the contaminant levels decrease naturally without intervention, so called natural attenuation [26, 28, 43], by either dilution or biodegradation. Hence, no expensive remediation techniques seem to be necessary. Whether natural

attenuation is an applicable remediation concept depends, for example, on the time period available before the contaminated site should be remediated, the allowable spreading of the contaminant plume and whether there is an acute danger for public health or environment.

In situ BIOREMEDIATION

The type of *in situ* remediation technique chosen to remediate a contaminated aquifer strongly depends on the type of contaminant, e.g. heavy metal, PAH, BTEX. etc. This thesis investigates aquifers that are polluted with an organic contaminant and where *in situ* bioremediation is used to treat the aquifer. At an injection well, treated groundwater enriched with an electron acceptor or electron donor is injected. Downstream, the contaminated groundwater is intercepted and subsequently treated. The main interest in this thesis is the processes occurring in the aquifer itself, i.e. transport, adsorption and biodegradation.

Organic contaminants can be present in the aqueous and the solid phase of the aquifer. In the aqueous phase, the dissolved contaminants are transported through the aquifer by the groundwater flow. In the solid phase, they are adsorbed to soil particles and immobile. Research has suggested that only organic contaminants present in the aqueous phase can be biodegraded by indigenous micro-organisms [29, 31]. Hence, a sorbed contaminant has to desorb from the soil particles before biodegradation can occur. This biodegradation may occur under aerobic or anaerobic conditions. Under aerobic conditions, indigenous aerobic bacteria use oxygen as the electron acceptor, whereas, under anaerobic conditions, indigenous anaerobic bacteria, i.e. iron or sulfate reducers, use respectively iron (Fe^{3+}) or sulfate as the electron acceptor. If oxygen, nitrate, iron and sulfate are simultaneously available, first oxygen then nitrate followed by iron and finally sulfate will be used as the electron acceptor [44]. In addition, under anaerobic conditions the contaminant may be used as electron acceptor and an electron donor is necessary to enhance biodegradation [7]. In both aerobic and anaerobic biodegradation, the contaminant is often used as carbon and energy source. Generally, the growth of the indigenous micro-organisms depends nonlinearly on the available organic contaminant and electron acceptor or electron donor and linearly on the present micro-organism population [30]. Research has shown that during the aerobic microbial growth on methane or phenol also the biotransformation of trichloroethylene occurs [1, 21]. This process is known as co-metabolism.

Environmental conditions that influence the organic contaminant biodegradation are the availability of either electron acceptors or donors and

of essential nutrients. Therefore, to enhance biodegradation we can alter the environmental conditions to create an optimal environment, e.g. we can inject electron acceptors or donors and nutrients. Guidelines are needed for choosing the best concentrations and injection rate for the *in situ* bioremediation. Development of such guidelines requires modeling, since due to slow kinetics of the involved biological processes, *in situ* experiments are expensive and time consuming. Furthermore, permission to conduct *in situ* experiments may not always be granted.

Because *in situ* bioremediation may involve the injection and extraction of the water phase of the soil, complex three-dimensional flow patterns develop. Simultaneous modeling of groundwater flow and the transport of the contaminant is performed by numerical models. An overview of different bioremediation models has been given by Baveye and Valocchi [2], de Blanc et al. [5], and Sturman et al. [45]. The different models distinguish themselves by the different assumptions made concerning e.g. the number of involved compounds, their mobility, whether mass transfer limitations are considered, the used biodegradation kinetics equations and the presentation of the micro-organism population.

These numerical models are often time consuming and relative inflexible. Therefore, research is carried out to develop analytical models. Oya and Valocchi [33] and Xin and Zhang [46] have studied *in situ* bioremediation analytically. Oya and Valocchi [33] present an analytical expression for the long-term degradation rate of the organic pollutant, derived from a simplified conceptual bioremediation model. Xin and Zhang [46] derive (semi)-analytical solutions, using a two component model by neglecting pore-scale dispersion and setting biomass kinetics to equilibrium. This thesis deals with the derivation of a semi-analytical solutions for a different conceptual model and uses these semi-analytical solutions to gain insight in the effect of physical and biochemical parameters of the soil on the performance of the *in situ* remediation technique.

HETEROGENEITY

In situ bioremediation, as all *in situ* remediation techniques, is strongly influenced by the natural variability of the soil properties caused by deposition of soil material, rock weathering and soil morphological processes. Also the variability of the physical and biochemical properties, such as the hydraulic conductivity, the porosity, the pH, the redoxpotential and organic matter, may have a strong effect on the transport of an organic contaminant that undergoes nonlinear biodegradation. A complication stemming from the spatial variability of properties, heterogeneity, is that for a detailed

deterministic model the properties have to be known at all considered positions. Hence, an enormous amount of data is needed whereas often the deterministic distribution of the properties are unknown. To circumvent this problem, stochastic approaches are developed where the spatially variable property is regarded as a statistically stationary random space function. Hence, the results of the approach are also given in statistical terms, i.e. moments (mean, variance, etc.).

Dagan [11], Dagan et al. [12], Cvetkovic and Dagan [9], and Dagan and Cvetkovic [14] have developed the Lagrangian stochastic approach that relates the statistics of the hydraulic conductivity to the statistical moments of the solute mass flux for instantaneously or continuously injected solutes. In this approach, the transport of conservative or reactive solutes is viewed as taking place along a set of random trajectories where the solute mass is advected and subjected to biochemical processes. Pore-scale dispersion and molecular diffusion are neglected. The Lagrangian approach is applied to conservative solutes [12, 40], linear sorbing solutes [10, 38, 39, 13], nonlinear sorbing solutes [42, 4] and to solutes that undergo linear sorption kinetics [8, 9, 14]. In this thesis the Lagrangian approach is applied to nonlinear biodegradable solutes. This was also done recently by Ginn et al. [16], Xin and Zhang [46] and Kaluarachchi et al. [23]. The work in this thesis differs from theirs because one electron acceptor, instead of none [16] or two [23], is considered and a semi-analytical solution, instead of a numerical method [23], is used to determine an expression for the averaged contaminant mass flux, instead of the resident concentration [46], in a heterogeneous aquifer. The changes in the averaged contaminant mass flux assess the interaction between heterogeneity and nonlinear biodegradation.

OBJECTIVES

As was outlined, environmental conditions influence the *in situ* biodegradation of organic contaminants. The first objective is to gain insight in the transport behavior of a nonlinear biodegradable contaminant in a homogeneous aquifer. During the transport different processes take place, e.g. flow, dispersion, linear adsorption and nonlinear biodegradation. The obtained insight tells whether and when one of these processes dominates and it leads to guidelines for choosing proper conditions to optimize the *in situ* bioremediation. To obtain this insight we develop a numerical biodegradation model and perform numerical simulations for a one-dimensional aquifer.

A second objective is to derive analytical models for which the solutions approximate the results of the numerical simulations. The advantage is

that the analytical approximations are determined very quickly and still all important processes are incorporated. To derive analytical models simplifications are often necessary. These simplifications restrict the applicability of the analytical model. During the study, the simplifications are decreased to weaken the restrictions such that the analytical model becomes more realistic and applicable.

A third objective is to determine the remediation conditions that optimize the *in situ* bioremediation using the developed analytical models. If a specific contaminated site is considered and an electron acceptor is chosen to remediate the site, the only adjustable properties are the injection concentration and the injection rate. Hence, the injection concentration and injection rate that optimize the *in situ* bioremediation are determined.

The final objective is to gain insight in the interaction between the physical heterogeneity and nonlinear biodegradation. In this way the results of this thesis could be applied to *in situ* bioremediation in field situations.

OUTLINE

This thesis is a compilation of several papers, published in or submitted to international scientific journals. In all chapters a nonlinear biodegradable organic contaminant is considered. In chapter 2 and 3 the contaminant is immobile, whereas in the other chapters the contaminant is mobile and sorbs linearly.

In chapter 2 the behavior of the organic contaminant is studied by numerical simulations. Three characteristic regimes are distinguished, a low electron acceptor consumption regime, an intermediate regime and a fast electron acceptor consumption or traveling wave regime. For the first regime an analytical model is derived that approximates the numerical results. Chapter 3 contains an analytical model that approximates the results of the traveling wave regime. In this chapter also an analysis of the effect of the physical and biochemical parameters on the developed traveling wave is performed.

In chapter 4, the analytical model of chapter 3 is extended such that a mobile and linearly sorbing contaminant can be considered. In chapter 5 this analytical solution is used to determine the performance of the *in situ* bioremediation. The performance is characterized by the 99% remediation time and the ratio of contaminant biodegraded to contaminant flushed out.

Physical heterogeneity may have a large impact on the *in situ* bioremediation. Therefore, in chapter 6 the Lagrangian approach developed by Dagan [11], Dagan et al. [12], Dagan and Cvetkovic [14], and Cvetkovic and Dagan [9] is extended to nonlinear biodegradation. This approach is

used to study the interaction between physical heterogeneity and nonlinear biodegradation.

Finally, in the last chapter some general conclusions evolving from this thesis are stated.

REFERENCES

- [1] Alvarez-Cohen, L., P.L. McCarty, E. Boulygina, R.S. Hanson, G.A. Brusseau & H.C. Tsien 1992. Characterization of a methane-utilizing bacterium from a bacterial consortium that rapidly degrades trichloroethylene and chloroform. *Appl. Environ. Microb.* 58:1886-1893.
- [2] Baveye, P. & A.J. Valocchi 1989. An evaluation of mathematical models of the transport of biologically reacting solutes in saturated soils and aquifers. *Water Resources Research* 25:1413-1421.
- [3] Berglund, S. & V.D. Cvetkovic 1995. Pump-and-treat remediation of heterogeneous aquifers: effects of rate-limited mass transfer. *Ground Water* 33:675-685.
- [4] Berglund, S. & V.D. Cvetkovic 1996. Contaminant displacement in aquifers: Coupled effects of flow heterogeneity and nonlinear sorption. *Water Resources Research* 32:23-32.
- [5] de Blanc, P.C., K. Sepehrnoori, G.E. Speitel & D.C. McKinney 1996. in: *Computational Methods in Water Resources XI*, Vol. 1, eds. A.A. Aldama, J. Aparicio, C.A. Brebbia, W.G. Gray, I. Herrera and G.F. Pinder, Computational Mechanics Publications, Boston, p.161.
- [6] Brown, C.L., G.A. Pope, L.M. Abriola & K. Sepehrnoori 1994. Simulation of surfactant-enhanced aquifer remediation. *Water Resources Research* 30:2959-2977.
- [7] de Bruin, W.P, M.J.J. Kotterman, M.A. Posthumus, G. Schraa & A.J.B. Zehnder 1992. Complete biological reductive transformation of tetrachloroethene to ethane. *Appl. Environ. Microb.* 58:1996-2000.
- [8] Cvetkovic, V.D. & G. Dagan 1994. Transport of kinetically sorbing solute by steady random velocity in heterogeneous porous formations. *J. Fluid Mech.* 265:189-215.
- [9] Cvetkovic, V.D. & G. Dagan 1996. Reactive transport and immiscible flow in geological media. II. Applications. *Proc. R. Soc. Lond. A* 452:303-328.
- [10] Cvetkovic, V.D. & A.M. Shapiro 1990. Mass arrival of sorptive solute in heterogeneous porous media. *Water Resources Research* 26:2057-2067.
- [11] Dagan, G. 1989. *Flow and transport in heterogeneous formations*, Springer-Verlag, New York.
- [12] Dagan, G., V.D. Cvetkovic & A.M. Shapiro 1992. A solute flux approach to transport in heterogeneous formations 1. The general framework. *Water Resources Research* 28:1369-1376.
- [13] Dagan, G. & V.D. Cvetkovic 1993. Spatial moments of a kinetically sorbing solute plume in a heterogeneous aquifer. *Water Resources Research* 29:4053-4061.
- [14] Dagan, G. & V.D. Cvetkovic 1996. Reactive transport and immiscible flow in geological media. I. General theory. *Proc. R. Soc. Lond. A* 452:285-301.
- [15] Fountain, J.C., A. Klimek, M. Beikirch & T.M. Middleton 1991. The use of surfactants for in situ extraction of organic pollutant from a contaminated aquifer. *J. Hazard. Mater.* 28:293-311.

- [16] Ginn, T.R., C.S. Simmons & B.D. Wood 1995. Stochastic-convective transport with nonlinear reaction: Biodegradation with microbial growth. *Water Resources Research* 31:2689-2700.
- [17] Groeber, M. & J.R. Boulding 1996. Granular activated carbon treatment. in: *EPA environmental engineering sourcebook*, eds. J.R. Boulding, Ann Arbor Press, Chelsea.
- [18] Hamby, D.M., 1996. Site remediation technique supporting environmental restoration activities - a review. *Sci. Total Environ.* 191:203-224.
- [19] Hinchee, R.E. 1994. *Air sparging for site remediation*, Lewis Publishers, Boca Raton, FL.
- [20] Hong, P.K.A., C.K.A. Li, S.K. Banerji & T.K. Regmi 1999. Extraction, recovery and biostability of EDTA for remediation of heavy metal contaminated soil. *J. Soil Contam.* 8:81-103.
- [21] Hopkins, G.D., L. Semprini & P.L. McCarty 1993. Microcosm and in situ field studies of enhanced biotransformation of trichloroethylene by phenol-utilizing microorganisms. *Appl. Environ. Microb.* 59:2277-2285.
- [22] Johnson, R.L., P.C. Johnson, D.B. McWhorther, R.E. Hinchee & I. Goodman 1993. An overview of in situ air sparging. *Groundwater Monitoring and Remediation* 127-135.
- [23] Kaluarachchi, J.J., V.D. Cvetkovic & S. Berglund 2000. Stochastic analysis of oxygen- and nitrate-bases biodegradation of hydrocarbons in aquifers. *J. Cont. Hydrology.* 41:335-365.
- [24] Keely, J.F. & J.R. Boulding 1996. Performance evaluation of pump and treat remediations. in: *EPA environmental engineering sourcebook*, eds. J.R. Boulding, Ann Arbor Press, Chelsea.
- [25] Langwaldt, J.H. & J.A. Puhakka 2000. On-site biological remediation of contaminated groundwater: a review. *Environ. Poll.* 107:187-197.
- [26] Lorah, M.M. & L.D. Olsen 1999. Natural attenuation of chlorinated volatile organic compounds in a freshwater tidal wetland: Field evidence of anaerobic biodegradation. *Water Resources Research* 35:3811-3827.
- [27] Mackay, D.M. & J.A. Cherry 1989. Groundwater contamination: pump-and-treat remediation. *Environ. Sci. Technol.* 23:630-636.
- [28] van der Meer, J.R., C. Werlen, S.F. Nishino & J.C. Spain 1998. Evolution of a pathway for chlorobenzene metabolism leads to natural attenuation in contaminated groundwater. *Appl. Environ. Microb.* 64:4185-4193.
- [29] Mihelcic, J.R., D.R. Lueking, R.J. Mitzell & J.M. Stapleton 1993. Bioavailability of sorbed- and separate-phase chemicals. *Biodegradation* 4:141-153.
- [30] Monod, J. 1949. The growth of bacterial cultures. *Ann. Rev. of Microb.* 3:371-394.
- [31] Ogram, A.V., R.E. Jessup, L.T. Ou & P.S.C. Rao 1985. Effects of sorption on biological degradation rates of (2,4-dichlorophenoxy)acetic acid in soils. *Appl. Environ. Microb.* 49:582-587.
- [32] Oostrom, M., C. Hofstee, R.C. Walker & J.H. Dane 1999. Movement and remediation of trichloroethylene in a saturated, heterogeneous porous medium 2. Pump-and-treat and surfactant flushing. *J. Cont. Hydrology* 37:179-197.
- [33] Oya, S. & A.J. Valocchi 1997. Characterization of traveling waves and analytical estimation of pollutant removal in one-dimensional subsurface bioremediation modeling. *Water Resources Research* 33:1117-1127.

- [34] Rawe, J. & J.R. Boulding 1996. Air stripping of aqueous solutions. in: *EPA environmental engineering sourcebook*, eds. J.R. Boulding, Ann Arbor Press, Chelsea.
- [35] Reed, B.E., R.E. Moore & S.R. Cline 1995. Soil flushing of a sandy loam contaminated with Pb(II), PbSO₄(s), PbCO₃(s), or Pb-naphthalene: column results. *J. Soil Contam.* 4:243-267.
- [36] Rulkens, W.H., T.A. Meeder & E.R. Soczó 1993. Saneringstechnieken voor verontreinigde landbodems. in: *Bodembescherming, Handboek voor milieubeheer*, eds. Th. Edelman, J.H.J. van der Gun & Th. M. Lexmond, Samsom H.D. Tjeenk Willink, The Netherlands.
- [37] Romantschuk, M., I. Sarand, T. Petänen, R. Peltola, M. Jonsson-Vihanne, T. Koivula, K. Yrjälä, K. Haahtela 2000. Means to improve the effect of in situ bioremediation of contaminated soil: an overview of novel approaches. *Environ. Poll.* 107:179-185.
- [38] Selroos, J.O. & V.D. Cvetkovic 1992. Modeling solute advection coupled with sorption kinetics in heterogeneous formations. *Water Resources Research* 28:1271-1278.
- [39] Selroos, J.O. & V.D. Cvetkovic 1994. Mass flux statistics of kinetically sorbing solute in heterogeneous aquifers: Analytical solution and comparison with simulations. *Water Resources Research* 30:63-69.
- [40] Shapiro, A.M. & V.D. Cvetkovic 1988. Stochastic analysis of solute arrival time in heterogeneous porous media. *Water Resources Research* 24:1711-1718.
- [41] Semer, R. & K.R. Reddy 1998. Mechanisms controlling toluene removal from saturated soils during in situ air sparging. *J. Hazard. Mater.* 57:209-230.
- [42] Simmons, C.S., T.R. Ginn & B.D. Wood 1995. Stochastic-convective transport with nonlinear reaction: Mathematical framework. *Water Resources Research* 31:2675-2688.
- [43] Soo Cho, J., J.T. Wilson, D.C. DiGiulio, J.A. Vardy & W. Choi 1997. Implementation of natural attenuation at a JP-4 jet fuel release after active remediation. *Biodegradation* 8:265-273.
- [44] Stumm, W. & J.J. Morgan 1981. *Aquatic Chemistry*, John Wiley & Sons, New York, p.780.
- [45] Sturman, P.J., P.S. Stewart, A.B. Cunningham, E.J. Bouwer & J.H. Wolfram 1995. Engineering scale-up of in situ bioremediation process: a review. *J. Cont. Hydrology* 19:171-203.
- [46] Xin, J. & D. Zhang 1998. Stochastic analysis of biodegradation fronts in one-dimensional heterogeneous porous media. *Adv. Water Resources* 22:103-116.

CHAPTER 2

Characteristic regimes for in-situ bioremediation of aquifers by injecting water containing an electron acceptor*

H. Keijzer, S.E.A.T.M. van der Zee and A. Leijnse

ABSTRACT

A one-dimensional model is developed for simulating in-situ bioremediation. The modeled processes are advective and dispersive transport, biotransformation and microbial growth. The biodegradation of the contaminant is limited by the supply of electron acceptor or microbial mass. We distinguish three regimes of oxygen consumption, a low oxygen consumption regime, an intermediate regime and a fast oxygen consumption regime. Parameter variation reveals the influence of the dimensionless numbers on the duration of the three regimes.

*Computational Geosciences 1998, 2, 1-22

INTRODUCTION

Contamination of ground water and soil by organic contaminants is widespread, and is often due to oil, BTEX or gasoline spills at industrial sites [15]. In-situ bioremediation is one of the techniques to remove these organic pollutants from an aquifer because they may biodegrade in the presence of oxygen or other electron acceptors [7]. When electron acceptors are absent, their injection may enhance bioremediation. Guidelines are needed for choosing the best concentration and injection rates of electron acceptors and nutrients for in-situ bioremediation of ground water. Development of such guidelines requires modeling, since due to the slow kinetics of the involved biological processes in-situ experiments are expensive and time consuming. Furthermore, permission to conduct in-situ experiments may not always be granted.

An overview of different bioremediation models has been given by Baveye and Valocchi [1], de Blanc et al. [2], and Sturman et al. [25]. Different bioremediation models distinguish themselves by the different assumptions made concerning e.g. the number of involved compounds, their mobility, whether mass transfer limitations are considered, and the used biodegradation kinetics equations. Whereas Zysset et al. [30] and Corapcioglu and Kim [9] only consider a contaminant and microbial mass, Borden and Bedient [4] and Schäfer and Kinzelbach [24] assume that the presence of an electron acceptor is needed for degradation. Therefore they account for a third compound: the electron acceptor. In aerobic conditions oxygen and in anaerobic conditions nitrate, sulfate or Fe(III) may be used as electron acceptor. Kinzelbach et al. [20] consider both aerobic and anaerobic conditions which involve different electron acceptors. The bioremediation model can be extended by taking degradation products into account which may also be degraded by micro-organisms [19], by considering different substrates and different species of micro-organism [8], and by accounting for nutrient availability.

Assuming that a biofilm is formed around soil particles. The microbial mass may be assumed to be immobile [8, 20, 24], whereas, Borden and Bedient [4] and Zysset et al. [30] consider a mobile microbial mass. Corapcioglu and Kim [9] consider mobile biocolloids to which the contaminant adsorbs which increases the mobility of the contaminant. In almost all models the electron acceptor is mobile and injected to enhance bioremediation. Often the contaminant is also mobile.

The number of phases involved in transport and biochemical processes differ for different models. Borden and Bedient [4], and Schäfer and Kinzelbach [24] only consider the liquid phase, in which biodegradation takes

place. To account for a biofilm a first order mass transfer between biofilm and liquid phase was assumed by Kinzelbach et al. [20], Chen et al. [8] and Dhawan et al. [11].

For the biodegradation kinetics different expressions were used. Kosson et al. [21] assume zero or first order biodegradation. Borden and Bedient [4], Zysset et al. [30] and Corapcioglu and Kim [9] consider Monod kinetics, but in the actual application of the model these expressions were approximated by first order kinetics [9, 30] or an instantaneous reaction is assumed [4]. Currently, mostly Monod kinetics is assumed [8, 20, 24].

In this paper we consider a formulation of the biodegradation process that is similar to that used by Borden and Bedient [4] and Schäfer and Kinzelbach [24]. We disregard first order mass transfer between the mobile liquid and the contaminant in this first approach and consider this limitation in the discussion. Furthermore, we do not account for transport of the contaminant. This approximation may hold physically if dissolution of capillary trapped contaminant droplets or desorption of sorbed contaminant buffer the contaminant concentration throughout the domain. However, this assumption may be considered as critical as we will show in the discussion that it affects the phenomena significantly. Our intention is to reveal with numerical simulations that both the behavior and the effectivity of bioremediation caused by injecting an electron acceptor changes significantly upon a change of physical and (bio)chemical parameters.

MATHEMATICAL FORMULATION

For steady state flow, reactive solute transport in a porous medium can be described by the advection-dispersion equation

$$\frac{\partial c}{\partial t}(\mathbf{x}, t) = \nabla \cdot (\mathbf{D} \cdot \nabla c(\mathbf{x}, t)) - v(\mathbf{x}) \cdot \nabla c(\mathbf{x}, t) + R_c, \quad \mathbf{x} = (x_1, x_2, x_3), \quad (2.1)$$

where c is the solute concentration, \mathbf{D} the dispersion tensor, v the velocity field and R_c the reaction term. This reaction term may include different processes like adsorption, decay and biodegradation.

In this paper we consider a homogeneous porous medium and a steady state flow in horizontal (x_1) direction. We assume that the microbial mass forms an immobile biofilm attached to the soil matrix. Furthermore, we assume that water flowing through a gasoline contaminated porous medium has removed all the mobile gasoline and hence, we consider the immobile capillary trapped gasoline fraction. The gasoline is biodegraded by microorganisms that consume both the electron acceptor, oxygen, and gasoline for their biosynthesis. The growth of the microbial mass is limited by

the supply of oxygen, gasoline or both, according to Monod kinetics. No natural decay of microbial mass is assumed and therefore no decrease of microbial mass occurs if neither oxygen nor gasoline are available. This does not effect the essence of our paper.

Both the physical and biodegradation parameters, e.g. dispersivity, density of the solute, the stoichiometric coefficients and the half saturation constants, are constant in time and space. These assumptions lead to the following set of equations

$$\frac{\partial C}{\partial t} = D \frac{\partial^2 C}{\partial x^2} - v \frac{\partial C}{\partial x} - m_C \frac{\partial M}{\partial t}, \quad (2.2)$$

$$\frac{\partial M}{\partial t} = \mu_m \left(\frac{C}{k_C + C} \right) \left(\frac{G}{k_G + G} \right) M, \quad (2.3)$$

$$\frac{\partial G}{\partial t} = -m_G \frac{\partial M}{\partial t}, \quad (2.4)$$

where C , M and G are the oxygen, microbial mass and gasoline concentrations, respectively. The stoichiometric parameters m_C and m_G describe the ratios of oxygen and gasoline consumption rate, respectively, over microbial growth rate, μ_m is the maximum specific growth rate, and k_C and k_G are the dissolved oxygen and gasoline half saturation constants.

Initially, at $t = 0$, we assume oxygen to be the limiting factor for biodegradation with initial concentration zero. The gasoline concentration is G_0 and constant in the domain and the microbial mass, M_0 , is constant but small. At the inlet of the domain the oxygen concentration is constant by injecting water that is saturated with oxygen and at the outlet we assume a purely convective mass flux of oxygen. Hence, the initial and boundary conditions are

$$C(0, t) = C_0, \quad (2.5)$$

$$\frac{\partial C}{\partial x}(L, t) = 0, \quad (2.6)$$

$$C(x, 0) = 0, \quad M(x, 0) = M_0, \quad G(x, 0) = G_0. \quad (2.7)$$

We introduce dimensionless quantities [9, 17]

$$\begin{aligned} \bar{x} &= \frac{x}{L}, & \bar{t} &= \frac{vt}{L}, \\ \bar{C} &= \frac{C}{C_0}, & \bar{M} &= \frac{M}{M_{max}}, & \bar{G} &= \frac{G}{G_0}, \end{aligned} \quad (2.8)$$

$$K_C = \frac{k_C}{C_0}, \quad K_G = \frac{k_G}{G_0}, \quad L_\mu = \frac{\mu_m L}{v}, \quad (2.8 \text{ cont.})$$

$$P_e = \frac{vL}{D}, \quad M_C = \frac{m_C M_{max}}{C_0}, \quad M_G = \frac{m_G M_{max}}{G_0},$$

where the Peclet number P_e and the Damkohler number L_μ describe the ratio of convection to dispersion and the ratio of reaction rate to transport rate respectively. M_{max} is the maximum microbial mass which can be derived by integration of equation (2.3) with respect to time and substitution of boundary conditions (2.7), $M(x, \infty) = M_{max}$ and $G(x, \infty) = 0$ (at infinite time the gasoline is consumed and the microbial mass is at its maximum),

$$M_{max} = \frac{G_0}{m_G} + M_0. \quad (2.9)$$

Substitution of (2.8) in equations (2.2), (2.3), (2.4), (2.5), (2.6) and (2.7) and omitting the bars gives the dimensionless equations

$$\frac{\partial C}{\partial t} = \frac{1}{P_e} \frac{\partial^2 C}{\partial x^2} - \frac{\partial C}{\partial x} - M_C \frac{\partial M}{\partial t}, \quad (2.10)$$

$$\frac{\partial M}{\partial t} = L_\mu \left(\frac{C}{K_C + C} \right) \left(\frac{G}{K_G + G} \right) M, \quad (2.11)$$

$$\frac{\partial G}{\partial t} = -M_G \frac{\partial M}{\partial t}, \quad (2.12)$$

with initial and boundary conditions

$$\begin{aligned} C(0, t) &= 1, \\ \frac{\partial C}{\partial x}(L, t) &= 0, \\ C(x, 0) &= 0, \quad M(x, 0) = M_0/M_{max}, \quad G(x, 0) = 1. \end{aligned} \quad (2.13)$$

IMPLEMENTATION OF THE MODEL

Model parameters

The dimensionless equations (2.10), (2.11) and (2.12) contain dimensionless numbers that depend on physical and biochemical properties of the aquifer (i.e. dispersivity, velocity and respectively the stoichiometric coefficients, the half saturation constants, maximum growth rate). These properties may contain uncertainties because determination of these properties in the field can be rather inaccurate. The longitudinal dispersivity may vary over different orders of magnitude. This variation is due to averaging for heterogeneous medium at different scales. Despite that 'local'

TABLE 2.1. The model parameters

Parameters	Values
v	0.02 m/day
α_L	0.05 m
L	1 m
μ_m	2 day ⁻¹
k_C	0.2 mg/l
k_G	2.0 mg/l
m_C	30 kg/kg
m_G	10 kg/kg
C_0	5 mg/l
G_0	4.5 mg/l
M_0	0.001 mg/l
M_{max}	0.451 mg/l

TABLE 2.2. The dimensionless numbers

Dimensionless numbers	Values
Peclet number: P_e	20
Damkohler number: L_μ	100
Oxygen half saturation constant: K_C	0.04
Carbon half saturation constant: K_G	0.4
Stoichiometric coefficient for C and M : M_C	2.7
Stoichiometric coefficient for G and M : M_G	1.0

mixing effects (hydrodynamic dispersion) control transfer of solute to interfaces where reactions occur, most numerical studies implicitly average at larger than 'local' scales [4, 20, 22, 24]. For this reason, we follow this convention and discuss appropriateness in the discussion.

The numerical values of the physical properties, the biological parameters and the initial and boundary conditions are chosen to be in agreement with Schäfer and Kinzelbach [24], Borden and Bedient [4], Table 2.1. Using these parameters, we obtain the reference case values for the dimensionless numbers of Table 2.2.

Numerical method

The model equations are highly non-linear and an analytical solution is not available. We use a numerical method to solve the dimensionless

equations. The nonlinear system of equations is split into a partial differential equation that involves the oxygen transport equation and which is solved with a Galerkin finite element method and into nonlinear differential equations involving the nonlinear biodegradation reactions, which are solved with a Euler implicit method. They are solved sequentially, using a Picard iteration to account for the nonlinearities. The obtained linearized equations are solved by a preconditioned conjugate gradient solver for nonsymmetric systems [26]. We prevent spurious oscillations and excessive numerical dispersion in the solution of the equations by taking the discretisation in such a way that the grid Peclet number is much smaller than two and the Courant number is much smaller than one.

The used Galerkin finite element method is rather standard [8, 22, 30] in bioremediation modeling. The stability criteria for this method are strict and ascertain no numerical dispersion and oscillations. One of the disadvantages of this method is the small necessary grid size to fulfill the Peclet condition. As we consider a one-dimensional model the number of gridpoints is still reasonable, therefore, the numerical model is satisfactory. For a two- or three-dimensional model a scheme adopted to advection-dominated transport may be preferable [17, 27].

To assess whether the numerical model correctly solves the governing equations we conducted a convergence analysis and a comparison between the numerical results and available analytical solutions. For the convergence analysis, the grid and timestep were repeatedly refined and the numerical results were compared until the agreement of the results were considered accurate.

By choosing appropriate limiting values for certain parameters of the biodegradation model, we tested whether the full model agrees with cases for which analytical solutions are available. These cases were given by van Genuchten and Alves [16] for absence of biodegradation (their case A3), zeroth (B7) or first order kinetics (C7).

For zero biodegradation, we take M_C very small. Zeroth order biodegradation implies a constant rate of oxygen consumption (i.e. independent of oxygen, gasoline and microbial mass). Choosing the oxygen and gasoline half saturation constants small compared to the oxygen and gasoline concentrations, the oxygen consumption rate becomes independent of the oxygen and gasoline concentration in (2.10). Furthermore the microbial mass has to remain constant which is arranged by taking the Damkohler number very small. As this would imply that $\frac{\partial M}{\partial t}$ would be small, we increase M_C as otherwise biodegradation is zero. The resulting zeroth order

biodegradation equation for oxygen is

$$\frac{\partial C}{\partial t} = \frac{1}{P_e} \frac{\partial^2 C}{\partial x^2} - \frac{\partial C}{\partial x} - M_C L_\mu M. \quad (2.14)$$

For first order biodegradation, the oxygen reaction term depends linearly on the oxygen concentration. Hence we choose the oxygen half saturation constant much larger than the injected oxygen concentration such that $\frac{C}{K_C+C} \approx \frac{C}{K_C}$. The other parameters are kept equal to the zero order degradation case, except for M_C which is increased such that biodegradation is significant. These parameter modifications result in the first order consumption and transport equation for oxygen

$$\frac{\partial C}{\partial t} = \frac{1}{P_e} \frac{\partial^2 C}{\partial x^2} - \frac{\partial C}{\partial x} - \frac{M_C L_\mu}{K_C} M C. \quad (2.15)$$

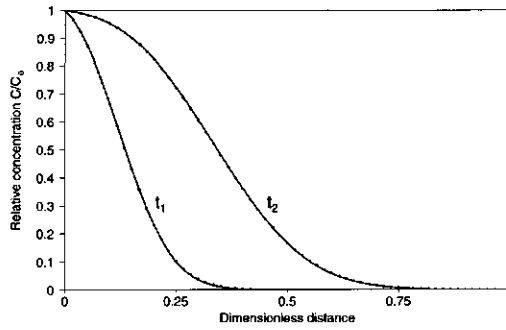
The numerical results and analytical solutions are in good agreement, see Figure 2.1.a-c. The small difference in Figure 2.1.b, is caused by the small oxygen concentrations that render K_C to be of the same order of magnitude. Then the reaction term (2.14) becomes oxygen dependent and the assumption of zeroth order degradation is invalid. We conclude that the numerical model approximates the limiting cases well and that the equations are solved correctly.

MODEL RESULTS

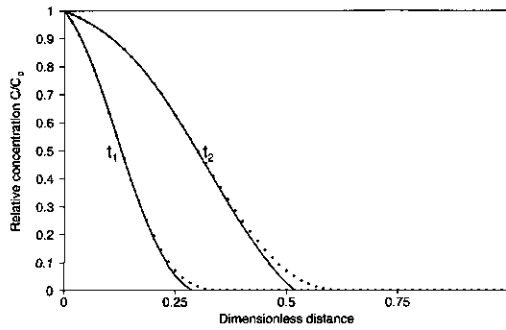
The simulation results using dimensionless numbers of Table 2.2 are provided in Figure 2.2, which shows the relative concentration fronts of oxygen, microbial mass and gasoline at different times. We observe for short times (until $t = 0.06$) a monotonous increase of oxygen concentration throughout the domain as a function of time. For larger times ($t = 0.06$ until $t = 0.11$) the oxygen concentrations at small distances decrease, i.e. this concentration does not decrease monotonically with increasing distance. At still larger times, different front shapes are observed for oxygen, microbial mass and gasoline which moves with constant a velocity.

These observations, which are also found by Murray and Xin (pers. comm., June 1997), lead us to consider three regimes of oxygen consumption. We distinguish these regimes as a function of time on the basis of spatial moments of the oxygen concentration front. The k th spatial moment is given by

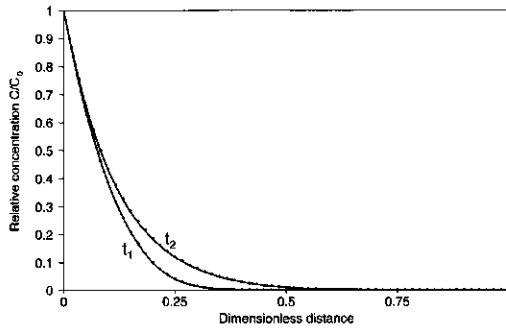
$$M_k = \int_{-\infty}^{\infty} x^k f(x) dx \quad (2.16)$$



(a)



(b)



(c)

FIGURE 2.1. Analytical (lines) and numerical (symbols) model solutions for different limiting cases at $t_1=0.01$, $t_2=0.03$. (a) No biodegradation. (b) Zeroth order biodegradation. (c) First order biodegradation.

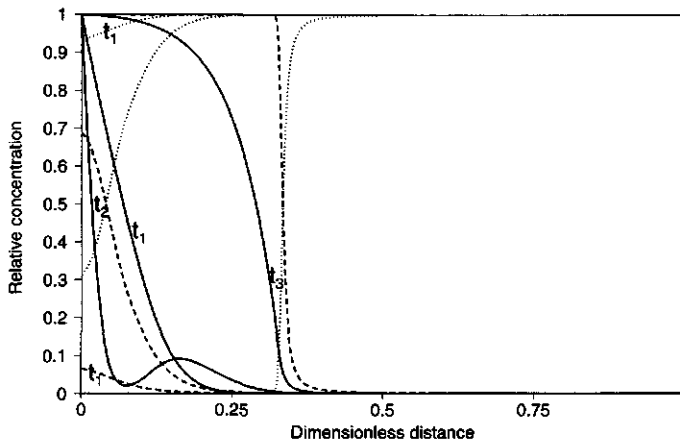


FIGURE 2.2. Relative oxygen (solid line), gasoline (dotted line) and microbial mass (dashed line) front for different times: $t_1=0.05$, $t_2=0.09$ and $t_3=1.0$.

and the k th central moment by

$$M_k^c = \int_{-\infty}^{\infty} (x - \mu)^k f(x) dx, \quad (2.17)$$

where μ is the first spatial moment (M_1). The oxygen front is related to the distribution function of traveled distance. Hence, the derivative of the oxygen concentration to x , is related to the probability density function $f(x)$, Bosma and van der Zee [5], which is given by

$$f(x) = -\frac{\partial C}{\partial x}. \quad (2.18)$$

From (2.16) and (2.17) it follows that the first moment is given by

$$M_1 = -\int_{-\infty}^{\infty} x \frac{\partial C}{\partial x} dx \quad (2.19)$$

which denotes the averaged front position. The second central moment,

$$M_2^c = -\int_{-\infty}^{\infty} (x - M_1)^2 \frac{\partial C}{\partial x} dx, \quad (2.20)$$

describes the variance (or spreading) of the front.

In the following we discuss the three oxygen consumption regimes separately and we show that it is more convenient to recognize the three regimes using the spatial moments than the oxygen concentration distributions.

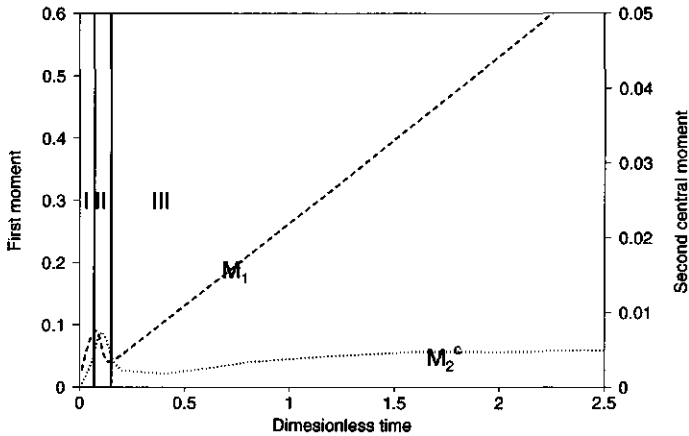


FIGURE 2.3. The first (M_1) and second central (M_2^c) moment as a function of dimensionless time and regime I, II and III.

Regime I

We observe a front that moves with almost the same speed as the water velocity. This regime is characterized by a small biodegradation rate because the microbial mass that is still close to its initial value (M_0/M_{max}), cannot consume the supplied oxygen (t_1 in Figure 2.2).

The oxygen moves fast into the domain and the averaged front position, the first moment, increases during this regime. Also the front spreads out, hence the second central moment becomes larger (Figure 2.3).

To investigate this in more detail we assume a constant small microbial mass and a constant large gasoline concentration, that are derived from the numerical results. This results in

$$\frac{\partial C}{\partial t} = \frac{1}{P_e} \frac{\partial^2 C}{\partial x^2} - \frac{\partial C}{\partial x} - M_C L_\mu \left(\frac{C}{K_C + C} \right) \left(\frac{\langle G \rangle}{K_G + \langle G \rangle} \right) \langle M \rangle, \quad (2.21)$$

where $\langle \cdot \rangle$ is the constant average of the concentration in regime I. To approximate the last term on the right hand side with a first order term, we linearize the nonlinear oxygen dependent term $\frac{C}{K_C + C}$ as $\frac{C}{K_C + \langle C \rangle}$, where $\langle C \rangle$ is the averaged oxygen concentration in this regime. This results in

$$\frac{\partial C}{\partial t} = \frac{1}{P_e} \frac{\partial^2 C}{\partial x^2} - \frac{\partial C}{\partial x} - M_C L_\mu \left(\frac{C}{K_C + \langle C \rangle} \right) \left(\frac{\langle G \rangle}{K_G + \langle G \rangle} \right) \langle M \rangle. \quad (2.22)$$

Comparing the analytical solution of the first order biodegradation equation (2.22) with the numerically obtained concentration fronts in this regime,

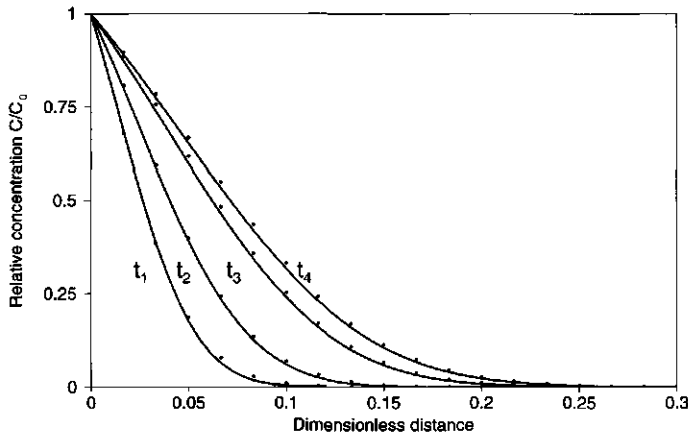


FIGURE 2.4. Numerical (symbols) and analytical results (lines) in regime I at $t_1=0.01$, $t_2=0.02$, $t_3=0.04$, and $t_4=0.05$.

we observe a close agreement (Figure 2.4) which indicates that this approximation is appropriate.

Regime II

Between $t = 0.06$ and $t = 0.11$ an intermediate regime is observed where the Monod kinetics start to play a role. Especially for small distances a rapid growth of the microbial mass occurs, as is shown in Figure 2.2 (t_2), and the oxygen consumption is large. For larger distances microbial growth is still slow and oxygen reduction is still small. Figure 2.2 shows it is possible to have a higher oxygen concentration at distances further in the domain than at distances near the inlet.

We observe a decrease in the first moment because the higher consumption of oxygen at small distances results in a decrease of the averaged front position. The front spreading, however, becomes larger because oxygen still spreads out to larger distances (Figure 2.3).

During this regime the large amount of oxygen supplied in the first regime is consumed during the rapid microbial growth until the oxygen supply and oxygen consumption used for gasoline degradation balance.

Regime III

We observe a front that moves with a constant velocity and a front shape that appears to be unaffected as it moves through the domain (t_3 in Figure 2.2). The front velocity is retarded compared with the water velocity.

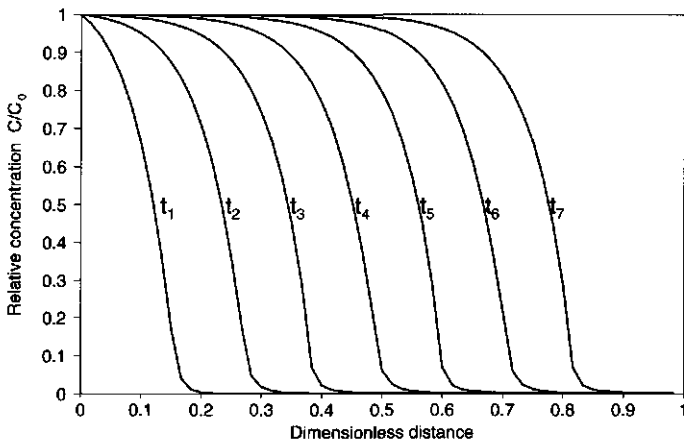


FIGURE 2.5. Relative oxygen concentration front in regime III only at $t_1=0.4$, $t_2=0.8$, $t_3=1.2$, $t_4=1.6$, $t_5=2.0$, $t_6=2.4$, and $t_7=2.8$.

For the first moment we observe a linear increase as a function of time which is caused by the constant velocity of the front. The second central moment approaches a finite limiting value (Figure 2.3). The striking resemblance of the concentration fronts can be seen by plotting the front for more times, Figure 2.5. These observations are similar to those observed by Bosma and Van der Zee [5], Oya and Valocchi [23], and Murray and Xin (pers. comm., June 1997) for a traveling wave.

A traveling wave connects the initial situation (large distance) with the final situation (small distance). An expression can be found for the traveling wave velocity based on mass balance considerations [12, 13, 14, 28]. The model equations (2.10) and (2.12) are transformed to a moving coordinate system given by

$$\eta = x - \alpha t \quad (2.23)$$

with α the traveling wave velocity. Applying this transformation gives

$$\frac{1}{P_e} \frac{d^2 C}{d\eta^2} = (1 - \alpha) \frac{dC}{d\eta} - \alpha M_C \frac{dM}{d\eta}, \quad (2.24)$$

$$-\alpha \frac{dG}{d\eta} = \alpha M_G \frac{dM}{d\eta}. \quad (2.25)$$

The boundary conditions are transformed too, which yield

$$C(\eta = -\infty) = 1, \quad C(\eta = \infty) = 0, \quad (2.26)$$

$$G(\eta = -\infty) = 0, \quad G(\eta = \infty) = 1. \quad (2.27)$$

Substituting (2.25) in (2.24), integrating with respect to η and substituting boundary conditions, we obtain for the traveling wave velocity

$$\alpha = \left(1 - \frac{M_C \Delta C}{M_G \Delta G} \right)^{-1}, \quad (2.28)$$

where ΔC and ΔG are the differences between the final and initial conditions for the oxygen and gasoline concentrations, respectively, which equal $\Delta C = 1$ and $\Delta G = -1$. The traveling wave velocity neither depends on the initial condition for the microbial mass (M_0) nor on the oxygen and gasoline half saturation constants (K_C and K_G). With the expression for the traveling wave velocity (2.28) the oxygen and gasoline removal rate can easily be derived, Oya and Valocchi [23].

Due to the balance between oxygen supply and its consumption to degrade the gasoline no biodegradation kinetics need to be evaluated. The only reaction parameters necessary are the stoichiometric coefficients (M_C and M_G). This instantaneous reaction approach is applicable if the traveling wave regime starts.

PARAMETER SENSITIVITY

We varied the dimensionless numbers to explore their influence on the duration of the different regimes. The duration of these regimes is assessed from the development of the first spatial moment. In the first regime, the first moment increases and during the second regime the first moment decreases. During the third regime, the first moment increases linearly with increasing time when the traveling wave has fully developed and the second central moment converge to a constant. The end of the first and second regime are denoted by t_I and t_{II} .

The time level t_I is defined as the time for which the first moment has a local maximum, and t_{II} is defined as the time for which the first moment has a local minimum. The local maximum and minimum value of the first moment, respectively $M_{1,max}$ and $M_{1,min}$, have to be related to the duration of the first two regimes. Because, if the first and second regime last longer, the oxygen concentration front reaches larger distances during these regimes. Hence, the averaged front position (first moment) increases and thus the local maximum and minimum increases. Therefore, we expect a positive correlation between t_I , t_{II} and $M_{1,max}$, $M_{1,min}$.

In view of uncertainties in the physical and biochemical properties in the field, the dimensionless numbers are varied over two orders of magnitude [22], where for each simulation only one of the dimensionless numbers is

varied. We compare the results with the results of the reference case (case ref, Table 2.3). A summary is given below.

The Peclet number relates advection with dispersion. Increasing the Peclet number (case a, Table 2.3) implies relatively less dispersion compared with advection and so, more oxygen is injected in time, whereas the oxygen consumption rate does not change. As a result the first two regimes will last longer. Because time is scaled with both the length of the domain and velocity this is also the case for t_I and t_{II} . Therefore, the Peclet number has no influence on t_I and t_{II} . This behavior is shown in Figure 2.6.a.

The Damkohler number relates the reaction rate with the transport rate of oxygen. If the Damkohler number increases (case b, Table 2.3) the reaction is faster compared with transport. This results in both a faster growth of microbial mass and a higher consumption of oxygen. Hence, t_I and t_{II} should decrease, and Figure 2.6.b confirms that this is the case. A closer inspection of the numerical results reveals

$$t_I = \frac{c1}{L_\mu} = \frac{6}{L_\mu} \quad (2.29)$$

$$t_{II} = \frac{c2}{L_\mu} = \frac{12}{L_\mu} \quad (2.30)$$

i.e., the Damkohler number is inversely proportional to t_I and t_{II} (Figure 2.7).

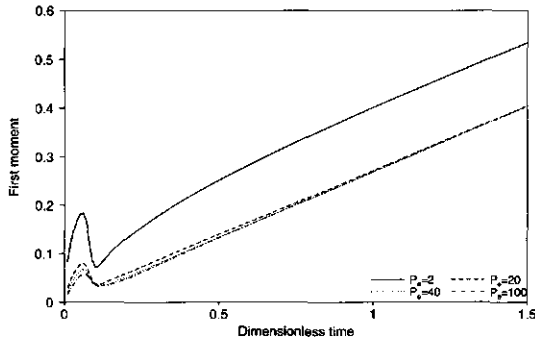
The dimensionless numbers K_C and K_G relate the dissolved oxygen and gasoline half saturation constants with the boundary condition of oxygen and the initial condition of gasoline. Both numbers occur similarly in the microbial mass equation (2.11). Therefore, they should have a similar effect on the duration of the first two regimes. If K_C or K_G increases (case c or d, Table 2.3) the Monod terms decrease, which results in a decrease of the growth rate of microbial mass and the consumption rate of oxygen. Thus t_I and t_{II} increase if K_C or K_G increases. Figure 2.6.c and 2.6.d confirm this behavior. Approximately we observe linear relations between K_C or K_G and t_I and t_{II} (Figure 2.7).

M_C gives the ratio between consumed oxygen and the formed microbial mass, and occurs only in the oxygen concentration equation (2.10). If M_C increases (case e, Table 2.3) more oxygen is necessary for the growth of the microbial mass, and oxygen decreases faster in the first two regimes. This results in a decrease of t_I and t_{II} as is shown in Figure 2.6.e.

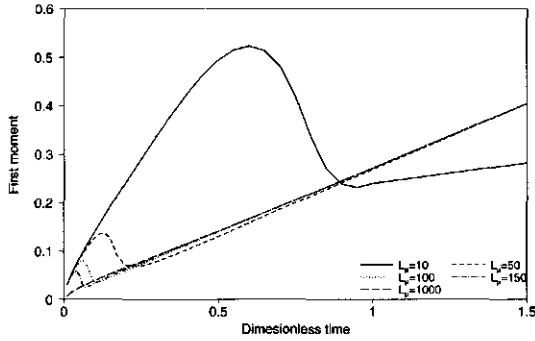
The dimensionless number M_G , which relates the consumed gasoline to the newly formed micro-organism, was not varied because it is impossible

TABLE 2.3. Dimensionless numbers and characteristic time t_I and t_{II} . P_e is varied for cases a, L_μ for cases b, K_C for cases c, K_G for cases d, M_C for cases e, and M_0 for cases f.

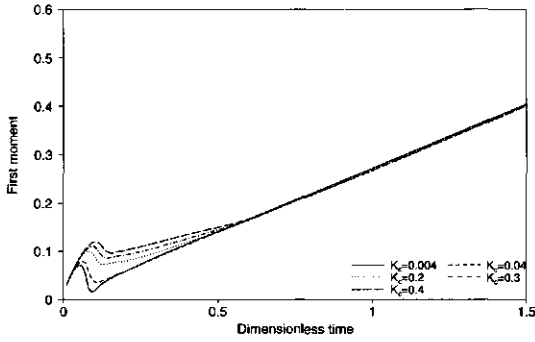
case	P_e	L_μ	K_C	K_G	M_C	M_0	t_I	t_{II}
ref	20	100	0.04	0.4	2.7	0.001	0.06	0.11
a1	2	-	-	-	-	-	0.06	0.10
a2	40	-	-	-	-	-	0.06	0.12
a3	80	-	-	-	-	-	0.06	0.12
a4	100	-	-	-	-	-	0.06	0.12
b1	-	10	-	-	-	-	0.6	0.95
b2	-	25	-	-	-	-	0.25	0.55
b3	-	50	-	-	-	-	0.13	0.25
b4	-	75	-	-	-	-	0.08	0.15
b5	-	150	-	-	-	-	0.04	0.07
c1	-	-	0.004	-	-	-	0.05	0.09
c2	-	-	0.02	-	-	-	0.06	0.10
c3	-	-	0.08	-	-	-	0.07	0.12
c4	-	-	0.2	-	-	-	0.08	0.13
c5	-	-	0.3	-	-	-	0.09	0.14
c6	-	-	0.4	-	-	-	0.10	0.15
d1	-	-	-	0.04	-	-	0.04	0.07
d2	-	-	-	0.2	-	-	0.05	0.09
d3	-	-	-	0.8	-	-	0.08	0.15
d4	-	-	-	2.0	-	-	0.14	0.25
d5	-	-	-	3.0	-	-	0.20	0.40
d6	-	-	-	4.0	-	-	0.25	0.50
e1	-	-	-	-	0.45	-	0.09	0.11
e2	-	-	-	-	1.35	-	0.07	0.11
e3	-	-	-	-	3.6	-	0.06	0.10
e4	-	-	-	-	4.0	-	0.05	0.10
e5	-	-	-	-	5.4	-	0.05	0.10
e6	-	-	-	-	6.75	-	0.05	0.10
f1	-	-	-	-	-	0.0001	0.09	0.19
f2	-	-	-	-	-	0.01	0.03	0.06



(a)

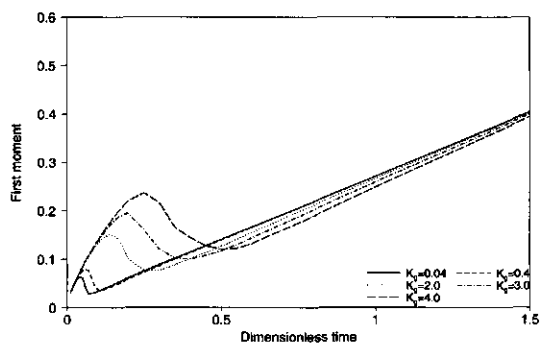


(b)

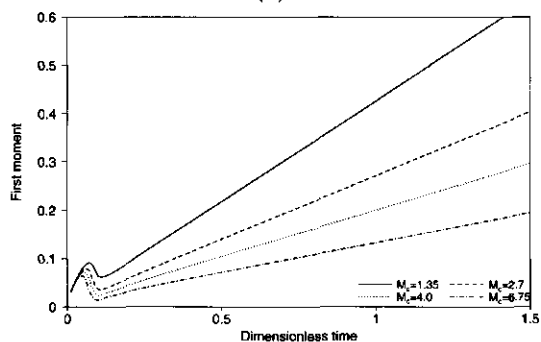


(c)

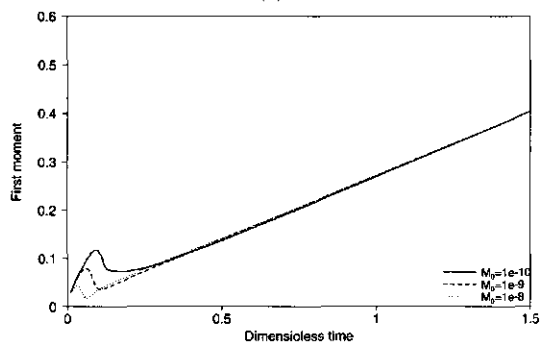
FIGURE 2.6. Influence of parameter variation on t_I and t_{II} . (a) Peclet number. (b) Damkohler number. (c) Oxygen half saturation constant.



(d)



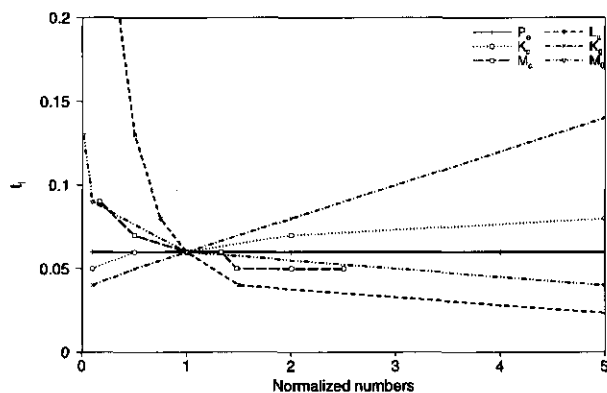
(e)



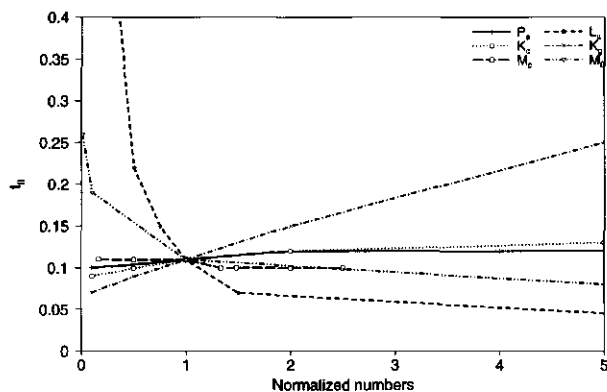
(f)

FIGURE 2.6. (Continued.) (d) Gasoline half saturation constant. (e) Stoichiometric coefficient. (f) Initial microbial mass.

to vary one of the underlying variables in M_G without changing M_C , as M_{max} implicitly depends on m_G and G_0 .



(a)



(b)

FIGURE 2.7. Dependence of t_I (a) and t_{II} (b) on the dimensionless numbers, which are normalized with respect to the reference case, for example $P_{e_n} = P_e/P_{e_{ref}}$.

The effect of the initial background value of the microbial mass M_0 was assessed by varying M_0 . If M_0 increases (case f, Table 2.3), immediately more oxygen is consumed and the microbial mass reaches its maximum value sooner. Therefore, the duration of the first two regimes shortens and t_I and t_{II} decrease, as shown in Figure 2.6.f.

The parameter variation reveals that t_I and t_{II} are influenced by the dimensionless numbers. This influence follows from the definition of these numbers and the model equations (2.10), (2.11) and (2.12). Figure 2.7 shows both t_I and t_{II} as a function of the dimensionless numbers, which

are normalized with respect to the reference case. Using Figure 2.7, we conclude that for small values of K_C or K_G and for large values of L_μ or M_0 , t_I and t_{II} are small. Therefore, the third regime will dominate. If on the other hand K_C or K_G are large or L_μ or M_0 are small, the first regime will dominate.

Furthermore, parameter variation reveals that the expected positive correlation between the duration of the first two regimes and the local maximum and minimum value of the first moment holds, Figure 2.6.b-2.6.f.

CONCLUSIONS AND DISCUSSION

We considered biodegradation of gasoline in a one-dimensional homogeneous porous medium as the result of injection of water that contains an electron acceptor such as oxygen. Biodegradation is described by Monod kinetics where the growth of microbial mass is limited by either the oxygen or gasoline concentration. We assumed that both gasoline and microbial mass are immobile and that the oxygen is mobile.

The numerical results of our model reveal three regimes of oxygen consumption, each of which is characterized by different dominating processes. The first regime is characterized by a supply of oxygen that is larger than the consumption rate of oxygen by microbial mass. In the following intermediate regime the biodegradation rate becomes of the similar magnitude as the oxygen injection rate and the degradation rate is strongly position dependent. In the third regime the injection and consumption rates of oxygen are almost equal, and the oxygen, gasoline and microbial mass fronts move with a constant velocity and fixed front shapes through the domain. These phenomena resemble a traveling wave, whose velocity we derived.

It is useful to assess whether or not the first or third regime dominates the numerical results. If the first regime dominates, we can simulate the results by first order kinetics. On the other hand, if the traveling wave regime is dominant, a balance between the oxygen supply and its consumption develops and we can consider an instantaneous reaction between oxygen and gasoline. This reaction does not depend on the biodegradation kinetics, and so, only the stoichiometric coefficients are needed. The modeling of biotransformation either by first order kinetics or by instantaneous reactions is attractive, because in the first situation an analytical solution is found and in the second situation only two instead of three equations have to be solved. Therefore more understanding of the circumstances under which the first order kinetics or instantaneous reaction approach is applicable is useful.

We defined two time levels, one for which the first regime ends (t_I) and one for which the traveling wave regime starts (t_{II}). Although the traveling wave is not yet developed at t_{II} we assume that the instantaneous reaction approach is valid at t_{II} . By parameter variation we gained insight in the influence of the dimensionless numbers on t_I and t_{II} . It showed that the effects of these numbers follow from the definition of these numbers and the model equations.

For some limiting situations only the first or the third regime will develop. For example, if the Damkohler number is large, the biodegradation reaction will be fast and an instantaneous reaction may be assumed [4]. Figure 2.6.b shows that this assumption is applicable for large Damkohler numbers because almost no first and second regime develops. In case the gasoline concentration is much smaller than the gasoline half saturation constant ($G \ll K_G$), the substrate is limiting the biodegradation [8, 23, 30] and only a small part of oxygen is consumed. Therefore the first regime will last and the third regime will not develop, which is also found by Oya and Valocchi [23]. The first order degradation approach is applicable in this situation.

We studied a simplified model, in specific cases some of the simplifications are questionable and we will discuss the influence if these simplifications were not made. In the analysis, we neglected to account for mass transfer limitations of the electron acceptor, oxygen, to reach the location where the contaminant and microbial mass reside and where the (bio)chemical degradation occurs. In most realistic porous media, this simplification is not appropriate. However, an extensive literature exists that describes the effect of first order mass transfer for homogeneous flow domains [29]. Except for a small ratio of travel distance over the scale of dispersive mixing, the effect of first order mass transfer can usually be represented as additional 'dispersion'. This was also shown to hold for the cases of nonlinear adsorption that lead to traveling waves [28]. Hence, accounting for first order mass transfer is likely to increase the duration of the regimes before a constant front of electron acceptor (in terms of first and second moment) develops as well as the final front thickness, but it does not affect the existence of the three regimes defined in this paper.

In our model we assumed an immobile contaminant. Our assumption may be considered critical if the retardation of the contaminant is small or if the low soluble contaminant is not capillary trapped. Oya and Valocchi [23] considered a mobile contaminant that adsorbs to the soil, they concentrated their study on the developed traveling wave. Extra effects

are recognized in the distribution of the electron acceptor and the contaminant, i.e. oscillations in the traveling wave velocity. These oscillations are due to the interaction between advective mixing enhanced by sorption of the substrate and biodegradation. It does not influence the existence of the three regimes as Oya and Valocch [23] also recognized an initial stage (regime II) during which the microbial mass drastically increases.

We also considered dispersivities that are much larger than would normally be in agreement with the local pore scale mixing that controls the likeliness of electron acceptor to reach the contaminant and microbial mass. For fine to coarse sand aquifers, dispersivities of 0.2-2 μm would be more appropriate [3]. Mass transfer limitations and physical heterogeneity at different scales lead to larger 'effective' dispersivities [10]. As almost all cited papers on in-situ bioremediation modeling on field scale use the large lumped 'effective' dispersivities, our results show relevant effects for such conventional modeling. For physical relevance, larger scale mixing should be represented by e.g. random conductivity field effects rather than additional diffusion. We did not explore this numerically, as if regime I dominates we expect similar effects as found by Kabala and Sposito [18]. If regime III dominates, results as found by Bosma and Van der Zee [6] may apply for continuous injection, and we concentrate on this situation. They considered nonlinear adsorption leading to local front steepening effects that are similar to ours, for the traveling wave regime. Furthermore, they considered chemical or physical heterogeneity. Hence, their results are applicable to the currently investigated situation. We mention their main conclusions. The combination of interactions that lead to a traveling wave in a homogeneous domain with physical or chemical random heterogeneity affect the averaged front variance (second central moment). If the heterogeneity scale is small (i.e., large ratio of transversal local dispersivity over integral scale), nonlinear interactions dominate and the front variance goes to a maximum as for a traveling wave. If the heterogeneity scale is large (the above ratio is small), the averaged front variance may increase linearly in agreement with Dagan [10]. Furthermore, a larger variability favors dominance of heterogeneity effects over nonlinearity of interactions. For most aquifers, we would expect the heterogeneity to dominate over nonlinear interactions effects, i.e., no stabilization of the averaged front variance for our initial and boundary conditions. Hence, we advise caution with regard to incorporating larger scale effects into an effective dispersivity for computational efficiency and speed.

NOTATION

C (\bar{C})	(Dimensionless) concentration electron acceptor [mg l^{-1}]
C_0	Feed concentration electron acceptor [mg l^{-1}]
D	Dispersion coefficient [$\text{m}^2 \text{day}^{-1}$]
L_μ	Damkohler number [1]
G (\bar{G})	(Diml.) concentration organic contaminant [mg l^{-1}]
G_0	Initial concentration organic contaminant [mg l^{-1}]
k_C (K_C)	(Diml.) electron acceptor half saturation constant [mg l^{-1}]
k_G (K_G)	(Diml.) contaminant half saturation constant [mg l^{-1}]
L	Length of domain [m]
M (\bar{M})	(Dimensionless) concentration microbial mass [mg l^{-1}]
M_0	Initial concentration microbial mass [mg l^{-1}]
M_{max}	Maximal concentration microbial mass [mg l^{-1}]
m_C (M_C)	(Dimensionless) stoichiometric coefficient [mg mg^{-1}]
m_G (M_G)	(Dimensionless) stoichiometric coefficient [mg mg^{-1}]
M_k	Kth spatial moment
M_k^c	Kth central moment
$M_{1,max}$	local maximum of first moment
$M_{1,min}$	local minimum of first moment
P_e	Peclet number [1]
R_c	Reaction term
t (\bar{t})	(Dimensionless) time [day]
t_I	Local maximum of first spatial moment [1]
t_{II}	Local minimum of first spatial moment [1]
v	Interstitial velocity [m day^{-1}]
x (\bar{x})	(Dimensionless) length [m]
α	Traveling wave velocity [m day^{-1}]
η	Moving coordinate
μ	First spatial moment
μ_m	Maximum specific growth rate [day^{-1}]

ACKNOWLEDGEMENT

This research was partly funded by Directorate General Science, Research and Development of the Commission of the European Communities, via the EC program ENVIRONMENT, contract no EV5V-CT94-0536, and by NOBIS via the biosparging project. We thank the reviewers, especially O. Cirpka (University of Stuttgart, Germany), for their helpful comments on the manuscript.

REFERENCES

- [1] Baveye, P. & A.J. Valocchi 1989. An evaluation of mathematical models of the transport of biologically reacting solutes in saturated soils and aquifers. *Water Resources Research* 25:1413-1421.
- [2] de Blanc, P.C., K. Sepehrnoori, G.E. Speitel & D.C. McKinney 1996. in: *Computational Methods in Water Resources XI*, Vol. 1, eds. A.A. Aldama, J. Aparicio, C.A. Brebbia, W.G. Gray, I. Herrera and G.F. Pinder, Computational Mechanics Publications, Boston, p.161.
- [3] Bolt, G.H. 1982. in: *Soil Chemistry B. Physico-Chemical models*, eds. G.H. Bolt, Elsevier, New York, p.285.
- [4] Borden, R.C. & P.B. Bedient 1986. Transport of dissolved hydrocarbons influenced by oxygen-limited biodegradation 1. Theoretical development. *Water Resources Research* 22:1973-1982.
- [5] Bosma, W.J.P. & S.E.A.T.M. van der Zee 1993. Transport of reactive solute in a one-dimensional chemically heterogeneous porous medium. *Water Resources Research* 29:117-131.
- [6] Bosma, W.J.P. & S.E.A.T.M. van der Zee 1995. Dispersion of a continuously injected, nonlinearly adsorbing solute in chemically or physically heterogeneous porous formations. *J. Cont. Hydrology* 18:181-198.
- [7] Bouwer, E.J. & A.J.B. Zehnder 1993. Biopremediation of organic compounds - putting microbial metabolism to work. *Trends Biotechn.* 11:360-367.
- [8] Chen, Y., L.M. Abriola, P.J.J. Alvarez, P.J. Anid & T.M. Vogel 1992. Modeling transport and biodegradation of benzene and toluene in sandy aquifer material: Comparisons with experimental measurements. *Water Resources Research* 28:1833-1847.
- [9] Corapcioglu, M.Y. & S. Kim 1995. Modeling facilitated contaminant transport by mobile bacteria. *Water Resources Research* 31:2639-2647.
- [10] Dagan, G. 1989. *Flow and transport in heterogeneous formations*, Springer-Verlag, New York.
- [11] Dhawan, S., L.E. Erickson & L.T. Fan 1993. Model development and simulation of bioremediation in soil beds with aggregates. *Ground Water* 31:271-284.
- [12] van Duijn, C.J. & P. Knabner 1992. Travelling waves in the transport of reactive solutes through porous media: adsorption and binary ion exchange - Part 1. *Transport in Porous Media* 8:167-194.
- [13] van Duijn, C.J. & P. Knabner 1992. Travelling waves in the transport of reactive solutes through porous media: adsorption and binary ion exchange - Part 2. *Transport in Porous Media* 8:199-225.
- [14] van Duijn, C.J., P. Knabner & S.E.A.T.M. van der Zee 1993. Travelling waves during the transport of reactive solute in porous media: combination of Langmuir and Freundlich isotherms. *Adv. Water Resources* 16:97-105.
- [15] Essaid, H.I., B.A. Bekins, E.M. Godsy, E. Warren, M.J. Baedecker & I.M. Cozzarelli 1995. Simulation of aerobic and anaerobic biodegradation processes at a crude oil spill site. *Water Resources Research* 31:3309-3327.
- [16] van Genuchten, M.Th. & W.J. Alves 1982. *Analytical solutions of the one-dimensional convective-dispersive transport equation*, USDA Techn. Bull. 1661, Washington D.C..

- [17] Ginn, T.R., C.S. Simmons & B.D. Wood 1995. Stochastic-convective transport with nonlinear reaction: Biodegradation with microbial growth. *Water Resources Research* 31:2689-2700.
- [18] Kabala, Z.J. & G. Sposito 1991. A stochastic model of reactive solute transport with time-varying velocity in a heterogeneous aquifer. *Water Resources Research* 27:341-350.
- [19] Kindred, J.S. & M.A. Celia 1989. Contaminant transport and biodegradation 2. Conceptual model and test simulations. *Water Resources Research* 25:1149-1159.
- [20] Kinzelbach, W., W. Schäfer & J. Herzer 1991. Numerical modeling of natural and enhanced denitrification processes in aquifers. *Water Resources Research* 27:1123-1135.
- [21] Kosson, Agnihocri and Ahlert 1985. Modeling of microbially active soil columns. *Computer Applications in Water Resources*, eds. H.C. Torno, p.266.
- [22] MacQuarrie, K.T.B. & E.A. Sudicky 1990. Simulation of biodegradable organic contaminants in groundwater. 2. Plume behavior in uniform and random flow fields. *Water Resources Research* 26:223-239.
- [23] Oya, S. & A.J. Valocchi 1997. Characterization of traveling waves and analytical estimation of pollutant removal in one-dimensional subsurface bioremediation modeling. *Water Resources Research* 33:1117-1127.
- [24] Schäfer, W. & W. Kinzelbach 1991. in: *In Situ Bioreclamation*, eds. R.E. Hinchee and R.F. Olfenbuttel, Butterworth-Heinemann, London, p.196.
- [25] Sturman, P.J., P.S. Stewart, A.B. Cunnungham, E.J. Bouwer & J.H. Wolfram 1995. Engineering scale-up of in situ bioremediation process: a review. *J. Cont. Hydrology* 19:171-203.
- [26] van der Vorst, H.A. *Bi-CGSTAB: a fast and smoothly converging variant of Bi-CG for the solution of nonsymmetric linear systems*, preprint 633, Dept. of Math., University Utrecht.
- [27] Wood, B.D., C.N. Dawson, J.E. Szecsody & G.P. Streile 1994. Modeling contaminant transport and biodegradation in a layered porous media system. *Water Resources Research* 30:1833-1845.
- [28] van der Zee, S.E.A.T.M. 1990. Analytical traveling wave solutions for transport with nonlinear and nonequilibrium adsorption. *Water Resources Research* 26:2563-2578. (Correction, 1991 *Water Resources Research* 27:983.)
- [29] van der Zee, S.E.A.T.M. & W.H. van Riemsdijk 1994. Transport of reactive solutes in soils. *Advances in Porous Media* 2:1-105.
- [30] Zysset, A., F. Stauffer & T. Dracos 1994. Modeling of reactive groundwater transport governed by biodegradation. *Water Resources Research* 30:2423-2434.

CHAPTER 3

Analytical approximation to characterize the performance of in-situ aquifer bioremediation*

H. Keijzer, M.I.J. van Dijke and S.E.A.T.M. van der Zee

ABSTRACT

The performance of in-situ bioremediation to remove organic contaminants from contaminated aquifers depends on the physical and biochemical parameters. We characterize the performance by the contaminant removal rate and the region where biodegradation occurs, the biologically active zone (BAZ). The numerical fronts obtained by one-dimensional in-situ bioremediation modeling reveal a traveling wave behavior: fronts of microbial mass, organic contaminant and electron acceptor move with a constant velocity and constant front shape through the domain. Hence, only one front shape and a linear relation between the front position and time is found for each of the three compounds. We derive analytical approximations for the traveling wave front shape and front position that agree perfectly with the traveling wave behavior resulting from the bioremediation model. Using these analytical approximations, we determine the contaminant removal rate and the BAZ. Furthermore, we assess the influence of the physical and biochemical parameters on the performance of the in-situ bioremediation technique.

*Advances in Water Resources 1999, 23, 217-228

INTRODUCTION

One of the approaches to remove organic contaminants from the aquifer is in-situ bioremediation. This approach is applicable if micro-organisms are present in the subsoil that can degrade organic contaminants with the help of an electron acceptor. If the micro-organisms aerobically degrade the organic contaminant, oxygen may act as an electron acceptor. At smaller redoxpotentials, other compounds (e.g. nitrate, Fe(III), or sulfate) may serve as the electron acceptor [20]. Provided that an electron acceptor is sufficiently available, the micro-organism population may grow during the consumption of organic contaminant. Hence, injection of a dissolved electron acceptor in a reduced environment may enhance the biodegradation rate.

In this study we use two factors to characterize the performance of bioremediation: the overall contaminant removal rate and the region where biodegradation occurs, the biologically active zone (BAZ) of the aquifer [15, 16]. The contaminant removal rate describes how fast the contaminant is removed from an aquifer. It is based on the averaged front position. The BAZ, which we base on the front shape of the electron acceptor, describes the transition of contaminant concentration from the remediated part to the contaminated part of the aquifer. If a small BAZ develops there is a clear distinction between the part of the aquifer that is still contaminated and the part that has already been remediated. If the BAZ is large, electron acceptor may already reach an extraction well while there is still a large amount of contaminant available. This indicates a less efficient use of injected electron acceptor.

The contaminant removal rate and the BAZ are affected by the physical and biochemical parameters of the soil. Insight in these effects is important for determining the performance of the in-situ bioremediation technique. Numerical models or analytical solutions can be used to determine the effects of the different parameters. Several researchers have developed numerical models that include transport and biodegradation. These models are used to simulate laboratory [5, 6, 25] or field [3, 13, 19] experiments or to gain better understanding of the underlying processes [11, 12, 15, 16]. The models differ with respect to assumptions made concerning, e.g. the number of involved compounds, the biodegradation kinetics, and the mobility of the compounds. A detailed overview of various numerical bioremediation models is given by Baveye and Valocchi [1] and Sturman et al. [21].

Moreover, Oya and Valocchi [15, 16] and Xin and Zhang [24] have studied in-situ bioremediation analytically. Oya and Valocchi [15, 16] present an analytical expression for the long-term degradation rate of the organic

pollutant, derived from a simplified conceptual bioremediation model. Xin and Zhang [24] derive (semi-)analytical solutions for the contaminant and electron acceptor front shapes, using a two component model. This two component model results from the model used by Oya and Valocchi by neglecting dispersion and setting the biomass kinetics to equilibrium. In our study we derive analytical approximations for the contaminant and electron acceptor front shapes for another simplified model. We also use the model of Oya and Valocchi and consider an immobile contaminant and a specific growth rate which is significantly larger than the decay rate. Our special interest goes to the influence of the physical and biochemical properties of the soil on the performance of the in-situ remediation. We use the analytical approximations of the front shapes to show in more detail how various model parameters affect the contaminant removal rate and the BAZ.

MATHEMATICAL FORMULATION

We consider the same one-dimensional bioremediation model as Keijzer et al. [11]. A saturated and homogeneous aquifer with steady state flow is assumed. The model includes three mass balance equations, one for the electron acceptor c , one for the organic contaminant g , and one for the microbial mass m . Several simplifying assumptions are made. We consider a mobile and non-adsorbing electron acceptor, e.g. oxygen or nitrate. The electron acceptor is injected to enhance biodegradation [3, 15, 16, 24]. Although the contaminant is often considered mobile [3, 15, 16, 24] we assume an immobile contaminant. This assumption reflects the situation where a contaminant is present at residual saturation, furthermore, the contaminant has a low solubility. We consider the effect of this assumption on the contaminant removal rate in the discussion and compare our findings with Oya and Valocchi [15] who have considered a mobile and linear-adsorbing contaminant. Moreover, we consider an immobile microbial mass that forms biofilms around the soil particles [5, 9, 13]. The micro-organisms are assumed to utilize the residual contaminant for their metabolism. The microbial growth is modeled by Monod kinetics [14, 15, 16, 24], the micro-organisms grow until the contaminant or electron acceptor is completely consumed. Furthermore, we neglect the decay of micro-organisms, assuming that the specific growth rate is significantly larger than the decay rate. Because of this assumption, we might obtain a large maximum microbial mass when the initial contaminant concentration is large.

These assumptions lead to the following mass balance equations for the three components

$$\frac{\partial c}{\partial t} = D \frac{\partial^2 c}{\partial x^2} - v \frac{\partial c}{\partial x} - m_c \frac{\partial m}{\partial t}, \quad (3.1)$$

$$\frac{\partial m}{\partial t} = \mu_m \left(\frac{c}{k_c + c} \right) \left(\frac{g}{k_g + g} \right) m, \quad (3.2)$$

$$\frac{\partial g}{\partial t} = -m_g \frac{\partial m}{\partial t}, \quad (3.3)$$

where D denotes the dispersion coefficient and v the effective velocity. The parameters in equation (3.2) are the maximum specific growth rate, μ_m , and the dissolved electron acceptor and organic contaminant half saturation constants, k_c and k_g . The stoichiometric parameters m_c and m_g in these equations describe, respectively, the ratios of consumed electron acceptor and organic contaminant to newly formed micro-organism.

Initially, at $t = 0$, we consider a constant contaminant concentration, g_0 , and a constant, small microbial mass, m_0 , in the domain. We assume the electron acceptor concentration to be the limiting factor for biodegradation which is initially equal to zero. At the inlet of the domain a prescribed mass flux of the electron acceptor is imposed and at the outlet ($x = L$) we assume a purely advective mass flux of electron acceptor. Hence, the initial and boundary conditions are

$$-D \frac{\partial c}{\partial x} + vc = vc_0 \quad \text{for } t > 0 \quad \text{at } x = 0, \quad (3.4)$$

$$\frac{\partial c}{\partial x} = 0 \quad \text{for } t > 0 \quad \text{at } x = L, \quad (3.5)$$

$$c = 0, \quad m = m_0, \quad g = g_0 \quad \text{for } x \geq 0 \quad \text{at } t = 0. \quad (3.6)$$

We introduce dimensionless quantities [6, 10, 11]

$$\begin{aligned} X &= \frac{x}{L}, & T &= \frac{vt}{L}, \\ C &= \frac{c}{c_0}, & M &= \frac{m}{m_{\max}}, & G &= \frac{g}{g_0}, \\ K_C &= \frac{k_c}{c_0}, & K_G &= \frac{k_g}{g_0}, & P_e &= \frac{vL}{D}, \\ L_\mu &= \frac{\mu_m L}{v}, & M_C &= \frac{m_c m_{\max}}{c_0}, & M_G &= \frac{m_g m_{\max}}{g_0}, \end{aligned} \quad (3.7)$$

where P_e is the Peclet and L_μ is the Damkohler number, which describe the ratios of advection rate over dispersion rate and of reaction rate over advection rate, respectively. Here m_{\max} is the maximum microbial mass, which is found by integration of equation (3.3) with respect to time and substitution of boundary conditions:

$$m_{\max} = \frac{g_0}{m_g} + m_0. \quad (3.8)$$

Substitution of (3.7) in the equations (3.1)-(3.3) yields the dimensionless equations

$$\frac{\partial C}{\partial T} = \frac{1}{P_e} \frac{\partial^2 C}{\partial X^2} - \frac{\partial C}{\partial X} - M_C \frac{\partial M}{\partial T}, \quad (3.9)$$

$$\frac{\partial M}{\partial T} = L_\mu \left(\frac{C}{K_C + C} \right) \left(\frac{G}{K_G + G} \right) M, \quad (3.10)$$

$$\frac{\partial G}{\partial T} = -M_G \frac{\partial M}{\partial T}. \quad (3.11)$$

The dimensionless boundary conditions become

$$-\frac{1}{P_e} \frac{\partial C}{\partial X} + C = 1 \quad \text{for } T > 0 \quad \text{at } X = 0, \quad (3.12)$$

$$\frac{\partial C}{\partial X} = 0 \quad \text{for } T > 0 \quad \text{at } X = 1, \quad (3.13)$$

$$C = 0, \quad M = \frac{m_0}{m_{\max}}, \quad G = 1 \quad \text{for } X \geq 0 \quad \text{at } T = 0. \quad (3.14)$$

The coupled system of non-linear partial differential equations (3.9)-(3.11) is solved numerically by Keijzer et al. [11]. The numerical results revealed three different time regimes of contaminant consumption. In the third regime, the biodegradation rate is maximal and opposes the dispersive spreading, hence a traveling wave behavior occurs: the fronts of the electron acceptor, the micro-organisms and the organic contaminant approach a constant velocity and fixed shapes while moving through the domain (Figure 3.1). Although the contaminant and the microbial mass are immobile, the fronts of these compounds show a traveling wave behavior because during the movement of electron acceptor, the micro-organisms consume the contaminant and electron acceptor and use them for their growth.

TRAVELING WAVE SOLUTION

For a traveling wave behavior, analytical solutions may be derived [2, 17, 22, 23]. The traveling wave solution describes the limiting behavior

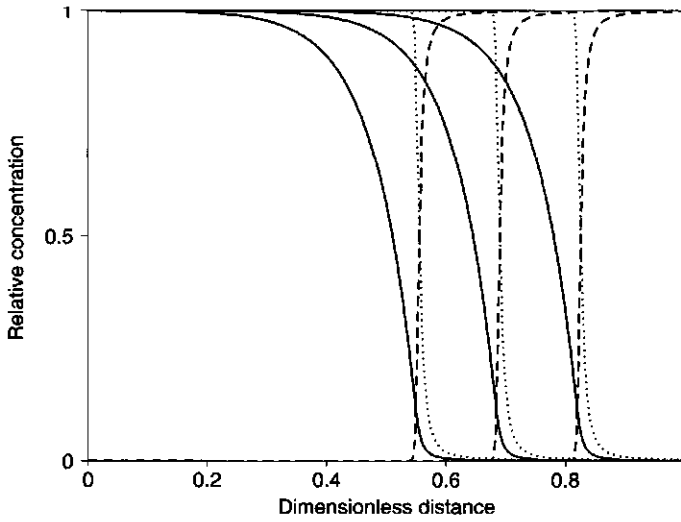


FIGURE 3.1. Relative concentration fronts for electron acceptor (solid line), contaminant (dashed line) and microbial mass (dotted line) at different observation times, obtained by the numerical model.

for infinite time and displacement. Keijzer et al. [11] showed that for large L_μ , small K_C or small K_G already after a short displacement of time a traveling wave behavior develops. To obtain a traveling wave solution the model equations are transformed to a moving coordinate system, with traveling coordinate η , given by

$$\eta = X - \alpha T, \quad (3.15)$$

with α the dimensionless traveling wave velocity. An analytical solution for the limiting front velocity follows from mass balance considerations [15, 22, 23], yielding for the present model [11]

$$\alpha = \left(1 - \frac{M_C \Delta G}{M_G \Delta C} \right)^{-1}, \quad (3.16)$$

where $\Delta C = 1$ and $\Delta G = -1$ are the differences between the final and initial conditions for the electron acceptor and contaminant, respectively.

Traveling wave front shape

Transformation of equations (3.9)-(3.11) to the moving coordinate system yields

$$\frac{1}{P_e} \frac{d^2 C}{d\eta^2} = (1 - \alpha) \frac{dC}{d\eta} - \alpha M_C \frac{dM}{d\eta}, \quad (3.17)$$

$$\alpha \frac{dM}{d\eta} = -L_\mu \left(\frac{C}{K_C + C} \right) \left(\frac{G}{K_G + G} \right) M, \quad (3.18)$$

$$\frac{dG}{d\eta} = -M_G \frac{dM}{d\eta}. \quad (3.19)$$

Assuming that the traveling wave solution is already a good approximation after a relatively short time, we impose the following boundary conditions for the transformed problem [15]

$$C(\eta) = 1, \quad M(\eta) = 1, \quad G(\eta) = 0, \quad \text{at } \eta = -\infty, \quad (3.20)$$

$$C(\eta) = 0, \quad M(\eta) = \frac{m_0}{m_{\max}}, \quad G(\eta) = 1, \quad \text{at } \eta = \infty, \quad (3.21)$$

where the boundary condition for $C(\eta = -\infty)$ is a reduction of the flux condition (3.12). It follows that, besides the above conditions, the following conditions also hold

$$\frac{dC}{d\eta} = 0, \quad \frac{dM}{d\eta} = 0, \quad \frac{dG}{d\eta} = 0, \quad \text{at } \eta = -\infty, \infty. \quad (3.22)$$

Rather than solving the system (3.17)-(3.19), we rewrite the system using the definition

$$w(C) = -\frac{dC}{d\eta}. \quad (3.23)$$

We obtain the following single order differential equation for $w(C)$, see Appendix A

$$\begin{aligned} \frac{dw}{dC} &= -P_e(1 - \alpha) \\ &+ P_e(1 - \alpha) \left(\frac{L_\mu M_G}{\alpha w} \right) \left(\frac{C}{K_C + C} \right) \left(\frac{G}{K_G + G} \right) \left(1 - \frac{G}{M_G} \right). \end{aligned} \quad (3.24)$$

with $0 \leq C \leq 1$ and

$$G = -\frac{w}{P_e(1 - \alpha)} - C + 1. \quad (3.25)$$

Furthermore, boundary condition (3.22) yields

$$w(0) = 0. \quad (3.26)$$

We integrate equation (3.24) numerically using a fourth-order Runge-Kutta method where the value of $w'(0)$ is found analytically by taking the limit of (3.24) for $C \rightarrow 0$ ($G \rightarrow 1$) using equation (3.25) and l'Hopital's rule

$$w'(C=0) = -\frac{P_e}{2}(1-\alpha) + \frac{1}{2} \sqrt{(P_e(1-\alpha))^2 + 4P_e(1-\alpha) \left(\frac{L_\mu M_G}{\alpha}\right) \left(\frac{1}{K_G+1}\right) \left(1 - \frac{1}{M_G}\right) \left(\frac{1}{K_C}\right)}. \quad (3.27)$$

With the resulting solution for $w(C)$ we find the front shape $C(\eta)$ by numerical integration of relation (3.23) from a reference point $\eta = \eta_r$, where we choose arbitrarily $C = 0.5$

$$\eta - \eta_r = - \int_{0.5}^C \frac{1}{w(C')} dC' \quad \text{for } 0 \leq C \leq 1. \quad (3.28)$$

The front shapes for $G(\eta)$ and $M(\eta)$ are found from (3.28), using equation (3.25) and (A1), respectively.

Traveling wave front position

The front shape is given with respect to an arbitrary reference point, see equation (3.28). We determine this point according to mass balance considerations. Assuming a large domain to prevent the electron acceptor from reaching the outlet, the total amount of electron acceptor injected into the domain, C_{inj} , is equal to the amount of electron acceptor still present in the domain, C_{pres} , plus the amount of electron acceptor consumed by the micro-organisms to biodegrade the contaminant, C_{cons} . The mass balance equation for C is

$$C_{inj} = C_{pres} + C_{cons}. \quad (3.29)$$

In Appendix B, we derive expressions for these quantities, using the dimensionless equation (3.9)-(3.11) and boundary conditions (3.12)-(3.13) for the original coordinate system.

If we combine equations (B1), (B2) and (B4), equation (3.29) becomes

$$T^* = \int_0^{X^*} C(X, T^*) dX + \frac{M_C}{M_G} \int_0^{X^*} (1 - G(X, T^*)) dX \quad (3.30)$$

with X^* the only unknown. To determine X^* , we use the traveling wave solutions for C and G , denoted by C_{TW} and G_{TW} respectively, as derived in section 3.1. We define $\eta^* = X^* - \alpha T^*$, such that $C_{TW}(\eta^*) = \epsilon$, and

$\eta_* = -\alpha T^*$. Hence, solving equation (3.30) for X^* is equivalent to finding $\eta^* - \eta_*$ from

$$T^* = \int_{\eta_*}^{\eta^*} C_{TW}(\eta) d\eta + \frac{M_C}{M_G} \int_{\eta_*}^{\eta^*} (1 - G_{TW}(\eta)) d\eta. \quad (3.31)$$

To achieve this, we use equation (3.28) to write η_r in terms of η^* ,

$$\eta^* - \eta_r = - \int_{1/2}^{\epsilon} \frac{1}{w(C')} dC'. \quad (3.32)$$

When X^* is found, η_r follows from (3.32) by the definition of $\eta^* = X^* - \alpha T^*$, which determines C_{TW} completely.

APPLICABILITY OF THE ANALYTICAL APPROXIMATION

We derived a traveling wave solution for the biodegradation equations. To show that the traveling wave solution provides a good approximation of the front shape and front position, we carry out a number of numerical simulations and compare the results with the analytical approximations. We apply the numerical method described by Keijzer et al. [11]. An operator-splitting method is applied. The transport part of the equations is solved with a Galerkin finite element method, whereas, the biodegradation reaction part is solved with an implicit Euler method. The two parts are solved using a Picard iteration.

For all simulations the following physical and biochemical parameters are kept constant, the numerical values are chosen in agreement with Schäfer and Kinzelbach [18] and Borden and Bedient [3]. The porosity and velocity are $n = 0.4$ and $v = 0.1$ m/day, respectively, and the length of the domain is $L = 10$ m. The initial available contaminant and microbial mass are $g_0 = 4.5$ mg/l and $m_0 = 0.001$ mg/l, respectively. We consider a relatively small initial contaminant concentration that results in a realistic maximal microbial mass. The imposed mass flux of electron acceptor at the inlet is vc_0 with $c_0 = 5.0$ mg/l. We choose the discretization and time step such that the grid Peclet and Courant conditions are fulfilled to avoid numerical dispersion and numerical instabilities. This results in $\Delta x = 0.025$ m and $\Delta t = 0.05$ day.

For the reference case (ref), the values of the dimensionless numbers are given in Table 3.1. The dimensionless numbers are obtained by using the following values for the remaining physical and biochemical parameters, i.e. $\mu_m = 1$ day⁻¹, $m_c = 30$, $m_g = 10$, $k_c = 0.2$ mg/l, $k_g = 2.0$ mg/l and $\alpha_l = 0.5$ m, respectively. The value of α_l may be too large to account for local mixing effects only but we use this value for the purpose of illustration.

TABLE 3.1. Dimensionless numbers and specific time (T^*) that were used to calculate the first and second central moment (M_1 and M_2^c) analytically (a) and numerically (n). P_e is varied for cases a, L_μ for cases b, K_C for cases c, K_G for cases d, M_C for cases e, and M_G for cases f.

	P_e	L_μ	K_C	K_G	M_C	M_G	T^*	M_{1n}	M_{2n}^c	M_{1a}	M_{2a}^c
ref	20	100	0.04	0.4	2.7	1.0022	2.5	0.624	0.0048	0.624	0.0047
a1	10	-	-	-	-	-	-	0.577	0.016	0.577	0.016
a2	100	-	-	-	-	-	-	0.664	0.0003	0.663	0.0003
b1	-	50	-	-	-	-	-	0.623	0.0051	0.622	0.0049
b2	-	200	-	-	-	-	-	0.624	0.0047	0.624	0.0044
c1	-	-	0.004	-	-	-	-	0.624	0.0046	0.624	0.0045
c2	-	-	0.2	-	-	-	-	0.623	0.0054	0.623	0.0056
d1	-	-	-	0.04	-	-	-	0.624	0.0047	0.624	0.0047
d2	-	-	-	4.0	-	-	-	0.622	0.0061	0.623	0.0061
e1	-	-	-	-	1.35	-	2.0	0.798	0.0077	0.800	0.0077
e2	-	-	-	-	27.0	-	6.0	0.167	0.0019	0.167	0.0019
f1	-	-	-	-	-	1.022	-	0.633	0.0048	0.633	0.0047
f2	-	-	-	-	-	1.22	-	0.725	0.0052	0.727	0.0051

Variation of one of the remaining physical or biochemical parameters results in a variation of one of the dimensionless numbers. The semi-analytical and numerical results are shown in dimensionless form.

We compare the semi-analytical and numerical results in two alternatives ways. First, we compare the obtained fronts for the electron acceptor, contaminant and microbial mass, as is done in Figure 3.2 for the reference case. We conclude that the semi-analytical fronts approximate the numerical fronts almost perfectly. Secondly, we can compare the spatial moments of the semi-analytically and numerically obtained fronts for the original coordinate system. Calculating the spatial moments, we only consider the electron acceptor front as the contaminant and microbial mass are functions of C and w , see respectively equation (3.25) and (A1). The first moment of the electron acceptor front describes the average front position [4, 11]

$$M_1 = \int_0^\infty X \frac{\partial C}{\partial X} dX. \quad (3.33)$$

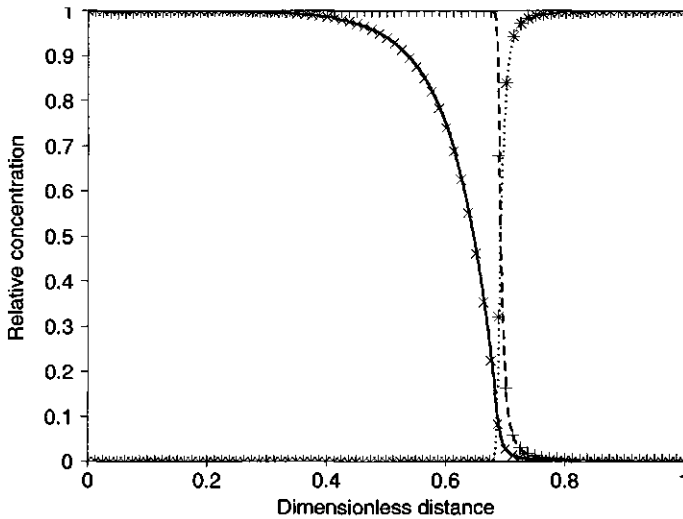


FIGURE 3.2. Relative concentration fronts resulting from analytical and numerical model. Semi-analytical and numerical front for electron acceptor: solid line and x, contaminant: dotted line and *, and microbial mass: dashed line and +.

The second central moment,

$$M_2^c = \int_0^\infty (X - M_1)^2 \frac{\partial C}{\partial X} dX, \quad (3.34)$$

describes the spreading (or variance) of the front. For both the semi-analytical and numerical fronts these moments can be derived numerically with the trapezoidal rule. The first and second central moment for semi-analytical (ana) and numerical (num) fronts are given in Table 3.1, at specific time T^* . Table 3.1 shows good agreement between the first and second central moments of the semi-analytical and numerical results for the different cases. We conclude that the traveling wave solution is valid for every value of the different dimensionless numbers, but only applicable to aquifers if the length of the aquifer is long enough [11, 15, 16].

PARAMETER SENSITIVITY

In section 3, we have derived a traveling wave solution that describes the averaged front position and the front shape. Using this solution, we assess the effect of the dimensionless numbers in terms of the averaged front position and the spreading of the front. In view of uncertainties in the physical and biochemical properties in field situations, the dimensionless numbers are varied over a wide range of values. In Figure 3.3, we show

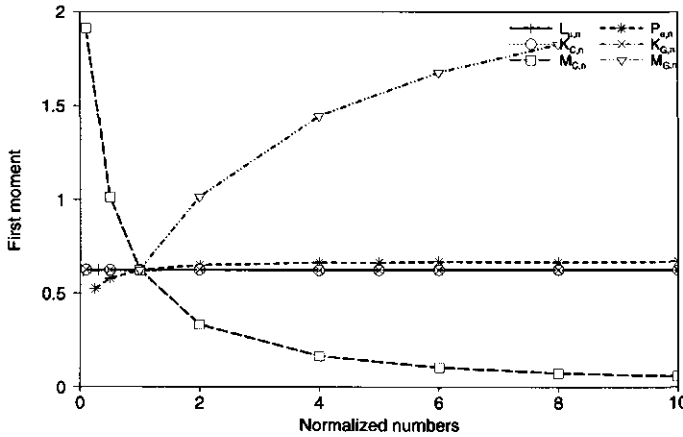


FIGURE 3.3. Dependence of the first moment on the dimensionless numbers, which are normalized with respect to the reference case, for example, $P_{e,n} = P_e/P_{e,r}$.

the first moment as a function of the dimensionless numbers which are normalized with respect to the reference case (subscript r):

$$\begin{aligned}
 P_{e,n} &= \frac{P_e}{P_{e,r}}, & L_{\mu,n} &= \frac{L_\mu}{L_{\mu,r}}, \\
 K_{C,n} &= \frac{K_C}{K_{C,r}}, & K_{G,n} &= \frac{K_G}{K_{G,r}}, \\
 M_{C,n} &= \frac{M_C}{M_{C,r}}, & M_{G,n} &= \frac{M_G}{M_{G,r}}.
 \end{aligned} \tag{3.35}$$

Observe that the Damkohler number, L_μ , and the two relative half saturation constants, K_C and K_G , barely affect the first moment, whereas the two relative stoichiometric coefficients, M_C and M_G , and the Peclet number, P_e , affect the first moment significantly. Because the traveling wave velocity depends on the stoichiometry [11, 15, 16], decreasing M_C or increasing M_G results in a larger traveling wave velocity. Hence, the front intrudes faster into the domain and the first moment grows faster with time. Although P_e is not part of equation (3.16) it affects the first moment because of the influx boundary condition (3.12).

In Figure 3.4, we present the second central moment as a function of the normalized dimensionless numbers (3.35). Increasing P_e , L_μ or M_C results in a smaller second central moment, whereas increasing K_C , K_G or M_G results in a larger second central moment. Increasing P_e implies less dispersion, which results in a steeper electron acceptor front and therefore

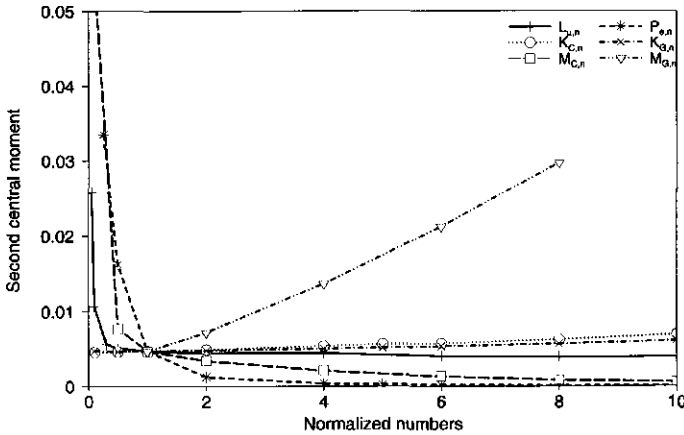


FIGURE 3.4. Dependence of the second central moment on the dimensionless numbers, which are normalized with respect to the reference case, for example, $P_{e,n} = P_e/P_{e,r}$.

a smaller second central moment. A steeper electron acceptor front also occurs when the microbial growth rate increases. This is indicated by larger L_μ values, see equation (3.10). Larger K_C or K_G , on the contrary, induce a smaller microbial growth rate and therefore a less steep electron acceptor front. Furthermore, increasing M_C results in a higher electron acceptor consumption which causes a steeper electron acceptor front, while increasing M_G results in a smaller electron acceptor consumption during the biodegradation of the contaminant, i.e., the electron acceptor front will flatten.

RESULTS AND DISCUSSION

We characterize the performance of *in-situ* bioremediation by the overall contaminant removal rate and the BAZ. We obtain the contaminant removal rate by the same approach as Oya and Valocchi [15, 16]. The dimensionless cumulative contaminant removal M_{RG} , for a finite domain, is given by

$$M_{RG} = n \left(L^* - \int_0^{L^*} G dX \right), \quad (3.36)$$

with n the porosity and L^* the length of the aquifer. The first term on the right-hand side is the total contaminant initially available and the second term is the total contaminant left in the domain. The other term in equation (24) of Oya and Valocchi [15] describes the amount of contaminant flowing out of the outlet. This term is omitted because there is no outflow of

contaminant at the outlet in our case. The complete term on the right-hand side is defined as the averaged front position of the contaminant [15]. We assume that the traveling wave has developed, the electron acceptor and contaminant front move with the same traveling wave velocity through the domain, thus $d(L^* - \int_0^{L^*} G dX)/dT = \alpha$. This leads to the dimensionless contaminant removal rate

$$R_G = \frac{dM_{rG}}{dT} = n \alpha = n \frac{1}{1 + \frac{M_C}{M_G}}. \quad (3.37)$$

The dimensionless contaminant removal rate is proportional to the dimensionless traveling wave velocity and does not depend on L_μ , P_e , K_C and K_G , see equation (3.16). This result is also found by Oya and Valocchi [15, 16] and Borden and Bedient [3]. Using the same approach as above, we obtain the dimensional removal rate

$$r_g = R_G v g_0, \quad (3.38)$$

which is linearly related to the flow velocity.

We determine the BAZ using the electron acceptor front shape. Although the second central moment describes the overall spreading of the electron acceptor front, it is important whether the entire front or only the part where biodegradation occurs spreads out. Figure 3.2, for example, shows that the electron acceptor front spreads mostly out to the left, but that the steep contaminant and microbial mass fronts are situated in a narrow region around the toe of the electron acceptor front. In this situation, the part of the electron acceptor front that is affected by the contaminant and microbial mass is small. If the contaminant front is less steep, a wider region of the electron acceptor front is affected. In this case it is possible that the electron acceptor reaches an extraction well, although still a large amount of contaminant is present in the aquifer.

To determine the influence of the different parameters on the BAZ, we divide the electron acceptor front in two parts. A part where the contaminant and micro-organism fronts are located, see Figure 3.2, which is dominated by biodegradation, and a part with virtually zero contaminant and maximal microbial mass, which is dominated by dispersion. We distinguish the two parts of the electron acceptor front on the basis of the function $w(C)$ which denotes the derivative of C with respect to η for each C value, see equation (3.23). According to equation (3.25), we define a critical electron acceptor concentration C_r which separates the two parts:

$$\begin{cases} 0 < C < C_r, & w = -P_e(1 - \alpha)[C + G - 1], & \text{biodegradation part,} \\ C_r < C < 1, & w = -P_e(1 - \alpha)[C - 1], & \text{dispersion part.} \end{cases} \quad (3.39)$$

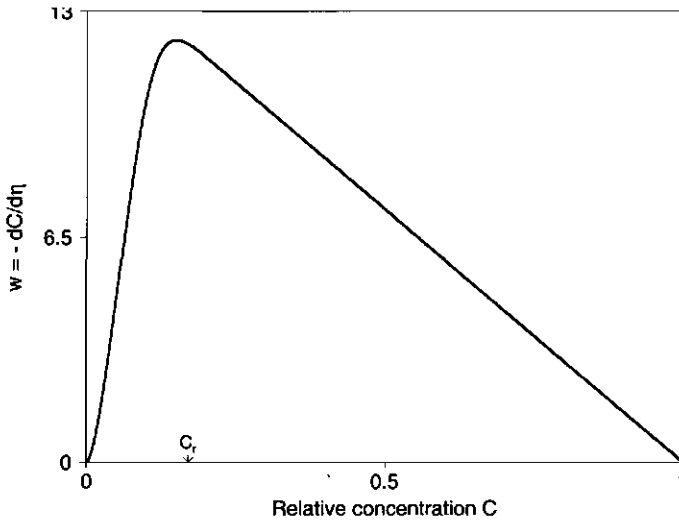


FIGURE 3.5. The function $w(C)$ and the critical electron acceptor concentration C_r for the reference case.

The latter part is linear in C , because $G \approx 0$. For example, Figure 2.5 shows $w(C)$ for the reference case, which is nonlinear for small C concentrations, the biodegradation-dominated, and virtually linear for larger C concentrations, the dispersion-dominated part, which corresponds to exponential behavior of the left part of the electron acceptor front in Figure 3.2.

Using the function $w(C)$, we discuss whether the dimensionless numbers influence the biodegradation or the dispersion-dominated part or both parts of the electron acceptor front. Variation of the Damkohler number L_μ (Figure 3.6.a) or one of the relative half saturation constants K_C or K_G (not shown) affects the biodegradation-dominated part of the electron acceptor front and the values of C_r , but not the slope of the linear part in the dispersion-dominated part. This slope is given by the effective Peclet number: $P_{e(\text{eff})} = P_e(1 - \alpha)$, see (3.39). This behavior is expected because L_μ , K_C or K_G are not included in $P_{e(\text{eff})}$ and influence only the microbial growth rate, see equation (3.10). On the other hand, variation of the Peclet number P_e (Figure 3.6.b) or one of the stoichiometric coefficients M_C or M_G (Figures 3.6.c and 3.6.d, respectively) affect also the dispersion-dominated part because $P_{e(\text{eff})}$ is affected too.

Furthermore, we use $w(C)$ to determine the influence of the dimensionless numbers on the BAZ. An increase in C_r leads to a larger biodegradation-dominated part, i.e., a larger BAZ, whereas an increase of $P_{e(\text{eff})}$ results

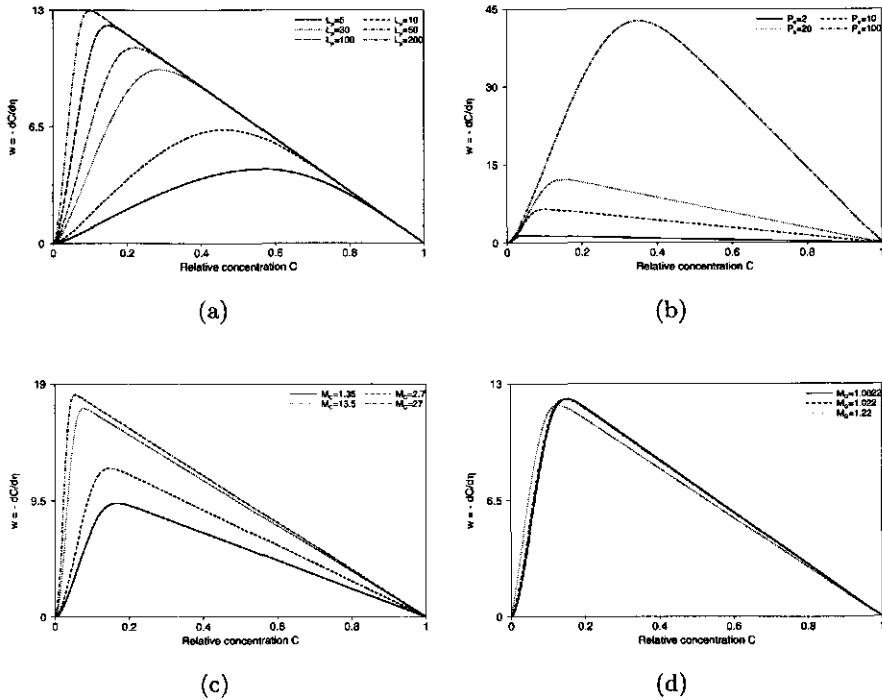


FIGURE 3.6. Influence of parameter variation on $w(C)$ and C_r . (a) Damkohler number L_μ . (b) Peclet number P_e . (c) Stoichiometric coefficient M_C . (d) Stoichiometric coefficient M_G .

in a steeper electron acceptor front and thus a smaller BAZ. Accordingly, these influences might counteract or intensify each other. We will start with L_μ , K_C and K_G and their limiting cases, next P_e and finally M_C and M_G .

Increasing L_μ (Figure 3.6.a) or decreasing K_C or K_G (not shown), we obtain a smaller C_r which leads to a larger dispersion-dominated part of the electron acceptor front and, because the slope of the linear part $P_{e(\text{eff})}$ is not affected, to a steeper front shape of the biodegradation-dominated part, see Figure 3.7. Hence, the BAZ decreases. This behavior is expected because L_μ , K_C and K_G affect the microbial growth, hence the consumption of electron acceptor.

Concerning L_μ , K_C and K_G , the following limiting cases are of interest: $L_\mu \rightarrow \infty$, indicating fast biodegradation kinetics leading to an equilibrium assumption, $K_C \ll 1$ or $K_G \ll 1$, indicating that electron acceptor or

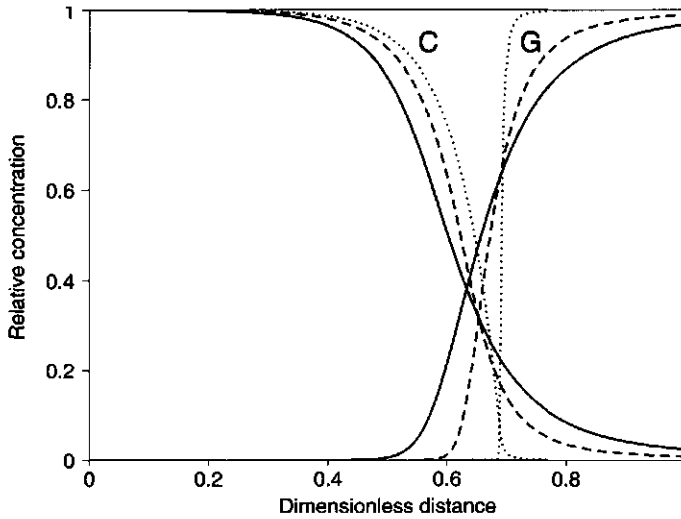


FIGURE 3.7. Relative electron acceptor and contaminant concentration fronts for different Damkohler numbers. (Solid line: $L_\mu = 5$, dashed line: $L_\mu = 10$ and dotted line: $L_\mu = 200$).

substrate respectively, are sufficiently available [15]. For these limiting situations C_r tends to zero, which implies that the entire electron acceptor front is dominated by dispersion and shows a complete exponential behavior, see Figure 3.7. The electron acceptor front shape can be derived analytically from (3.39)

$$C(\eta - \eta_r) = 1 - e^{P_e(1-\alpha)(\eta - \eta_r)}, \quad (3.40)$$

with η_r calculated as explained in section 3.2. The length of the BAZ is negligible. The contaminant concentration front changes abruptly from initial to zero and is given by a step function. On the other hand, if $L_\mu \ll 1$, indicating slow biodegradation kinetics, $K_C \gg 1$ or $K_G \gg 1$, indicating that electron acceptor or contaminant respectively, are limiting factors [15], C_r is equal to one. This implies that the entire electron acceptor front shape is dominated by biodegradation, and the electron acceptor concentration changes only gradually from one to zero, see Figure 3.7. Thus a large BAZ is found. Moreover, Keijzer et al. [11] and Oya and Valocchi [15, 16] showed that for these specific cases, a long enough aquifer is necessary before the traveling wave can develop.

P_e , M_C and M_G influence both C_r and $P_{e(\text{eff})}$. Figure 3.6.b shows that increasing P_e leads to a larger value of C_r , but also to a larger value of

$P_{e(\text{eff})}$. Effectively, w grows with increasing P_e in the biodegradation-dominated part of the electron acceptor front, resulting in a steeper shape of this part of the front. Hence, a smaller BAZ is found.

Figure 3.6.c shows that increasing M_C results in a smaller value of C_r and a larger value of $P_{e(\text{eff})}$, because an increase of M_C results in a smaller traveling wave velocity, see equation (3.16). As a result, the biodegradation-dominated part becomes smaller and the electron acceptor front steepens for increasing M_C . Hence, a smaller BAZ is obtained.

Furthermore, Figure 3.6.d shows that an increase of M_G leads to a smaller value of C_r , but also a smaller value of $P_{e(\text{eff})}$, as an increase of M_G results in a larger traveling wave velocity, see equation (3.16). In the biodegradation-dominated part of the electron acceptor front a larger w is found. Hence, effectively w grows with increasing M_G in the biodegradation-dominated part, resulting in a steeper shape for this part of the front. This implies a decreasing BAZ. We conclude that increasing L_μ , M_C , M_G or P_e results in a smaller BAZ, whereas, increasing K_C or K_G results in a larger BAZ. A smaller BAZ implies a more efficient use of electron acceptor, thus increasing L_μ , M_C , M_G or P_e or decreasing K_C or K_G results in a better performance of the bioremediation technique.

When we apply the in-situ bioremediation technique at a specific contaminated site we may increase the contaminant removal rate, or decrease the BAZ or both, by varying one of the dimensionless numbers. At a specific site, we consider a particular set of contaminant, microbial mass and electron acceptor, for which the following biochemical parameters are fixed: the stoichiometric coefficients (m_c and m_e), the half saturation constants (k_c and k_g), and the specific growth rate (μ_m). Furthermore, the initially available contaminant concentration (g_0), microbial mass (m_0) and the considered contaminated aquifer length (L) are fixed field data. Thus the only parameters with which we can steer the operation are the injection velocity (v) and the injected electron acceptor concentration (c_0). This implies that we can vary L_μ , K_C and M_C , whereas the other dimensionless numbers are fixed, see (3.7). However, we can not increase the injection velocity to arbitrary high values because of physical limits and the concentration of injected electron acceptor is limited by the concentration at saturation. This concentration depends on the electron acceptor used, e.g. nitrate has a larger concentration at saturation than oxygen.

The increase of the injection velocity leads to a smaller Damkohler. A smaller L_μ implies a larger BAZ, see Figure 3.7, because a tailing in the biodegradation-dominated part of the electron acceptor front occurs. However,

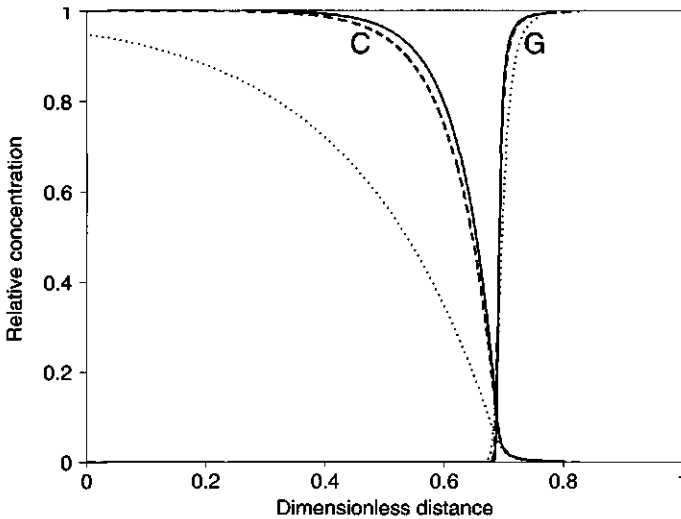


FIGURE 3.8. Relative electron acceptor and contaminant concentration front for different injected electron acceptor concentrations. (Solid line: $C_0 = 2.5$ mg/l, dashed line: $C_0 = 5.0$ mg/l, and dotted line: $C_0 = 50.0$ mg/l).

the increase of the injection velocity leads also to a higher dimensional contaminant removal rate, see equation (3.38).

The increase of the injected electron acceptor concentration leads to a smaller half saturation constant K_C and a smaller stoichiometric coefficient M_C . The resulting effects counteract because a smaller K_C implies a smaller BAZ, yet, a smaller M_C implies a larger BAZ. Figure 3.8 presents the electron acceptor and contaminant fronts for different values of c_0 . For larger values of c_0 (e.g., dotted line) a less steep front shape for the biodegradation-dominated part occurs. Hence, the negative effect of M_C dominates over the positive effect of K_C , resulting in a larger BAZ. This follows directly from equation (A5), where K_C is included in term $C/(K_C + C)$ and M_C in $M_G L_\mu / \alpha (= (M_G + M_C) L_\mu)$. Whatever value we choose for c_0 , the first term will always be between zero and one, whereas the other term will always be larger than one. Accordingly, the increase of c_0 influences the term $(M_G + M_C) L_\mu$ more strongly than the term $C/(K_C + C)$. However, the increase of c_0 leads also to a larger dimensionless traveling wave velocity and thus a higher contaminant removal rate, see equation (3.38).

We conclude that increasing the injection velocity or the injected electron acceptor concentration results in a higher contaminant removal rate

and a larger BAZ. A higher removal rate and a larger BAZ have counteracting effects on the performance of the bioremediation technique. A higher removal rate causes a faster clean up, whereas, a large BAZ indicates that a large part of the aquifer contains contaminant concentrations between the initial and zero concentration. Therefore, it can take a long time before the contaminant is completely removed by the micro-organisms even though the removal rate expresses differently. If we are interested only in the contaminant removal rate or the BAZ, respectively increasing or decreasing the injection velocity or the injected electron acceptor concentration results in an improvement of the bioremediation technique.

CONCLUSIONS

We investigated the performance of the in-situ bioremediation technique under simplifying assumptions. Because of these simplifying assumptions we can derive an analytical expression for the traveling wave velocity and a semi-analytical solution for the traveling wave front shape of the electron acceptor front. We showed that these solutions perfectly approximate the traveling wave behavior which was found in the numerical results. Furthermore, it is found that this traveling wave solution is valid for all combinations of dimensionless numbers, although in some situations it can take a long time (or traveled distance) before the solution is applicable.

Using the analytical traveling wave velocity and the semi-analytical solution for the front shape, we can determine the contaminant removal rate and the region where biodegradation occurs, the biologically active zone (BAZ). These two factors characterize the performance of the bioremediation technique. We showed that the contaminant removal rate is proportional to the traveling wave velocity. Thus a higher traveling wave velocity results in a faster clean up. The BAZ depends on the front shape of the electron acceptor, especially the biodegradation-dominated part of the electron acceptor concentration front. A tailing in the biodegradation-dominant part implies a large BAZ. A large part of the aquifer contains contaminant between initial and zero concentration. Therefore, it can take a long time before the aquifer is cleaned.

Furthermore, we assessed the influence of the different model parameters on the performance of the in-situ bioremediation technique. We showed that only the stoichiometric coefficients, M_C and M_G , influence the traveling wave velocity. Therefore, decreasing M_C or increasing M_G results in a higher contaminant removal rate. All dimensionless numbers influence the biodegradation-dominated part of the electron acceptor front and thus the BAZ. Increasing the Damkohler number, the stoichiometric coefficients

or the Peclet number, or decreasing the relative half saturation constants results in a smaller BAZ and thus in an improvement of the bioremediation technique.

To improve the performance of in-situ bioremediation at a specific contaminated site of fixed length, we can only vary the injection velocity or the injected electron acceptor concentration because all other physical and biochemical parameters are fixed. Increasing the injection velocity or the injected electron acceptor concentration results in a higher contaminant removal rate and a larger BAZ, which have counteracting effects on the performance of the bioremediation technique. A higher removal rate implies a faster clean-up, whereas, a larger BAZ indicates the total clean-up of the aquifer can last a long time.

Although the obtained traveling wave solution is based on a simplified biodegradation model, it is useful to predict the effect of physical and biochemical parameters on the performance of the in-situ bioremediation technique. Furthermore, it can give rough and quick estimations of the contaminant removal rate and the BAZ by simplifying the conditions at a real site. One can argue that we consider a one-dimensional homogeneous aquifer, whereas in practice, an aquifer is neither one-dimensional nor is the permeability of the aquifer constant. In fact, the permeability is space dependent and thus the assumption of homogeneity does not hold. If we envision an aquifer as an ensemble of one-dimensional streamtubes and each streamtube has different physical and biochemical soil properties (e.g. permeability, initially available contaminant) we can mimic a three-dimensional heterogeneous porous media. Using the stochastic-convective approach discussed by other researchers [7, 8, 10] we may consider field-scale results. This method is only applicable if the transverse dispersion is negligible.

NOTATION

c (C)	(Dimensionless) concentration electron acceptor [mg l^{-1}]
c_0	Feed concentration electron acceptor [mg l^{-1}]
C_{cons}	Amount of electron acceptor consumed [mg]
C_{inj}	Amount of injected electron acceptor [mg]
C_{pres}	Amount of electron acceptor present in domain [mg]
C_r	Critical electron acceptor concentration [mg l^{-1}]
D	Dispersion coefficient [$\text{m}^2 \text{day}^{-1}$]
g (G)	(Dimensionless) concentration organic contaminant [mg l^{-1}]
g_0	Initial concentration organic contaminant [mg l^{-1}]
G_C	Consumed contaminant concentration [mg l^{-1}]

$k_c (K_C)$	(Diml.) electron acceptor half saturation constant [mg l ⁻¹]
$k_g (K_G)$	(Diml.) contaminant half saturation constant [mg l ⁻¹]
L	Length of initial contaminated aquifer [m]
L_μ	Damkohler number
$m (M)$	(Dimensionless) concentration microbial mass [mg l ⁻¹]
m_0	Initial concentration microbial mass [mg l ⁻¹]
m_{\max}	Maximal concentration microbial mass [mg l ⁻¹]
$m_c (M_C)$	(Dimensionless) stoichiometric coefficient [mg mg ⁻¹]
$m_g (M_G)$	(Dimensionless) stoichiometric coefficient [mg mg ⁻¹]
M_{RG}	Dimensionless cumulative contaminant removal
M_1	First moment [m]
M_2^c	Second central moment [m ²]
n	Porosity
P_e	Peclet number
$r_g, (R_G)$	(Dimensionless) contaminant removal rate [mg day ⁻¹]
$t (T)$	(Dimensionless) time [day]
v	Flow velocity [m day ⁻¹]
$x (X)$	(Dimensionless) length [m]
α	Dimensionless traveling wave velocity
α_l	Dispersivity [m]
ϵ	Small number [mg l ⁻¹]
η	Moving coordinate
μ_m	Maximum specific growth rate [day ⁻¹]

APPENDIX A EVALUATION OF THE SINGLE FIRST ORDER DIFFERENTIAL EQUATION

To rewrite the system (3.17)-(3.19), we first integrate equation (3.19) using boundary conditions (3.20) and (3.21), which leads to the explicit relation between M and G

$$M = 1 - \frac{G}{M_G}. \quad (\text{A1})$$

Substitution of $dM/d\eta$ following from (3.19) in equation (3.17) and (3.18) yields

$$\frac{d^2C}{d\eta^2} = P_e(1 - \alpha)\frac{dC}{d\eta} + P_e\alpha\frac{M_C}{M_G}\frac{dG}{d\eta}, \quad (\text{A2})$$

$$\frac{dG}{d\eta} = \frac{M_G L_\mu}{\alpha} \left(\frac{C}{K_C + C} \right) \left(\frac{G}{K_G + G} \right) M. \quad (\text{A3})$$

Using definition (3.16) for the dimensionless traveling wave velocity and equation (A1), we obtain

$$\frac{d^2C}{d\eta^2} = P_e(1 - \alpha) \left[\frac{dC}{d\eta} + \frac{dG}{d\eta} \right], \quad (\text{A4})$$

$$\frac{dG}{d\eta} = \frac{M_G L_\mu}{\alpha} \left(\frac{C}{K_C + C} \right) \left(\frac{G}{K_G + G} \right) \left(1 - \frac{G}{M_G} \right). \quad (\text{A5})$$

Substitution of expression (A5) for $dG/d\eta$ in equation (A4) and using definition (3.23) for $w(C)$ gives equation (3.24). Furthermore, we derive an explicit relation between G , C and $w(C)$ by integrating equation (A4) from $\eta = -\infty$ to η and using the definition for $w(C)$, which yields equation (3.25).

APPENDIX B EVALUATION OF THE MASS BALANCE QUANTITIES

The total amount of electron acceptor injected into the domain at a specific time, T^* , is equal to the total influx of electron acceptor at the left boundary,

$$C_{\text{inj}}(T^*) = \int_0^{T^*} \text{flux}|_{X=0} dT = T^*, \quad (\text{B1})$$

where the flux is given by boundary condition (3.12). The amount of electron acceptor still present in the domain at T^* is given by

$$C_{\text{pres}}(T^*) = \int_0^{X^*} C(X, T^*) dX, \quad (\text{B2})$$

where X^* characterizes the length of the domain that still contains electron acceptor, defined by

$$C(X^*, T^*) = \epsilon \quad \text{and} \quad C(X, T^*) > \epsilon \quad \text{for} \quad X < X^*,$$

with ϵ a small number, say $\epsilon=0.001$. To derive C_{cons} , we define the consumed contaminant front, $G_C(X, T)$, which equals the initial available contaminant minus the contaminant still present

$$G_C(X, T) = 1 - G(X, T). \quad (\text{B3})$$

C_{cons} at T^* is related to G_C by the stoichiometric coefficients, M_C and M_G . M_C describes the amount of electron acceptor necessary to produce a certain amount of microbial mass, and M_G describes the amount of contaminant necessary to produce the same amount of microbial mass, therefore,

C_{cons} is given by

$$C_{\text{cons}}(T^*) = \frac{M_C}{M_G} \int_0^{X^*} G_C(X, T^*) dx = \frac{M_C}{M_G} \int_0^{X^*} (1 - G(X, T^*)) dX, \quad (\text{B4})$$

where X^* satisfies additionally

$$1 - G(X^*, T^*) \leq \epsilon \quad \text{and} \quad 1 - G(X, T^*) > \epsilon \quad \text{for} \quad X < X^*.$$

REFERENCES

- [1] Baveye, P. & A.J. Valocchi 1989. An evaluation of mathematical models of the transport of biologically reacting solutes in saturated soils and aquifers. *Water Resources Research* 25:1413-1421.
- [2] Bolt, G.H. 1982. in: *Soil Chemistry B. Physico-Chemical models*, eds. G.H. Bolt, Elsevier, New York, p.285.
- [3] Borden, R.C. & P.B. Bedient 1986. Transport of dissolved hydrocarbons influenced by oxygen-limited biodegradation 1. Theoretical development. *Water Resources Research* 22:1973-1982.
- [4] Bosma, W.J.P. & S.E.A.T.M. van der Zee 1993. Transport of reactive solute in a one-dimensional chemically heterogeneous porous medium. *Water Resources Research* 29:117-131.
- [5] Chen, Y., L.M. Abriola, P.J.J. Alvarez, P.J. Anid & T.M. Vogel 1992. Modeling transport and biodegradation of benzene and toluene in sandy aquifer material: Comparisons with experimental measurements. *Water Resources Research* 28:1833-1847.
- [6] Corapcioglu, M.Y. & S. Kim 1995. Modeling facilitated contaminant transport by mobile bacteria. *Water Resources Research* 31:2639-2647.
- [7] Cvetkovic, V.D. & A.M. Shapiro 1990. Mass arrival of sorptive solute in heterogeneous porous media. *Water Resources Research* 26:2057-2067.
- [8] Destouni, G. & V.D. Cvetkovic 1991. Field scale mass arrival of sorptive solute into the groundwater. *Water Resources Research* 27:1315-1325.
- [9] Ghiorse, W.C. & D.L. Balkwill 1983. Enumeration and morphological characterization of bacteria indigenous to subsurface environments. *Dev. Ind. Microb.* 24:213-224.
- [10] Ginn, T.R., C.S. Simmons & B.D. Wood 1995. Stochastic-convective transport with nonlinear reaction: Biodegradation with microbial growth. *Water Resources Research* 31:2689-2700.
- [11] Keijzer, H., S.E.A.T.M. van der Zee & A. Leijnse 1998. Characteristic regimes for in-situ bioremediation of aquifers by injecting water containing an electron acceptor. *Computational Geosciences* 2:1-22.
- [12] Kindred, J.S. & M.A. Celia 1989. Contaminant transport and biodegradation 2. Conceptual model and test simulations. *Water Resources Research* 25:1149-1159.
- [13] Kinzelbach, W., W. Schäfer & J. Herzer 1991. Numerical modeling of natural and enhanced denitrification processes in aquifers. *Water Resources Research* 27:1123-1135.
- [14] Monod, J. 1949. The growth of bacterial cultures. *Ann. Rev. of Microb.* 3:371-394.

- [15] Oya, S. & A.J. Valocchi 1997. Characterization of traveling waves and analytical estimation of pollutant removal in one-dimensional subsurface bioremediation modeling. *Water Resources Research* 33:1117-1127.
- [16] Oya, S. & A.J. Valocchi 1998. Analytical approximation of biodegradation rate for in situ bioremediation of groundwater under ideal radial flow conditions. *J. Cont. Hydrology* 31:65-83.
- [17] Reiniger, P. & G.H. Bolt 1972. Theory of chromatography and its application to cation exchange in soils. *Neth. J. Agric. Sci.* 20:301-313.
- [18] Schäfer, W. & W. Kinzelbach 1991. in: *In Situ Bioreclamation*, Numerical Investigation into the effect of aquifer heterogeneity on in situ bioremediation, eds. R.E. Hinchee and R.F. Olfenbuttel, Butterworth-Heinemann, London, p.196.
- [19] Semprini, L. & P.L. McCarty 1991. Comparison between model simulations and field results for in-situ bioremediation of chlorinated aliphatics: Part 1. Biostimulation of methanotrophic bacteria. *Ground Water* 29:365-374.
- [20] Stumm, W. & J.J. Morgan 1981. in: *Aquatic Chemistry*, John Wiley & Sons, New York, p.780.
- [21] Sturman, P.J., P.S. Stewart, A.B. Cunningham, E.J. Bouwer & J.H. Wolfram 1995. Engineering scale-up of in situ bioremediation process: a review. *J. Cont. Hydrology* 19:171-203.
- [22] Van der Zee, S.E.A.T.M. 1990. Analytical traveling wave solutions for transport with nonlinear and nonequilibrium adsorption. *Water Resources Research* 26:2563-2578. (Correction, 1991 *Water Resources Research* 27:983.)
- [23] van Duijn, C.J., P. Knabner & S.E.A.T.M. van der Zee 1993. Travelling waves during the transport of reactive solute in porous media: combination of Langmuir and Freundlich isotherms. *Adv. Water Resources* 16:97-105.
- [24] Xin, J. & D. Zhang 1998. Stochastic analysis of biodegradation fronts in one-dimensional heterogeneous porous media. *Adv. Water Resources* 22:103-116.
- [25] Zysset, A., F. Stauffer & T. Dracos 1994. Modeling of reactive groundwater transport governed by biodegradation. *Water Resources Research* 30:2423-2434.

Semi-analytical traveling wave solution of one-dimensional aquifer bioremediation*

H. Keijzer, R.J. Schotting and S.E.A.T.M. van der Zee

ABSTRACT

We consider a one-dimensional biodegradation model that describes transport and biodegradation of contaminant and electron acceptor and, moreover growth and decay of micro-organisms. We derive a semi-analytical solution for the contaminant, electron acceptor and microbial mass traveling wave fronts under the condition that the microbial decay rate is much smaller than the microbial growth rate. We compare the semi-analytical solution with the numerically determined traveling wave front of the complete biodegradation model and the closed form solution of a reduced biodegradation model derived by Xin and Zhang. We show that the semi-analytical solution describes the complete biodegradation model almost perfectly. Even under nutrient-deficient conditions, the semi-analytical solution is a better approximation than the closed form solution of Xin and Zhang.

*Communications on Applied Nonlinear Analysis 2000, 7, 1-20

INTRODUCTION

Bioremediation is one of the promising techniques to remove degradable organic contaminants from the subsurface. Micro-organisms present in the subsurface can either aerobically or anaerobically biodegrade these contaminants if either electron acceptors or electron donors and nutrients are sufficiently available. If all these compounds are simultaneously present, a biological active zone [6, 10, 11] is formed where biodegradation occurs. In most cases, biodegradation is limited because one of the necessary compounds is scarce under natural conditions. If these compounds are injected into an aquifer to enhance biodegradation, we call this 'in situ bioremediation'. Even if compounds are injected, biodegradation can still be limited by other factors, e.g. heterogeneity of the soil, which can prevent mixing between the compounds.

Research concerning in situ bioremediation is carried out both through experiments and model simulations. These experiments [16] and models [5, 6, 10, 11, 17] show that after an initial start up period, contaminant, electron acceptor and microbial mass fronts move with constant velocity and constant front shapes through the aquifer. This behavior is known as the traveling wave behavior. The traveling wave behavior also occurs for other non-linear reactions, e.g. ion exchange and non-linear adsorption [1, 2, 12, 14, 15], and (semi-)analytical expressions for the traveling wave velocity and front shapes are found. If biodegradation is included as a non-linear sink term in the convection-dispersion transport equation for contaminant and electron acceptor, (semi-)analytical solutions for the developed traveling wave front shapes can be derived, as is shown by Oya and Valocchi [10, 11], Xin and Zhang [17] and Keijzer et al. [6]. They analyze slightly different conceptual models, because different assumptions are made.

The model of Oya and Valocchi [10] includes transport and biodegradation of contaminant and electron acceptor, microbial growth and first-order microbial decay. Oya and Valocchi derive expressions for the traveling wave velocity and the long-term biodegradation rate, using a plug flow approximation to represent the contaminant and electron acceptor fronts. The influence of front shapes is not included and expressions for the developed traveling front shapes are not derived. Xin and Zhang [17] reduce the model of Oya and Valocchi to a two component model, assuming nutrient-deficient conditions (K_C and K_G large compared with C_0 and G_0) and/or a microbial growth rate smaller than the microbial decay rate. Furthermore, they neglect dispersion in their paper, which enable them to derive closed form solutions for the traveling wave front shapes. Keijzer et al. [6] reduce

the model of Oya and Valocchi considering an immobile contaminant and neglecting microbial decay, assuming a microbial decay rate much smaller than the microbial growth rate. They determine a semi-analytical solution for traveling wave front shapes.

In this paper, we derive a semi-analytical solution for the model of Oya and Valocchi under the condition that the microbial decay rate is much smaller than the microbial growth rate. We compare the semi-analytical solution with numerical results of Oya and Valocchi's model. Considering nutrient-deficient conditions, we compare the semi-analytical traveling wave solution with the closed form solution of Xin and Zhang and the numerical results of the complete model.

MODEL FORMULATION

Consider steady-state flow in a one-dimensional saturated and homogeneous aquifer. In this aquifer, biodegradation occurs if contaminant, either electron acceptor or electron donor and micro-organisms are simultaneously present. Several simplifying assumptions are made [10]. We consider a mobile and reversible linearly-sorbing contaminant. The sorption/desorption process is represented by a constant retardation factor R . For brevity, we consider aerobic degradation but the concept is also applicable to anaerobic degradation. Thus an electron acceptor is considered and assumed to be a mobile non-sorbing compound, e.g. oxygen or nitrate. Moreover, we consider an immobile microbial mass assuming that it forms biofilms covering soil particles [3, 4, 13]. Research [7, 9] suggests that micro-organisms can only use contaminant and electron acceptor that are present in the aqueous phase for their growth. Microbial growth is modeled by Monod kinetics [8] and microbial decay by a first order sink term.

These assumptions lead to a system of second order partial differential equations (2nd order PDE) for the electron acceptor C , contaminant G and microbial mass M given (in dimensionless form) by

$$\frac{\partial C}{\partial T} = \frac{1}{P_e} \frac{\partial^2 C}{\partial X^2} - \frac{\partial C}{\partial X} - M_C L_\mu \left(\frac{C}{K_C + C} \right) \left(\frac{G}{K_G + G} \right) M, \quad (4.1)$$

$$R \frac{\partial G}{\partial T} = \frac{1}{P_e} \frac{\partial^2 G}{\partial X^2} - \frac{\partial G}{\partial X} - M_G L_\mu \left(\frac{C}{K_C + C} \right) \left(\frac{G}{K_G + G} \right) M, \quad (4.2)$$

$$\frac{\partial M}{\partial T} = L_\mu \left(\frac{C}{K_C + C} \right) \left(\frac{G}{K_G + G} \right) M - L_d (M - 1), \quad (4.3)$$

where P_e is the Peclet number, L_μ is the Damkohler number and L_d the decay number, which describe the ratios of advection rate over dispersion rate, of growth rate over advection rate and decay rate over advection

rate, respectively. The relative stoichiometric parameters M_C and M_G describe, respectively, the ratios of consumed electron acceptor and organic contaminant to newly formed micro-organisms. K_C and K_G are the relative dissolved electron acceptor and organic contaminant half saturation constants.

We consider initially a contaminant and microbial mass homogeneously distributed over the subsurface. Initially the electron acceptor concentration is the limiting factor for biodegradation and is equal to zero. We inject the electron acceptor to enhance biodegradation by imposing a prescribed mass flux at the inlet of the domain, whereas obviously no contaminant is injected. At the outlet of the domain we assume a purely advective mass flux for both the contaminant and electron acceptor. The resulting dimensionless initial and boundary conditions are

$$C = 0, \quad G = 1, \quad M = 1 \quad \text{for } X \geq 0 \quad \text{at } T = 0, \quad (4.4)$$

$$-\frac{1}{P_e} \frac{\partial C}{\partial X} + C = 1, \quad -\frac{1}{P_e} \frac{\partial G}{\partial X} + G = 0 \quad \text{for } T > 0 \quad \text{at } X = 0, \quad (4.5)$$

$$\frac{\partial C}{\partial X} = 0, \quad \frac{\partial G}{\partial X} = 0 \quad \text{for } T > 0 \quad \text{at } X = 1. \quad (4.6)$$

Numerical results of biodegradation models [5, 6, 10, 11] have revealed traveling wave behavior. This behavior implies that contaminant, electron acceptor and microbial mass fronts move with constant velocity and constant front shapes through the aquifer. This is caused by counteracting effects of dispersion and biodegradation. Dispersion results in a spreading of the fronts, while biodegradation results in a steepening of the front. Traveling wave behavior results if the two effects balance.

SEMI-ANALYTICAL TRAVELING WAVE SOLUTION

We derive a semi-analytical solution for the developed traveling wave fronts under the condition that the microbial decay rate is small compared to the microbial growth rate ($L_d \ll L_\mu$). In this derivation, the 2nd order PDE system (4.1)-(4.3) is transformed into a system of second order ordinary differential equations (2nd order ODE). The resulting system is solved using Newton's method. To determine the front position, we consider mass balances for the contaminant and electron acceptor and the semi-analytically derived front shapes.

Front shape

As a first step, the 2nd order PDE system (4.1)-(4.3) is transformed to a moving coordinate system

$$\eta = X - \alpha T, \quad (4.7)$$

where α denotes the traveling wave velocity, yielding

$$\frac{d^2 C}{d\eta^2} = P_e(1 - \alpha) \frac{dC}{d\eta} - P_e \alpha M_C \frac{dM}{d\eta}, \quad (4.8)$$

$$\frac{d^2 G}{d\eta^2} = P_e(1 - R\alpha) \frac{dG}{d\eta} - P_e \alpha M_G \frac{dM}{d\eta}, \quad (4.9)$$

$$\frac{dM}{d\eta} = -\frac{L_\mu}{\alpha} \left(\frac{C}{K_C + C} \right) \left(\frac{G}{K_G + G} \right) M. \quad (4.10)$$

Note that the second term on the right-hand side of equation (4.3) has vanished in equation (4.10) because of the assumption $L_d \ll L_\mu$. Using equations (4.8)-(4.10), we obtain an expression for the traveling wave velocity [6, 10] (see Appendix A for a derivation)

$$\alpha = \left(\frac{1 + \frac{M_C}{M_G}}{1 + R \frac{M_C}{M_G}} \right). \quad (4.11)$$

We assume that the traveling wave solution is already a good approximation after a relatively short time so that the following boundary conditions can be used for the transformed problem [10, 14]

$$C(-\infty) = 1, \quad G(-\infty) = 0, \quad M(-\infty) = M_{max}, \quad (4.12)$$

$$C(\infty) = 0, \quad G(\infty) = 1, \quad M(\infty) = 1, \quad (4.13)$$

where M_{max} is the maximal microbial mass. Although we neglect microbial decay, the microbial mass does not grow without bounds because the microbial growth is limited by the availability of contaminant and electron acceptor. An expression can be derived for the maximal microbial mass, using the transformed equations (4.8)-(4.10) (see again Appendix A)

$$M_{max} = \frac{1 - \alpha}{\alpha M_C} + 1. \quad (4.14)$$

It follows from conditions (4.12) and (4.13), that also the following conditions hold

$$\frac{dC}{d\eta} = 0, \quad \frac{dG}{d\eta} = 0, \quad \frac{dM}{d\eta} = 0 \quad \text{at} \quad \eta = -\infty, \infty. \quad (4.15)$$

Rather than solving the 2nd order ODE system (4.8)-(4.10) on the infinite domain for η , we search for a solution for the functions u and v on

a finite domain for C ($C \in [0, 1]$). The functions $u(C)$ and $v(C)$ are defined by

$$u = -\frac{dC}{d\eta}, \quad (4.16)$$

$$v = \frac{dG}{d\eta}. \quad (4.17)$$

Substitution of (4.16)-(4.17) in equation (4.8)-(4.10) yields a 1st order ODE system

$$u' = -P_e(1 - \alpha) + P_e M_C \frac{F}{u}, \quad (4.18)$$

$$v' = -P_e(1 - R\alpha) \frac{v}{u} - P_e M_G \frac{F}{u}, \quad (4.19)$$

$$\frac{dM}{d\eta} = -\frac{F}{\alpha}, \quad (4.20)$$

where primes ' denotes differentiation with respect to C , and F is defined as

$$F = L_\mu \left(\frac{C}{K_C + C} \right) \left(\frac{G}{K_G + G} \right) M. \quad (4.21)$$

The boundary conditions for this 1st order ODE system follow from equation (4.15)

$$u(0) = 0 \quad \text{and} \quad v(0) = 0. \quad (4.22)$$

In order to obtain an ODE system that depends only on C , u and v , we derive explicit expressions for M and G in terms of C , u and v (see Appendix A)

$$M = \frac{u + P_e(1 - \alpha)(C - 1)}{P_e \alpha M_C} + M_{max}, \quad (4.23)$$

and

$$G = \frac{-u - P_e(1 - \alpha)(C - 1) - \frac{M_C}{M_G} v}{P_e(1 - \alpha)}. \quad (4.24)$$

These explicit expressions for M and G are substituted in the first order system (4.18)-(4.20). The result is

$$u' = -P_e(1 - \alpha) + \frac{L_\mu \bar{F}}{\alpha u}, \quad (4.25)$$

$$v' = \frac{P_e(1-\alpha)M_G v}{M_C} u - \frac{L_\mu M_G \bar{F}}{\alpha M_C} u, \quad (4.26)$$

$$\frac{dM}{d\eta} = -\frac{L_\mu}{P_e \alpha^2 M_C} \bar{F}, \quad (4.27)$$

where

$$\begin{aligned} \bar{F} = & \left(\frac{C}{K_G + C} \right) \times \\ & \left(\frac{-u - P_e(1-\alpha)(C-1) - \frac{M_G v}{M_C}}{K_G P_e(1-\alpha) - u - P_e(1-\alpha)(C-1) - \frac{M_G v}{M_C}} \right) \times \\ & (u + P_e(1-\alpha)(C-1) + P_e \alpha M_C M_{max}). \end{aligned} \quad (4.28)$$

We differentiate equation (4.25) and (4.26) with respect to C , yielding the 2nd order ODE system

$$uu'' + u'^2 = -P_e(1-\alpha)u' + \frac{L_\mu}{\alpha} \bar{F}, \quad (4.29)$$

$$uv'' + u'v' = \frac{P_e(1-\alpha)M_G}{M_C} v' - \frac{L_\mu M_G}{\alpha M_C} \bar{F}, \quad (4.30)$$

with

$$\bar{F} = \frac{d\bar{F}}{dC}, \quad (4.31)$$

subject to boundary conditions for u and v for $C = 0$ and $C = 1$ (see (4.15))

$$u(0) = v(0) = 0 \quad \text{and} \quad u(1) = v(1) = 0. \quad (4.32)$$

The numerical procedure to solve this 2nd order ODE system (4.29) and (4.30) subject to boundary conditions (4.32) is based on Newton's method. See Appendix B for details. Using this procedure, we find u and v as functions of C . To determine the front shape $C(\eta)$, we integrate relation (4.16) numerically from a reference point $\eta = \eta_r$, where we may choose arbitrarily $C = 0.5$ [14]

$$\eta - \eta_r = - \int_{0.5}^C \frac{1}{u(C)} dC \quad \text{for} \quad 0 \leq C \leq 1. \quad (4.33)$$

The front shapes for $G(\eta)$ and $M(\eta)$ are found by substitution of $C(\eta)$, $u(C)$ and $v(c)$ in equation (4.24) and (4.23).

Front position

The front shape is given with respect to an arbitrary reference point, see equation (4.33). We determine this point using mass balance considerations. To this end, a large domain (with length L) is considered to prevent the electron acceptor from reaching the outlet. Therefore the amount of electron acceptor injected into the domain, C_{inj} , is equal to the amount of electron acceptor still present in the domain, C_{pres} , plus the amount of electron acceptor consumed by the micro-organisms, C_{cons} . Hence, the mass balance equation for C is given by

$$C_{inj} = C_{pres} + C_{cons}. \quad (4.34)$$

Here, C_{cons} is related to the amount of contaminant consumed G_{cons} by the relative stoichiometric coefficients, M_C and M_G . M_C describes the amount of electron acceptor necessary to produce a certain amount of microbial mass, and M_G describes the amount of contaminant necessary to produce the same amount of microbial mass.

G_{cons} is equal to the amount of contaminant initially available, G_{init} , minus the amount of contaminant still present in the domain, G_{pres} , minus the amount of contaminant flushed out of the domain, G_{out} . Hence, the mass balance for G is given by

$$G_{cons} = G_{init} - G_{pres} - G_{out}. \quad (4.35)$$

Substitution of the mass balance equation for G in equation (4.34) yields

$$C_{inj} = C_{pres} + \frac{M_C}{M_G}(G_{init} - G_{pres} - G_{out}). \quad (4.36)$$

Expressions for the quantities in equation (4.36) can be derived, using the dimensionless equations (4.1)-(4.2) and boundary conditions (4.5)-(4.4) in the original coordinate system.

The amount of electron acceptor injected into the domain at a specific time, T^* , is equal to the total influx of electron acceptor at the inlet boundary

$$C_{inj}(T^*) = n \int_0^{T^*} J_c(0) dT = nT^*, \quad (4.37)$$

where n is the porosity and $J_c(0)$ is the boundary condition (4.5). The amount of electron acceptor still present in the domain at T^* is given by

$$C_{pres}(T^*) = n \int_0^L C(X, T^*) dX. \quad (4.38)$$

The amount of contaminant present in the domain at T^* is

$$\begin{aligned} G_{\text{pres}}(T^*) &= n \int_0^L RG(X, T^*)dX \\ &= n \int_0^L RG(X, 0)dX - n \int_0^L [R(G(X, 0) - G(X, T^*))] dX \\ &= nRL - nR \int_0^L [1 - G(X, T^*)]dX, \end{aligned} \quad (4.39)$$

where R is included because we consider the adsorbed contaminant as well as the contaminant in the water phase. The amount of contaminant initially available is given by

$$G_{\text{init}} = n \int_0^L RG(X, 0) dX = nRL. \quad (4.40)$$

Finally, the amount of contaminant flushed out of the domain at a T^* is equal to

$$G_{\text{out}} = n \int_0^{T^*} G(L, T)dT = nT^*, \quad (4.41)$$

because the contaminant concentration at the outlet of the domain is equal to $G(L, T) = 1$ for all T , since we consider a sufficiently large domain.

Substitution of the quantities (4.37)-(4.41) in equation (4.36) gives

$$T^*(1 + \frac{M_C}{M_G}) = \int_0^L C(X, T^*)dX + \frac{M_C}{M_G}R \int_0^L 1 - G(X, T^*)dX. \quad (4.42)$$

Here, X^* is defined as the length of the domain that still contains electron acceptor, but where the relative contaminant concentration is less than one

$$\begin{aligned} C(X, T^*) &\leq \epsilon && \text{for} && X > X^*, \\ 1 - G(X, T^*) &\leq \epsilon && \text{for} && X > X^*, \end{aligned}$$

with ϵ a small number, say $\epsilon=0.001$. Using the definition for X^* , one can recast equation (4.42) into

$$T^*(1 + \frac{M_C}{M_G}) = \int_0^{X^*} C(X, T^*)dX + \frac{M_C}{M_G}R \int_0^{X^*} 1 - G(X, T^*)dX, \quad (4.43)$$

with X^* the only unknown. To determine X^* , we use the traveling wave solutions for C and G , denoted by C_{TW} and G_{TW} respectively, as derived previously. We define $\eta^* = X^* - \alpha T^*$, such that $C_{TW}(\eta^*) = \epsilon$, and $\eta_* =$

$-\alpha T^*$. Hence, solving equation (4.43) for X^* is equivalent to finding $\eta^* - \eta_*$ from

$$T^* \left(1 + \frac{M_C}{M_G}\right) = \int_{\eta_*}^{\eta^*} C_{TW}(\eta) d\eta + \frac{M_C}{M_G} R \int_{\eta_*}^{\eta^*} (1 - G_{TW}(\eta)) d\eta. \quad (4.44)$$

To achieve this, we use equation (4.33) to write η_r in terms of η^*

$$\eta^* - \eta_r = - \int_{1/2}^c \frac{1}{u(C)} dC. \quad (4.45)$$

When X^* is found, η_r follows from (4.45) using the definition of η^* , which determines the traveling wave front $C(X, T^*)$ completely.

Applicability of the semi-analytical solution

In the derivation of the traveling wave front shapes, we used definitions for u and v , respectively (4.16) and (4.17). The variables u and v will be larger or equal to zero for all C values, because the electron acceptor front is monotonically decreasing and the contaminant front is monotonically increasing, while both are bounded, see boundary conditions (4.12) and (4.13). Combining the boundary conditions of u and v (4.32) with the constraint that u and v are larger or equal to zero, we obtain the following conditions for the derivatives of u and v with respect to C for $C = 0$ and $C = 1$

$$u'(0) \geq 0, \quad u'(1) \leq 0, \quad (4.46)$$

$$v'(0) \geq 0, \quad v'(1) \leq 0. \quad (4.47)$$

These conditions result in restrictions for the model parameters, see Appendix C

$$\frac{L_\mu}{P_e K_C (K_G + 1)} < \frac{(1 + \frac{M_C}{M_G})(R - 1)^2}{M_C (1 + R \frac{M_C}{M_G})^2}, \quad (4.48)$$

and

$$\frac{L_\mu}{P_e K_G (K_C + 1)} < \frac{M_C (R - 1)^2 (1 + \frac{M_C}{M_G})^2}{M_G (1 + R \frac{M_C}{M_G})^2 (R - 1 + M_C + M_G)}. \quad (4.49)$$

On the left-hand side we find the Damkohler number divided by the Peclet number. In general the Peclet number is much larger than the Damkohler number which results in a small term on the left-hand side of (4.48) and (4.49). Only when either K_C or K_G are small, the term on the left-hand side might become large. In that case the traveling wave fronts are very steep and a plug flow approximation can be applied [6, 10].

TABLE 4.1. Input dimensionless numbers in first simulation.

Dimensionless number	Data
P_e	2000.0
L_μ	30.0
L_d	7.0
M_C	0.128
M_G	0.085
K_C	0.1
K_G	0.1
R	3.0

RESULTS

To establish whether the semi-analytical solution provides a good approximation for the traveling wave behavior of the original model (4.1)-(4.3), we perform numerical simulations and compare the results with the semi-analytical solutions. The numerical method described by Keijzer et al. [5] in which microbial decay is incorporated is applied. The transport part of the equations is solved using a Galerkin-finite element method, while the biodegradation reaction part is solved using an implicit Euler method. The two parts are solved using Picard iterations. In the simulation the following parameter values are used. The porosity is $n = 0.4$ and the dimensionless length of the domain is $L = 1$. The values of the other (dimensionless) numbers are given in Table 4.1. The discretisation and time step are chosen such that the grid Peclet and Courant conditions are fulfilled to avoid numerical dispersion and numerical instabilities. The semi-analytical and numerical results are shown in their dimensionless form.

Figure 4.1 shows the semi-analytically and numerically obtained electron acceptor, contaminant and microbial mass fronts. The semi-analytical fronts for electron acceptor and contaminant approximate the numerical fronts almost perfectly. The semi-analytically and numerically obtained microbial mass fronts show some difference. Specially the part of the front where the contaminant becomes the limiting factor in the microbial growth and the microbial decay start to play a role. As a result, microbial mass grows to a lower value in the numerical results than in the semi-analytical solution. When the contaminant is completely biodegraded only microbial decay occurs and the microbial front shows an exponential decrease. If we decrease microbial decay rate even more, the contaminant and electron front approximate the numerical fronts even better (not shown). Thus, if

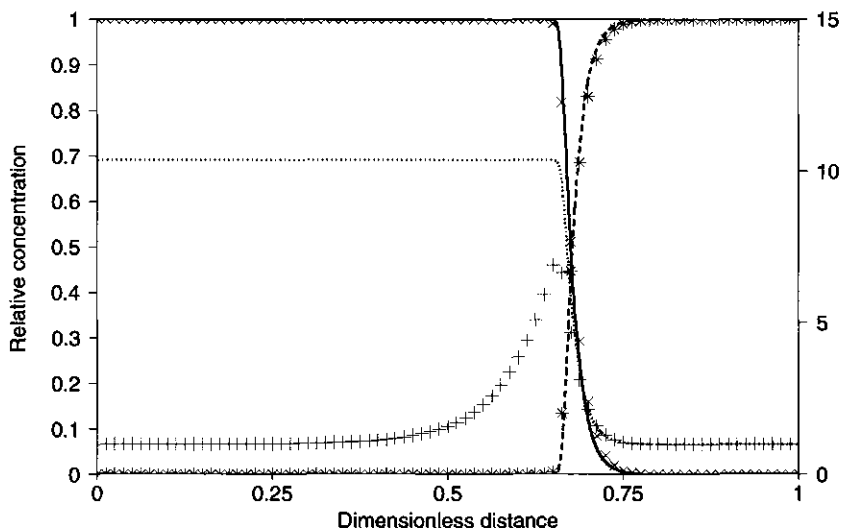


FIGURE 4.1. Dimensionless fronts resulting from semi-analytical and numerical solutions. Semi-analytical and numerical front for electron acceptor: solid line and \times , contaminant: dotted line and $*$, and microbial mass: dashed line and $+$ (right y axis).

microbial decay can be neglected, we can use the semi-analytical solution to approximate the contaminant and electron acceptor front.

Xin and Zhang [17] reduce original model (4.1)-(4.3) to a two component model, assuming nutrient-deficient conditions and/or a microbial growth rate smaller than the decay rate. In case of nutrient-deficient conditions, they derive a closed form solution for the traveling fronts. Using our semi-analytical solution, we can also determine the traveling wave fronts under nutrient-deficient conditions ($K_C \gg 1$ and $K_G \gg 1$). We compare the semi-analytical solution with the closed form solution of Xin and Zhang and the numerical solution of our original model. To fulfill the conditions made by Xin and Zhang, the dimensionless parameter values are used as given in Table 4.2.

Figure 4.2 shows the electron acceptor and contaminant front obtained, using the semi-analytical solution, Xin and Zhang's closed form solution and the numerical solution of the original model. The semi-analytical solution is a better approximation for the traveling wave fronts of the original model than the closed form solution of Xin and Zhang. This is expected since Xin and Zhang neglect the terms $K_C C$, $K_G C$ and CG in the denominator of the Monod terms (equation (4.3)) because these term are much smaller than the

TABLE 4.2. Input dimensionless numbers in second simulation.

Dimensionless number	Data
P_e	4000.0
L_μ	100.0
L_d	7.0
M_C	1.708
M_G	0.854
K_C	3.16
K_G	3.16
R	1.5

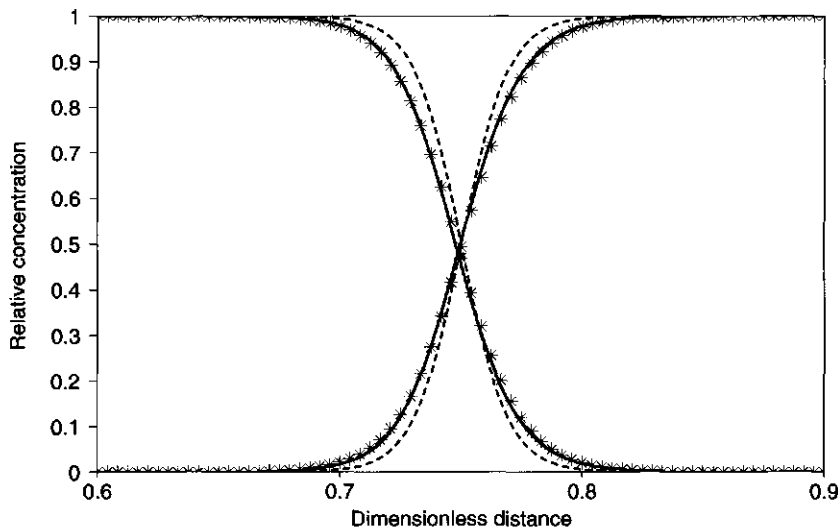


FIGURE 4.2. Dimensionless electron acceptor and contaminant fronts resulting from semi-analytical solution (solid lines), closed form solution of Xin and Zhang [17] (dashed lines) and numerical method (symbols).

term $K_C K_G$. In our model we only neglect microbial decay. As we already showed, this hardly influences the electron acceptor and contaminant front.

SUMMARY

In this study, we have considered a conceptual model which describes transport and biodegradation by two advection-dispersion-reaction equations for contaminant and electron acceptor, and one equation for the microbial mass, which includes microbial growth and microbial decay. We

derived an analytical expression for the traveling wave velocity and a semi-analytical solution for the developed contaminant, electron acceptor and microbial mass traveling wave fronts. We compared the semi-analytically obtained traveling wave fronts with fronts obtained from a numerical model developed by Keijzer et al. [5] for the original system, see equations (4.1)-(4.3). The semi-analytical solution of the contaminant and electron acceptor approximate the traveling wave fronts almost perfectly.

Xin and Zhang [17] reduced the original model in order to derive a closed form solution for the traveling wave fronts. If we compare the semi-analytical solution with the closed form solution of Xin and Zhang and the numerically obtained fronts for the original model, the semi-analytically solution approximate the numerically obtained traveling wave fronts better than the closed form solution of Xin and Zhang. We conclude that although Xin and Zhang derive a closed form solution, the semi-analytical solution presented in this paper is more applicable because less restrictive assumptions are made.

APPENDIX A

Determination of α , M_{max} , M and G

In this appendix different properties of the traveling wave solution are determined in more detail. First of all, we determine the traveling wave velocity (α), secondly the maximal microbial mass (M_{max}) and finally we determine M and G as functions of C , u and v .

To calculate the traveling front velocity, we combine equation (4.8) and (4.9)

$$\frac{d^2C}{d\eta^2} - P_e(1 - \alpha)\frac{dC}{d\eta} = \frac{M_C}{M_G} \left(\frac{d^2G}{d\eta^2} - P_e(1 - \alpha R)\frac{dG}{d\eta} \right). \quad (A1)$$

Integration from $\eta = -\infty$ to η leads to

$$\frac{dC}{d\eta} - P_e(1 - \alpha)[C - 1] = \frac{M_C}{M_G} \left(\frac{dG}{d\eta} - P_e(1 - \alpha R)G \right). \quad (A2)$$

Using the conditions at $\eta = \infty$, we obtain the expression for the traveling wave velocity (4.11).

To obtain M_{max} , we integrate equation (4.8) from $\eta = -\infty$ to η , yielding

$$\frac{dC}{d\eta} - P_e(1 - \alpha)[C - 1] + P_e\alpha M_C[M - M_{max}] = 0. \quad (A3)$$

Using the conditions at $\eta = \infty$, we obtain

$$P_e(1 - \alpha) + P_e\alpha M_C[1 - M_{max}] = 0, \quad (A4)$$

which results in equation (4.14).

To determine M as a function of C we use the definition of u (equation (4.16)) in equation (A3), yielding

$$u = -P_e(1 - \alpha)[C - 1] + P_e\alpha M_C[M - M_{max}]. \quad (\text{A5})$$

Hence, an explicit relation (4.23) between M , C and u is found. Note that, when $C \downarrow 0$ then $M \downarrow 1$ and when $C \uparrow 1$ then $M \uparrow M_{max}$. To obtain G as function of C , we use the definition of u and v (respectively, equation (4.16) and (4.17)) in equation (A2), which yields

$$-u - P_e(1 - \alpha)[C - 1] = \frac{M_C}{M_G}(v - P_e(1 - \alpha R)G), \quad (\text{A6})$$

and relation (4.24) is determined. Note that, when $C \downarrow 0$ then $G \uparrow 1$, when $C \uparrow 1$ then $G \downarrow 0$.

APPENDIX B

Numerical procedure

The second order ODE system (4.29)-(4.30) involves non-linear second order ordinary differential equations for u and v . Therefore, the computation of u and v as function of C requires an iterative procedure to converge to the solution.

Figure 4.3 illustrates the flow chart of the numerical procedure. At the first iteration step, we start with initial guesses for u and v which fulfill the boundary conditions of the system. When solving equation (4.29) for u , we substitute the initial guess for v and we apply Newton's method which results in an approximated solution for u . In turn, the computed u is used for computing v from equation (4.30) applying Newton's method again. We check whether the difference between the approximated solution and initial guesses of u and v are within a specified error interval. If the difference is unacceptable, the next iteration is performed after replacing the initial u and v with the improved solution.

APPENDIX C

Restrictions

We analytically determine the derivative of u and v with respect to C for $C = 0$, using equation (4.21). We consider the limit of $C \downarrow 0$, hence $G \uparrow 1$ and $M \downarrow 1$, and apply l'Hopital's rule. First we evaluate the limit

$$\lim_{C \downarrow 0, G \uparrow 1, M \downarrow 1} \frac{F}{u} = \lim_{C \downarrow 0, G \uparrow 1, M \downarrow 1} \frac{L_\mu \left(\frac{C}{K_C + C} \right) \left(\frac{G}{K_G + G} \right) M}{u}$$

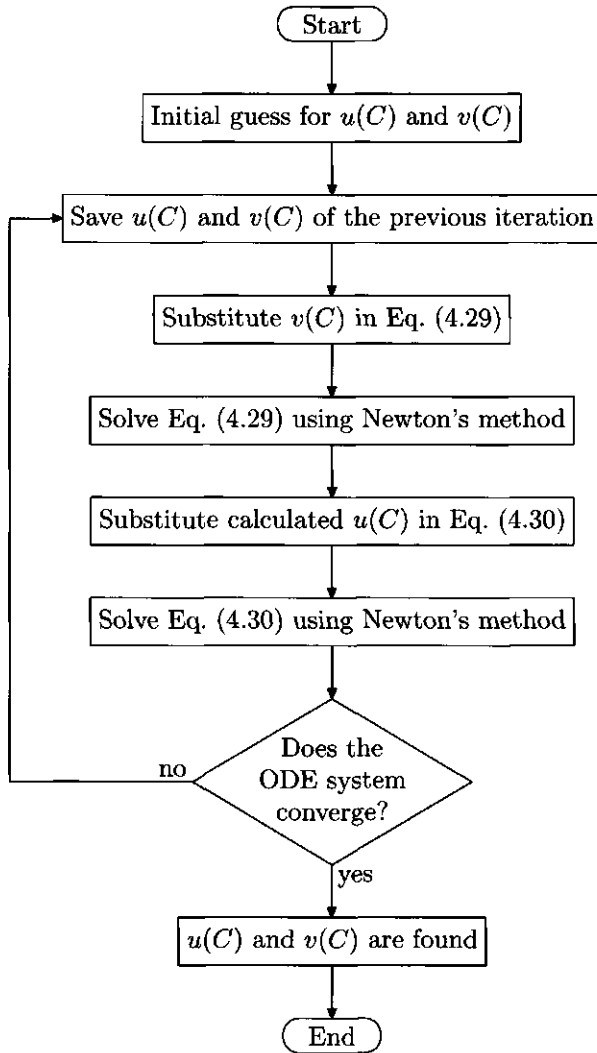


FIGURE 4.3. Flow chart of the numerical procedure.

$$\begin{aligned}
 &= \lim_{C \downarrow 0, G \uparrow 1, M \downarrow 1} \frac{L_\mu \left(\frac{C}{K_C + C} \right) \left(\frac{1}{K_G + 1} \right)}{u} \\
 &= \frac{L_\mu}{K_C} \frac{1}{K_G + 1} \frac{1}{u}.
 \end{aligned} \tag{C1}$$

Next, substitution of (C1) in equation (4.25) and (4.26) yields

$$(u')^2 + P_e(1 - \alpha)u' - P_e M_C \frac{L_\mu}{K_C} \frac{1}{K_G + 1} = 0, \quad (\text{C2})$$

$$u'v' + P_e(1 - R\alpha)v' + P_e M_G \frac{L_\mu}{K_C} \frac{1}{K_G + 1} = 0. \quad (\text{C3})$$

According to equation (C2), $u'(0)$ is given by

$$u'(0) = -\frac{P_e}{2}(1 - \alpha) \pm \frac{1}{2} \sqrt{(P_e(1 - \alpha))^2 + 4P_e M_C \left(\frac{L_\mu}{K_C}\right) \left(\frac{1}{K_G + 1}\right)}. \quad (\text{C4})$$

The sign must be positive to satisfy $u'(0) \geq 0$. Furthermore, according to equation (C3), $v'(0)$ is

$$v'(0) = \frac{P_e M_G \frac{L_\mu}{K_C} \frac{1}{K_G + 1}}{P_e(R\alpha - 1) - u'(0)}. \quad (\text{C5})$$

To satisfy $v'(0) \geq 0$, we obtain restriction (4.48) for the model parameters.

To determine the derivative of u and v with respect to C for $C = 1$, we consider the limit for $C \uparrow 1$, hence $G \downarrow 0$ and $M \uparrow M_{max}$, and apply again l'Hopital's rule. First we evaluate the limit

$$\begin{aligned} \lim_{C \uparrow 1, G \downarrow 0, M \uparrow M_{max}} \frac{F}{u} &= \lim_{C \uparrow 1, G \downarrow 0, M \uparrow M_{max}} \frac{L_\mu \left(\frac{C}{K_C + C}\right) \left(\frac{G}{K_G + G}\right) M}{u} \\ &= \lim_{C \uparrow 1, G \downarrow 0, M \uparrow M_{max}} \frac{L_\mu \left(\frac{1}{K_C + 1}\right) M_{max} \left(\frac{G}{K_G + G}\right)}{u} \\ &= \frac{L_\mu}{K_G} \frac{M_{max}}{K_C + 1} \lim_{G \rightarrow 0} \frac{G}{u}. \end{aligned} \quad (\text{C6})$$

Next, substitution of equation (4.24) and applying l'Hopital's rule yields

$$\lim_{C \uparrow 1, G \downarrow 0, M \uparrow M_{max}} \frac{F}{u} = \frac{L_\mu}{K_G} \frac{M_{max}}{K_C + 1} * \left[-\frac{1}{P_e(1 - \alpha)} - \frac{1}{u'} - \frac{M_C}{M_G P_e(1 - \alpha)} \frac{v'}{u'} \right]. \quad (\text{C7})$$

Multiplying equation (4.25) by M_G and equation (4.26) by M_C and adding the results, we obtain an explicit equation for $v'(1)$ in terms of $u'(1)$ only

$$v'(1) = \frac{u'(1)^2 + P_e(1 - \alpha)u'(1)}{P_e(1 - \alpha) - \frac{M_C}{M_G} u'(1)}. \quad (\text{C8})$$

Substituting (C7) and hereafter (C8) in equation (4.25), we obtain a third order equation in terms of u' :

$$\begin{aligned} u'^3 &+ \left[\frac{M_C}{M_G} P_e(1-\alpha) - P_e(1-\alpha) \right] u'^2 \\ &+ \left[\frac{M_C}{M_G} P_e^2(1-\alpha)^2 + M_G P_e A \right] u' + M_G P_e^2(1-\alpha) A = 0, \\ (u' + P_e(1-\alpha)) &(-u'^2 + \frac{M_C}{M_G} P_e(1-\alpha) u' + M_G P_e A) = 0, \end{aligned} \quad (C9)$$

where $A = \frac{L_\mu}{K_G} \frac{M_{max}}{K_C+1}$. The solution of this equation is

$$u'(1) = -P_e(1-\alpha), \quad (C10)$$

and

$$\begin{aligned} u'(1) = -\frac{P_e}{2}(1-R\alpha) \\ \pm \frac{1}{2} \sqrt{(P_e(1-R\alpha))^2 + 4P_e M_G \left(\frac{L_\mu}{K_G} \right) \left(\frac{M_{max}}{K_C+1} \right)}. \end{aligned} \quad (C11)$$

The sign must be negative in order to satisfy $u'(1) < 0$. To satisfy $v'(1) \leq 0$, the denominator of (C8) should be negative which leads to restriction (4.49).

REFERENCES

- [1] Bolt, G.H. 1982. in: *Soil Chemistry B. Physico-Chemical models*, eds. G.H. Bolt, Elsevier, New York, p.285.
- [2] Bosma, W.J.P. & S.E.A.T.M. van der Zee 1993. Analytical approximation for nonlinear adsorbing solute transport and first-order degradation. *Transport Porous Media* 11:33-43.
- [3] Harvey, R.W. & L.B. Barber II 1992. Association of free-living bacteria and dissolved organic compounds in a plume of contaminated groundwater. *J. Cont. Hydrology* 9:91-103.
- [4] Harvey, R.W., R.L. Smith & L. George 1984. Effect of organic contamination upon microbial distributions and heterotrophic uptake in a Cape Cod, Mass., aquifer. *Appl. Environ. Microb.* 48:1197-1202.
- [5] Keijzer, H., S.E.A.T.M. van der Zee & A. Leijnse 1998. Characteristic regimes for in-situ bioremediation of aquifers by injecting water containing an electron acceptor. *Computational Geosciences* 2:1-22.
- [6] Keijzer, H., M.I.J. van Dijke & S.E.A.T.M. van der Zee 1999. Analytical approximation to characterize the performance of in situ aquifer bioremediation. *Adv. Water Resources* 23:217-228.
- [7] Mihelcic, J.R., D.R. Lueking, R.J. Mitzell & J.M. Stapleton 1993. Bioavailability of sorbed- and separate-phase chemicals. *Biodegradation* 4:141-153.
- [8] Monod, J. 1949. The growth of bacterial cultures. *Ann. Rev. of Microb.* 3:371-394.

- [9] Ogram, A.V., R.E. Jessup, L.T. Ou & P.S.C. Rao 1985. Effects of sorption on biological degradation rates of (2,4-dichlorophenoxy)acetic acid in soils. *Appl. Environ. Microb.* 49:582-587.
- [10] Oya, S. & A.J. Valocchi 1997. Characterization of traveling waves and analytical estimation of pollutant removal in one-dimensional subsurface bioremediation modeling. *Water Resources Research* 33:1117-1127.
- [11] Oya, S. & A.J. Valocchi 1998. Analytical approximation of biodegradation rate for in situ bioremediation of groundwater under ideal radial flow conditions. *J. Cont. Hydrology* 31:65-83.
- [12] Reiniger, P. & G.H. Bolt 1972. Theory of chromatography and its application to cation exchange in soils. *Neth. J. Agric. Sci.* 20:301-313.
- [13] Vandevivere, P. & P. Baveye 1992. Effect of bacterial extracellular polymers on the saturated hydraulic conductivity of sand columns. *Appl. Environ. Microb.* 58:1690-1698.
- [14] Van der Zee, S.E.A.T.M. 1990. Analytical traveling wave solutions for transport with nonlinear and nonequilibrium adsorption. *Water Resources Research* 26:2563-2578. (Correction, 1991 *Water Resources Research* 27:983.)
- [15] Van Duijn, C.J., P. Knabner & S.E.A.T.M. van der Zee 1993. Travelling waves during the transport of reactive solute in porous media: combination of Langmuir and Freundlich isotherms. *Adv. Water Resources* 16:97-105.
- [16] Wood, B.D., C.N. Dawson, J.E. Szecsody & G.P. Streile 1994. Modeling contaminant transport and biodegradation in a layered porous media system. *Water Resources Research* 30:1833-1845.
- [17] Xin, J. & D. Zhang 1998. Stochastic analysis of biodegradation fronts in one-dimensional heterogeneous porous media. *Adv. Water Resources* 22:103-116.

Effect of physical, chemical and biochemical processes on the performance of in situ aquifer bioremediation

H. Keijzer and S.E.A.T.M. van der Zee

ABSTRACT

We consider an aquifer polluted with a linear sorbing organic contaminant. The contaminant can be biodegraded by indigenous micro-organisms provided that an electron acceptor is available. The indigenous micro-organisms use the contaminant for their growth. To enhance the biodegradation, the electron acceptor is injected into the aquifer which we refer to as in situ bioremediation. During in situ bioremediation the contaminant is either biodegraded or flushed out of the domain. We characterize the in situ bioremediation performance with the 99% remediation time, τ , and the ratio of contaminant biodegraded to contaminant flushed out, χ . The 99% remediation time is the time necessary to remove 99% of the initially present contaminant. The ratio χ reveals whether the largest fraction of the initially present contaminant is biodegraded or flushed out. In this paper τ and χ are derived semi-analytically and analytically depending on whether or not the front shape is considered. The in situ bioremediation performance is influenced by physical, chemical and biochemical processes, e.g. transport, adsorption and biodegradation respectively. To assess how these processes influence the performance and how we can improve the performance, we determine their effect on τ and χ . Considering a specific polluted site where only the injected electron acceptor concentration c_0 and the injection velocity v can be controlled, we use the effect of c_0 and v on τ and χ for dimensioning the in situ bioremediation performance.

INTRODUCTION

Many aquifers in the world are contaminated with organic contaminants. Research has shown that some of these organic contaminants can be biodegraded by micro-organisms provided that electron acceptors or electron donors and nutrients are sufficiently available. If these compounds are present, a biologically active zone [10] is formed where biodegradation occurs. In most cases, biodegradation is limited because one of the necessary compounds is scarce. If these compounds are injected into the aquifer to enhance biodegradation, we call this in situ bioremediation.

During in situ bioremediation the contaminant is either biodegraded or flushed out of the considered domain or both. If the contaminant is biodegraded, it may be transformed into harmless rest products, whereas if the contaminant is flushed out of the domain, the contaminant is still present in the extraction fluid or elsewhere in the environment. Hence, biodegradation results in a more sustainable removal than flushing. Therefore, if we want to determine whether the in situ bioremediation performance is satisfactory, not only the time necessary to remove the contaminant but also the way the contaminant is removed should be considered. For this reason, we characterize the in situ bioremediation performance, using the 99% remediation time, denoted by τ , and the ratio of contaminant biodegraded to contaminant flushed out, denoted by χ . If τ is small and χ is large, i.e. a short time period is necessary to remove the contaminant and much more contaminant is biodegraded than flushed out, the in situ bioremediation performance is considered satisfactory. Furthermore, especially χ can be used to determine whether natural attenuation occurs. If a very small χ is measured at a polluted site, this implies that no natural attenuation takes place since the fraction of contaminant biodegraded is very small. To remediate such a site, requires in situ bioremediation.

Whether the performance of in situ bioremediation is satisfactory, strongly depends on the physical, chemical and biochemical processes, i.e. transport, adsorption and biodegradation respectively, occurring in the aquifer. The transport of dissolved contaminant and electron acceptor through the aquifer is caused by the injection velocity. Increasing the injection velocity results in a faster supply of electron acceptor and a faster flushing of the contaminant out of the domain. Then, both biodegradation and flushing increase. Due to adsorption less contaminant resides in the aqueous phase and thus adsorption diminished the flushing rate compared with the case of no adsorption. Since micro-organisms are believed to only degrade contaminant in the aqueous phase [7, 9] adsorption also

suppresses the biodegradation rate. As biodegradation itself results in less contaminant in the aqueous phase it limits flushing.

Transport, adsorption and biodegradation occur simultaneously and their effects on the amount of contaminant biodegraded and flushed out might be either synergistic or antagonistic. For example, both fast transport and a high biodegradation rate influence the in situ bioremediation performance positively. In combination, though, the small residence time implied by fast transport adversely affects the fraction of contaminant biodegraded. Therefore, fast transport and a high biodegradation rate act antagonistically. Similarly, both small adsorption and a high biodegradation rate influence the in situ bioremediation performance positively. In combination, the larger fraction of contaminant in the aqueous phase and the faster transport velocity implied by the small adsorption favorably affect the biodegradation and flushing. Especially the fraction of contaminant biodegraded is favorably affected because of the high biodegradation rate. Hence, low adsorption and a high biodegradation rate act synergistically.

To assess the influence of transport, adsorption and biodegradation on the in situ bioremediation performance, we determine their effect on τ and χ . Both τ and χ can be calculated when the development of the contaminant distribution in the aquifer is known. If a (semi-)analytical expression for this contaminant distribution is available, τ and χ can be determined (semi-)analytically. Otherwise numerical simulations are necessary. Fry and Istok [2] analytically determine a 99.9% remediation time, considering first order desorption kinetics where the rate of mass transfer of contaminant from the solid phase to the aqueous phase depends on the concentration gradient between the two phases. They represent the biodegradation of the contaminant by first order degradation. First order degradation approximates Monod kinetics when the contaminant concentration is rate limiting for the microbial growth. Moreover, they assume that the electron acceptor is sufficiently available and that the micro-organism population is at steady state. Schäfer and Kinzelbach [12], on the other hand, numerically determine a 90% remediation time, considering a linear sorbing contaminant, a non-sorbing electron acceptor and an immobile micro-organism population. The biodegradation of the contaminant, the microbial growth, and the consumption of the electron acceptor are related according to Monod kinetics. Their interest goes to the influence of aquifer heterogeneity on this 90% remediation time.

Keijzer et al. [5] and Oya and Valocchi [10] numerically show that during in situ bioremediation a contaminant, electron acceptor and microbial mass front develop which travel with a constant traveling wave velocity

and constant front shapes through the domain. The constant velocity and constant front shapes develop because the spreading effect of dispersion is balanced by the steepening effect of biodegradation. Keijzer et al. [6] determine a semi-analytical solution for the developed contaminant front. In this paper we use this semi-analytical expression, to determine semi-analytically the 99% remediation time (τ_s) and the ratio of contaminant biodegraded to contaminant flushed out (χ_s). In addition, we determine analytically the 99% remediation time, τ_a , and the ratio of contaminant biodegraded to contaminant flushed out, χ_a , assuming plug flow behavior [10]. The difference between τ_s and τ_a is considered, to determine whether the contaminant front shape should be considered during the assessment of the in situ bioremediation performance or whether we can suffice with a plug flow approximation. Moreover, a 99% remediation time is numerically determined to determine whether τ_s or τ_a is more accurate. Furthermore, we use τ_s and χ_s to assess how physical, chemical and biochemical processes influence the in situ bioremediation performance and how we can improve the in situ bioremediation performance applied to a polluted site where only the injection concentration of the electron acceptor and the injection velocity can be adapted.

Our study is closely related to the work of Xin and Zhang [13] in that (semi-)analytical solutions are used to determine the amount of contaminant removed. However, the following aspects differ: different assumption are made concerning the microbial growth and decay rate, they consider the contaminant removal rate as we consider the 99% remediation time and the ratio of contaminant biodegraded to contaminant flushed out, and they determine the influence of aquifer heterogeneity on the developed front, whereas, we assess the influence of physical and biochemical processes on the in situ bioremediation performance.

MODEL FORMULATION

Consider steady-state flow in a one-dimensional saturated and homogeneous aquifer. In the aquifer, aerobic biodegradation occurs if contaminant, electron acceptor and micro-organisms are simultaneously present. Several simplifying assumptions are made [5]. We consider a mobile and reversible sorbing contaminant. Although many contaminants undergo kinetic sorption [9], linear equilibrium sorption is assumed which approximates first order sorption kinetics when sorption is at local equilibrium. Furthermore, we consider a mobile non-sorbing electron acceptor, e.g. oxygen or nitrate. In case another electron acceptors is taken into account such as sulfate, electron acceptor adsorption would also have to be dealt with.

Then a relative retardation factor, $R = R_g/R_c$ could be considered, where R_g and R_c are the retardation factor of the contaminant and electron acceptor. An immobile microbial mass is assumed because micro-organisms form biofilms around the soil particles [3]. Research suggests that micro-organisms can only use both contaminant and electron acceptor that are present in the aqueous phase for microbial growth [7, 9]. The microbial growth and subsequent contaminant biodegradation and electron acceptor consumption is modeled by Monod kinetics [8] and we disregard the decay of micro-organisms, assuming that the specific growth rate is significantly larger than the decay rate. Keijzer et al. [6] show that this simplification has only a small effect on the distribution of the contaminant and electron acceptor concentration. Furthermore, we point out that the results considered in this paper in principle hold also for the anaerobic biodegradation of a contaminant that would require an electron donor instead of an electron acceptor.

These assumptions lead to mass balance equations of the concentrations of the electron acceptor, c [mg l^{-1}], the contaminant, g [mg l^{-1}], and the microbial mass, m [mg l^{-1}] given by

$$\frac{\partial c}{\partial t} = D \frac{\partial^2 c}{\partial x^2} - v \frac{\partial c}{\partial x} - m_c \frac{\partial m}{\partial t}, \quad (5.1)$$

$$R \frac{\partial g}{\partial t} = D \frac{\partial^2 g}{\partial x^2} - v \frac{\partial g}{\partial x} - m_g \frac{\partial m}{\partial t}, \quad (5.2)$$

$$\frac{\partial m}{\partial t} = \mu_m \left(\frac{c}{k_c + c} \right) \left(\frac{g}{k_g + g} \right) m, \quad (5.3)$$

where D denotes the dispersion coefficient [$\text{m}^2 \text{day}^{-1}$], v the effective velocity [m day^{-1}] and R the relative retardation factor. The stoichiometric parameters m_c [$\text{mg}_c \text{mg}_m^{-1}$] and m_g [$\text{mg}_g \text{mg}_m^{-1}$] describe the ratios of consumed electron acceptor and organic contaminant, respectively, to newly formed micro-organism. The parameters in equation (5.3) are the maximum specific growth rate, μ_m [day^{-1}] and the dissolved electron acceptor and organic contaminant half saturation constants, k_c [mg l^{-1}] and k_g [mg l^{-1}]. The independent variables are the spatial coordinate x [m] and the time t [day].

Initially at $t = 0$, we consider a contaminant and microbial mass homogeneously distributed over the aquifer with contaminant concentration in the solution, g_0 [mg l^{-1}], and microbial background mass, m_0 [mg l^{-1}]. We assume that the electron acceptor concentration is the limiting factor for biodegradation, and it is initially equal to zero. The electron acceptor is injected to enhance biodegradation. Hence, we consider injected water

that contains electron acceptor but no contaminant. Thus, we impose a prescribed mass flux of the electron acceptor and contaminant at the inlet of the domain. At the outlet ($x = L$) we assume a purely advective mass flux of electron acceptor and contaminant. Hence, the initial and boundary conditions are

$$c = 0, \quad g = g_0, \quad m = m_0 \quad \text{for } x \geq 0 \quad \text{at } t = 0, \quad (5.4)$$

$$-D \frac{\partial c}{\partial x} + vc = vc_0, \quad -D \frac{\partial g}{\partial x} + vg = 0 \quad \text{for } t > 0 \quad \text{at } x = 0, \quad (5.5)$$

$$\frac{\partial c}{\partial x} = 0, \quad \frac{\partial g}{\partial x} = 0 \quad \text{for } t > 0 \quad \text{at } x = L. \quad (5.6)$$

BIOREMEDIATION CHARACTERISTICS

The 99% remediation time, τ

Because τ is the time at which 99% of the initially present contaminant is removed, it equals the time at which 1% of the initially present contaminant still resides in the considered domain. The amount of contaminant still present in the domain can be expressed by

$$G(t) = n \int_0^L Rg(x, t) dx. \quad (5.7)$$

Hence, τ can be derived from

$$G(\tau) = 0.01 G(0), \quad (5.8)$$

with $G(0)$ the amount of contaminant initially present in the domain [mg]. The quantity $G(0)$ is given by

$$G(0) = n \int_0^L Rg(x, 0) dx = nRLg_0. \quad (5.9)$$

There are two ways to determine $G(t)$. We can either use the semi-analytically derived contaminant concentration front of Keijzer et al. [6] or we can use a plug flow approximation [10].

Keijzer et al. [6] derive a semi-analytical solution for the system of equations (5.1)-(5.3) for initial and boundary conditions (5.4)-(5.6). To solve this system of equations, Keijzer et al. [6] transform it into a nonlinear second order ordinary differential equation (ODE) system, using two newly defined functions of the electron acceptor c : u and w . The nonlinear second order ODE system is solved using an iterative procedure. In each iteration step, u and w are determined by Newton's method. After the iteration, the function u is integrated numerically from a reference point which results in the front shape of c and g . Because the front shapes are given with

respect to an arbitrary reference point, Keijzer et al. [6] use mass balances for c and g to determine their position. Substituting the semi-analytically derived $g(x, t)$, equation (5.7) and (5.9) in equation (5.8), we obtain

$$\int_0^L g(x, \tau) dx = 0.01 L g_0, \tag{5.10}$$

where τ is the only unknown. From equation (5.10) we can determine τ semi-analytically, using for example the trapezoidal rule, which yields τ_s .

If we consider a plug flow approximation for $g(x, t)$,

$$g(x, t) = g_0 H(x - x_p(t), t), \tag{5.11}$$

where H is the Heaviside function

$$H(x - x_p(t), t) = \begin{cases} 0 & \text{if } x < x_p(t), \\ 1 & \text{if } x > x_p(t), \end{cases} \tag{5.12}$$

and $x_p(t)$ the shock front position at t . The expression for $G(t)$ becomes

$$G(t) = nRg_0 \int_0^L H(x - x_p(t), t) dx = nRg_0(L - x_p(t)). \tag{5.13}$$

Substitution of equation (5.9) and (5.13) in equation (5.8), yields

$$x_p(\tau) = 0.99 L. \tag{5.14}$$

The front position for the plug flow is related to the front or traveling wave velocity α [5, 6] and the time passed and is defined by $x_p(t) = \alpha t$ [10] with α is analytically derived by Keijzer et al. [6]

$$\alpha = v \left(\frac{c_0 + \frac{m_c}{m_g} g_0}{c_0 + R \frac{m_c}{m_g} g_0} \right). \tag{5.15}$$

Using the definition of x_p , we obtain a simple analytical expression for 99% remediation time

$$\tau_a = 0.99 \frac{L}{\alpha}. \tag{5.16}$$

We emphasize that the semi-analytically or analytically derived 99% bioremediation times, τ_s and τ_a , can only be determined in case the traveling wave has developed. Keijzer et al. [4] and Oya and Valocchi [10] showed that the traveling waves develop after a limited start up period. Keijzer et al. [4] identify the end of this period qualitatively, whereas Oya [11] quantitatively defines a peak biodegradation time that approximates the time at which this period ends.

The ratio χ

The quantity of contaminant biodegraded at t , $G_b(t)$, can be derived from the contaminant mass balance. It equals the quantity of contaminant initially present minus the sum of the quantities of contaminant still present and flushed out, $G_f(t)$, at t which yields

$$G_b(t) = G(0) - (G(t) + G_f(t)), \quad (5.17)$$

where $G(0)$ and $G(t)$ are given in equation (5.9) and (5.7). The quantity of contaminant flushed out is given by

$$G_f(t) = nv \int_0^t g(L, t) dt. \quad (5.18)$$

We determine the ratio of contaminant biodegraded to flushed out as a function of time, using equation (5.17) and (5.18)

$$\chi(t) = \frac{G_b(t)}{G_f(t)} = \frac{G(0) - G(t) - G_f(t)}{G_f(t)}. \quad (5.19)$$

The ratio $\chi(t)$ can be determined semi-analytically by substitution of the quantities $G(0)$, $G(t)$ and $G_f(t)$, i.e. equation (5.9), (5.7) and (5.18), and the semi-analytically derived $g(x, t)$ and $g(L, t)$ in equation (5.19). Henceforth, when we mention the semi-analytically determined χ_s , we refer to

$$\chi_s = \chi_s(\tau_s) \quad (5.20)$$

The ratio χ can also be determined analytically, if we again consider a plug flow approximation for $g(x, t)$. Then the quantity of contaminant flushed out becomes

$$G_f(t) = nv \int_0^t g_0 H(L - \alpha t, t) dt = \begin{cases} nv g_0 t & \text{if } \alpha t < L, \\ nv g_0 t_m & \text{if } \alpha t > L, \end{cases} \quad (5.21)$$

where $t_m = L/\alpha$. Substitution of the analytical expressions of the quantities $G(0)$, $G(t)$ and $G_f(t)$, i.e. equation (5.9), (5.13) and (5.21), in equation (5.19) leads to a analytically determined χ_a ,

$$\chi_a = \frac{R\alpha - v}{v} = R\alpha' - 1, \quad (5.22)$$

where $\alpha' = \alpha/v$ is the dimensionless traveling wave velocity. Notice that χ_a only depends on the retardation factor and the dimensionless traveling velocity and not on t .

Bioremediation parameters

Physical, chemical and biochemical processes in the aquifer are characterized by different properties. Transport is characterized by the injection velocity, v , the dispersivity, α_l , the porosity, n and the length of the contaminated aquifer, L . Adsorption is characterized by the retardation factor, R . Biodegradation and microbial growth are characterized by, respectively the stoichiometric coefficients, m_g and m_c , the specific growth rate, μ_m and the half saturation constants, k_g and k_c . Both biodegradation and microbial growth are also influenced by the initially present contaminant concentration and microbial mass, i.e., by g_0 and m_0 , and by the injected electron acceptor concentration, c_0 .

If we consider a site polluted with a specific organic contaminant and we assume that indigenous micro-organism populations are present, some of the physical, chemical and biochemical parameters are fixed, in the sense that their values can not be influenced e.g. for dimensioning purposes. The physical parameters α_l , n and L are fixed because both the structure and the relevant length of the contaminated aquifer are known, and the biochemical parameters k_g , m_g , g_0 , μ_m and m_0 are fixed because they represent the present contaminant and micro-organisms. In situ bioremediation can therefore be influenced by adapting the physical parameter v as different injection and extraction velocities can be imposed during bioremediation, and by adapting the biochemical parameters k_c , m_c and c_0 because different electron acceptors and electron acceptor injection concentrations can be chosen. These adaptable parameters are henceforth referred to as control parameters. We also consider R to be a control parameter because, depending on the chosen electron acceptor, the electron acceptor can also react with soil particles so that R can be seen as a relative retardation factor ($R = R_g/R_c$).

For the reference case we consider a site polluted with a contaminant which is rather resistant to biodegradation. Therefore, the steepening effect of biodegradation that opposes dispersion is not dominant and the developed traveling wave front is rather spread out, as is shown in Figure 5.1. The control parameter values used to obtain Figure 5.1 are given in Table 5.1 (ref). The parameter values that are the same for all calculations are given in Table 5.2.

RESULTS

Applicability of τ_s , τ_a , χ_s and χ_a

One of our aims is to determine whether the contaminant front shape should be considered during the assessment of the in situ bioremediation

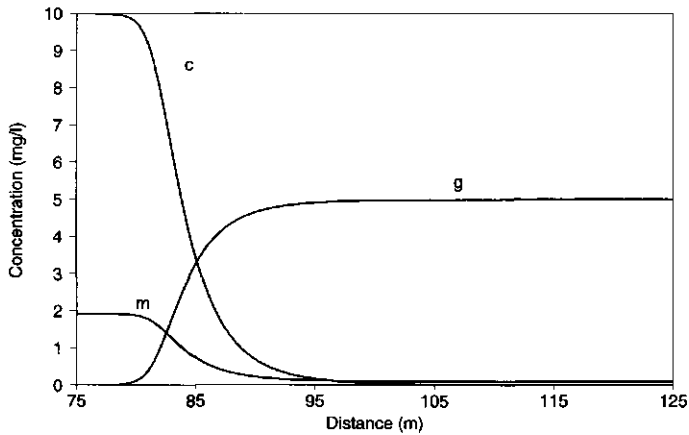


FIGURE 5.1. Semi-analytical contaminant (g), electron acceptor (c) and microbial mass (m) front at $t = 1000$ days.

TABLE 5.1. Values of the bioremediation control parameters for different cases.

case	k_c	m_c	c_0	v	R
ref	1.0	1.0	10.0	0.1	3.0
sim 1	10.0	-	-	-	-
sim 2	20.0	-	-	-	-
sim 3	-	0.2	-	-	-
sim 4	-	0.5	-	-	-
sim 5	-	-	1.0	-	-
sim 6	-	-	3.0	-	-
sim 7	-	-	-	0.5	-
sim 8	-	-	-	1.0	-
sim 9	-	-	-	-	1.1
sim 10	-	-	-	-	9.0

TABLE 5.2. Parameter values that are the same for all calculations.

k_g	m_g	g_0	μ_m	m_0	n	α_l	L
2.0	5.0	5.0	0.05	0.1	0.4	0.005	200

performance. Therefore, we vary the control parameters separately over a broad but plausible range of values and derive for each value τ_s , τ_a , χ_s and χ_a . To determine the influence of the front shape, we can either consider the difference between τ_s and τ_a or χ_s and χ_a since τ_s and χ_s are derived using the contaminant front shape, whereas, τ_a and χ_a are derived

using a plug flow approximation. In the following we will focus on the difference between τ_s and τ_a . The ratio of τ_s to τ_a , denoted by τ^* is used to determine this difference. If the traveling wave front shape is steep, it can be approximated by a shock front and τ_s is approximated by τ_a , i.e. $\tau^* = 1$. If the traveling wave front is diffuse, it is poorly approximated by a shock front and τ_s and τ_a differ, i.e. $\tau^* > 1$ or $\tau^* < 1$. Whether or not the traveling wave front is diffuse depends on the balance between the spreading effect of dispersion and the steepening effect of nonlinear biodegradation [10, 5].

To assess whether τ_s or τ_a is more accurate, we carry out numerical simulations to determine the 99% remediation time, τ_n . Only two numerical simulations per control parameter are performed (see Table 5.1) because the numerical simulations are very time consuming. For example for the reference case, on an AlphaStation 500/333 it requires 10 hours to determine τ numerically, whereas it requires only 1 minute to determine τ semi-analytically. To obtain τ numerically, we solve the system of equation (5.1)-(5.3) as described by Keijzer et al. [5] and we choose the spatial discretization and time step such that the grid Peclet and Courant conditions are fulfilled to avoid numerical dispersion and numerical instabilities. This results in $\Delta x = 0.025$ m and $\Delta t = 0.05$ day. We compare the numerical 99% remediation time divided by τ_a , denoted by τ_n^* , with τ^* . If both the numerical and semi-analytical 99% remediation time are larger or smaller than the analytical 99% remediation time, i.e. $\tau_n^* > 1$ and $\tau^* > 1$ or $\tau_n^* < 1$ and $\tau^* < 1$, then the semi-analytical 99% remediation time is the best approximation. If both the numerical and semi-analytical 99% remediation time equal the analytical 99% remediation time, i.e. $\tau_n^* = 1$ and $\tau^* = 1$, then both the semi-analytical and analytical 99% remediation times are good approximations and it is sufficient to use a plug flow approximation.

Figure 5.2 shows the ratio τ^* and the ratio τ_n^* for the simulations given in Table 5.1 as a function of the normalized control parameters. It can be seen that for small c_0 or large k_c or v values τ^* becomes larger than one. Large k_c or small c_0 values indicate a limited microbial growth due to electron acceptor deficiency so less contaminant biodegradation occurs. Therefore, the steepening effect of biodegradation becomes less significant. Large v values, on the other hand, indicate fast flushing and the spreading effect of dispersion becomes more significant. For all these cases the contaminant front shape becomes more diffuse [5, 10] and more time is necessary to remove 99% of the initially present contaminant, hence τ^* increases, i.e. τ_s and τ_a differ. Furthermore, Figure 5.2 also shows that for these parameter values, i.e. small c_0 , large k_c or v values, τ^* approximates τ_n^* very well. Therefore, it is necessary to determine the 99% remediation time

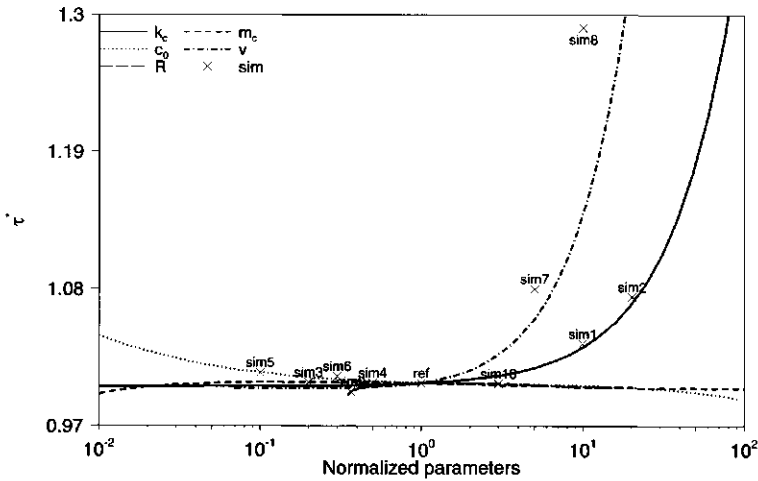


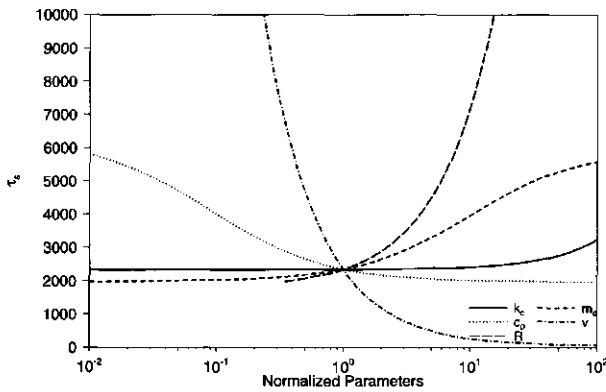
FIGURE 5.2. The ratio τ^* for different values of the control parameters k_c , m_c , c_0 , v and R which are normalized with respect to their reference value. The symbol x shows τ_n^* for the different numerical simulations.

semi-analytically. For all other values of the control parameters, i.e. large c_0 , small k_c , small v , all m_c and R values, both τ_n^* and τ_n are close to one, i.e. the semi-analytical, analytical and numerical 99% remediation time are comparable. Even though the semi-analytical is a better approximation of τ_n^* it is sufficient to determine τ analytically by a plug flow approximation.

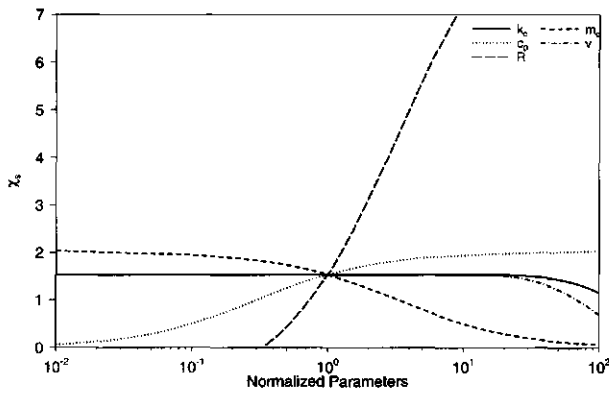
We conclude from Figure 5.2 that if the contaminant front shape is diffuse, the 99% remediation time should be determined semi-analytically. If this is not the case then a plug flow approximation is justified and τ can be determined analytically. We emphasize that τ_s and τ_a can only be determined if the traveling waves develop before they reach the end of the domain. Oya and Valocchi [10] and Keijzer et al. [5] show that for very large k_c or v values the traveling waves might not develop in time. But even for these values Figure 5.2 shows that the semi-analytical 99% remediation time approximates the numerical 99% remediation time better than the analytical one.

Sensitivity analysis

The in situ bioremediation characteristics τ and χ are used to assess the effect of transport, adsorption and biodegradation. Figure 5.3.a and b show τ_s and χ_s as a function of the normalized control parameters. From Figure 5.3.a it can be seen that increasing c_0 or v , or decreasing m_c or R result in a decrease in τ_s . This behavior is expected because increasing c_0 or v , or



(a)



(b)

FIGURE 5.3. Semi-analytically determined 99% remediation time τ_s (a) and ratio χ_s (b) for different values of the control parameters k_c , m_c , c_0 , v and R which are normalized with respect to their reference value.

decreasing m_c or R results in an increase in the traveling wave velocity as follows from equation (5.15) and therefore in a decrease in τ_s . Furthermore, Figure 5.3.a shows that τ_s increases for large k_c values, though the traveling wave is not affected by k_c . This is a result of the electron acceptor deficiency which causes a more diffuse front [10, 5].

Figure 5.3.b shows that increasing c_0 or decreasing m_c leads to a decrease in χ_s . This is expected since this leads to an increase in the traveling wave velocity and more contaminant is flushed out. Though the traveling

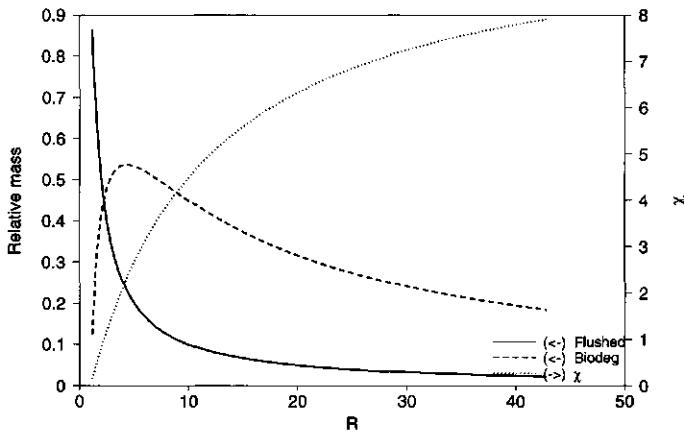


FIGURE 5.4. Semi-analytical fraction of contaminant flushed out (solid line), fraction of contaminant biodegraded (dashed line) and ratio of contaminant biodegraded to flushed out (dotted line) at $t = 2000$ for the reference case.

wave is not affected by k_c , χ_s decreases for large k_c values because large k_c indicate a limited microbial growth due to electron acceptor deficiency and less contaminant biodegradation occurs.

The effect of v and R on χ_s is more complex. Increasing v results in an faster traveling wave velocity and a faster supply of electron acceptor. Therefore both more contaminant is flushed out and more contaminant is biodegraded and thus χ_s remains unaffected. This is confirmed by the expression of χ_a , equation (5.16), that shows an independence of v . For large v values the contaminant front becomes more diffuse since the spreading effect of the dispersion dominates over the steepening effect of biodegradation and χ_s decreases.

R influences both biodegradation and flushing as R influences the traveling wave velocity according to equation (5.15) and the amount of contaminant present in the aqueous phase. Notice that the traveling wave velocity is bounded by the original contaminant velocity (v/R) and the original electron acceptor velocity (v), $v/R \leq \alpha \leq v$. We use Figure 5.4 to explain the effect of R on χ_s . It shows the fraction of contaminant biodegraded, flushed out and χ_s at $t = 2000$. For R values close to one, the original contaminant velocity almost equals the original electron acceptor velocity, thus the overlap between contaminant and electron acceptor is small and the fraction of contaminant biodegraded is small. For larger values of R , the original contaminant velocity is smaller than the original electron acceptor velocity which implies a larger overlap and the fraction of

contaminant biodegraded increases. For even larger R values, the overlap still increases but only a small fraction of the contaminant is present in the aqueous phase which limits biodegradation. Hence, a R is found for which the fraction of contaminant biodegraded has a maximum. Such a R is also found by Oya and Valocchi [11] and Chiang et al. [1]. The effect of R on fraction of contaminant flushed out is rather straight forward. If R increases, the traveling wave velocity decreases and less contaminant is present in the aqueous phase. Hence, the fraction of contaminant flushed out decreases, see Figure 5.4. Both Figure 5.3.b and 5.4 show that χ_s increases as R increases because for small R values the contaminant removal is dominated by flushing and for large R values the removal is dominated by biodegradation. Again this effect is confirmed by the expression of χ_a , equation (5.16), that shows χ_a is proportional to R .

The combination of Figure 5.3.a and b shows that an increase in c_0 or a decrease in m_c results in a decrease in τ and an increase in χ , hence a better in situ bioremediation performance is obtained. The control parameter k_c has only a small effect on both τ_s and χ_s , thus it has almost no effect on the in situ bioremediation performance. The injection velocity, on the other hand, has a large effect on τ_s which decreases when v increases, whereas it has almost no effect on χ_s . If we are only interested in decreasing the remediation time, increasing v would be a good option. If we want to remove the contaminant by biodegradation, increasing v does not help. Furthermore, if we decrease R , both τ_s and χ_s decreases, hence the in situ bioremediation performance might stay the same on change only a little.

Performance

Depending on the optimization feature of the in situ bioremediation performance, e.g. fast removal of contaminant, minimum use of electron acceptor, it is in principle feasible to identify an electron acceptor which is most suitable. If this electron acceptor is injected to enhance the biodegradation, the k_c , m_c and R values are no longer subjects of choice. The remaining two control parameters that can still be adapted are the injected electron acceptor concentration c_0 and the injection velocity v . They are related with, respectively, the biodegradation rate, since electron acceptor deficiency limits the biodegradation, and the flushing of the contaminant.

We consider the in situ bioremediation performance to be satisfactory if both fast removal of contaminant occurs and removal is dominated by biodegradation, i.e. if τ_s is small and χ_s is large. To determine for which c_0 and v values the in situ bioremediation performance is satisfactory, we vary these two control parameters simultaneously. Figure 5.5 shows τ_s and

χ_s as a function of v and c_0 . This figure can be used to determine whether the in situ bioremediation performance is limited by electron acceptor deficiency or flushing and thus the feasibility of using in situ bioremediation to decrease the remediation time. Furthermore, it can be used to determine how we can improve the in situ biodegradation performance. The values of the other physical, chemical and biochemical parameter used to obtain Figure 5.5 are given in Table 5.1 (ref) and 5.2.

Figure 5.5 shows that when the injected electron acceptor concentration is large and the imposed injection velocity is low, flushing limits the decrease in the 99% remediation time and removal of contaminant occurs mainly by biodegradation, i.e. τ_s and χ_s are large. Increasing the imposed injection velocity results in an immediate decrease in the 99% remediation time since more flushing as well as biodegradation occurs because, respectively, more contaminant is flushed out of the domain and a faster supply of electron acceptor takes place. Since both flushing and biodegradation increases, the ratio χ_s does not change immediately. If v increases even more, flushing starts to dominate over biodegradation and χ_s decreases. When, on the other hand, the injected electron acceptor concentration is small and the imposed injection velocity is high, electron acceptor deficiency limits the contaminant biodegradation and thus the decrease in the 99% remediation time and removal of contaminant occurs mainly by flushing, i.e. τ_s is large and χ_s is small. Increasing the injected electron acceptor concentration results in an immediate decrease in the 99% remediation time and increase in the ratio χ_s since more biodegradation occurs.

Furthermore, from Figure 5.5 it can be seen that the combination of a medium c_0 and v leads to a small 99% remediation time but also to a relatively small χ_s . Lets take, for example, $c_0 = 0.4$ and $v = 1.25$ then $\tau_s = 300$ but $\chi_s = 1.0$. Thus the quantity of contaminant biodegraded equals the quantity of contaminant flushed out. If we want more contaminant to be removed by biodegradation, c_0 has to be increased significantly. For example, if we want to obtain $\chi_s = 2.0$ instead of $\chi_s = 1.0$, we have to use a ten times larger injection concentration. Whether this is feasible depends on the solubility of the electron acceptor.

We emphasize that we consider a specific polluted site for which specific values are chosen for all model parameters (Table 5.1 (ref) and 5.2). The results shown in Figure 5.5, will differ if one of these parameter values changes. Still we could create the same figure for other polluted sites, using their specific model parameter values and the associated semi-analytically

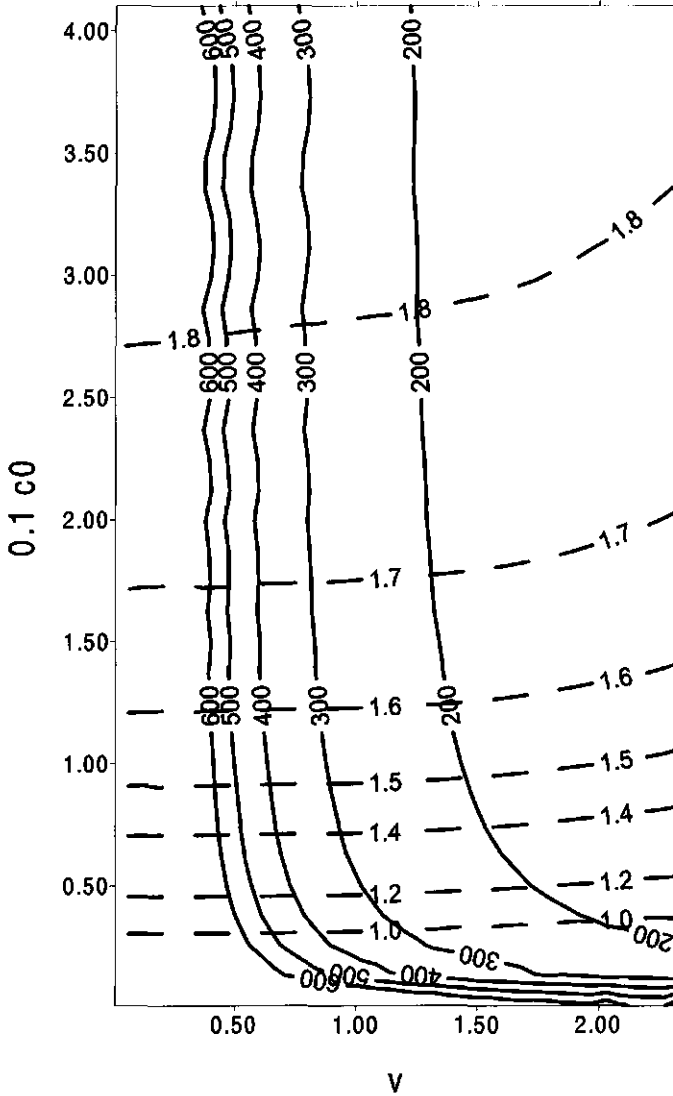


FIGURE 5.5. Semi-analytically determined 99% remediation time (solid lines) and ratio of contaminant biodegraded to flushed out (dashed lines) as a function of the injected electron acceptor concentration (c_0) and the injection velocity (v).

determined τ_s and χ_s . In the same way as discussed above, we could determine how we can improve the in situ bioremediation performance at these sites.

CONCLUSION AND DISCUSSION

We have considered steady-state flow in a one-dimensional saturated and homogeneous aquifer. The aquifer is polluted with an organic contaminant which is biodegraded if contaminant, electron acceptor and micro-organisms are simultaneously present. To enhance the contaminant biodegradation the electron acceptor is injected which is called in situ bioremediation. The in situ bioremediation performance is characterized by a 99% remediation time, τ , and a ratio of contaminant biodegraded to flushed out, χ . We have shown that τ and χ can either be determined semi-analytically, using the semi-analytical solution of Keijzer et al. [6], or analytically, using a plug flow approximation.

Using the semi-analytically and analytically determined 99% remediation time, respectively τ_s and τ_a , we assess whether the contaminant front shape should be taken into account. The results show that if a diffuse contaminant front shape develops, i.e. if c_0 is small or k_c or v is large, τ_s and τ_a differ. Using a numerically determined 99% remediation time, τ_n , we show that for such a diffuse contaminant front τ_s is more accurate than τ_a . Hence, the 99% remediation time should be determined semi-analytically. If, on the other hand, the contaminant front shape is rather steep, i.e. large c_0 , small k_c , small v , all m_c or all R values, τ_s , τ_a and τ_n are comparable and it is sufficient to determine the 99% remediation time analytically. Since no explicit range of c_0 , k_c and v is found for which a diffuse front shape develops, it is better to determine τ semi-analytically for all c_0 , k_c and v values. Especially because the determination of τ_s and χ_s is not time consuming and they are better approximations for τ and χ than τ_a and χ_a .

We consider the in situ bioremediation performance to be satisfactory if both fast removal of contaminant occurs and removal is dominated by biodegradation, i.e. if τ_s is small and χ_s is large. Therefore, both τ_s and χ_s are used to determine the influence of transport, adsorption and biodegradation on the in situ bioremediation performance and to determine how we improve the performance. If we consider these processes separately, we see that the injection velocity has a large effect on τ_s which decreases when v increases, whereas it has almost no effect on χ_s . Thus if we are only interested in decreasing the remediation time, increasing v would be a good option but if we want to remove the contaminant by biodegradation, increasing v does not help. If adsorption decreases, i.e. R decreases, both τ_s and χ_s decreases, hence the in situ bioremediation performance might stay the same on change only a little. An increase in c_0 or a decrease in m_c results in a decrease in τ and an increase in χ , hence a better in situ

bioremediation performance is obtained. Whereas, k_c has only a small effect on both τ_s and χ_s and thus a small effect on the in situ bioremediation performance.

At a specific site contaminated with organic contaminant, an electron acceptor can be found for which fast removal of contaminant occurs and removal is dominated by biodegradation. Then the only two remaining control parameters are the injected electron acceptor concentration, c_0 , and the injection velocities, v . The other parameters can be measured. We provide a figure that shows τ_s and χ as a function of c_0 and v . Using this figure, we can determine whether the in situ bioremediation performance is limited by electron acceptor deficiency or contaminant flushing. It shows that if the injected electron acceptor concentration is large and the imposed injection velocity is low, flushing limits the performance. Whereas, if the injected electron acceptor concentration is small and the imposed injection velocity is high, electron acceptor deficiency limits the performance. We could create such figures for different polluted sites, using the semi-analytically determined τ and χ .

Not only the performance but also the costs made during in situ bioremediation are an important factor. The costs strongly depend on the amount of electron acceptor injected and the injection velocity imposed. Large injected electron acceptor concentrations and large injection velocities may result in high remediation cost. If the involved cost are known for all possible combinations of injected electron acceptor concentrations and injection velocities, we could create an overlay for Figure 5.5. Using this overlay, we can determine for which injected electron acceptor concentration and which injection velocity the in situ bioremediation is satisfactory and the involved costs are minimal.

REFERENCES

- [1] Chiang, C.Y., C.N. Dawson & M.F. Wheeler 1991. Modeling of in-situ bioremediation of organic compounds in groundwater. *Transport in Porous Media* 6:667-702.
- [2] Fry, V.A., & J.D. Istok 1994. Effects of rate-limited desorption on the feasibility of in situ bioremediation. *Water Resources Research* 30:2413-2422.
- [3] Ghiorse, W.C. & D.L. Balkwill 1983. Enumeration and morphological characterization of bacteria indigenous to subsurface environments. *Dev. Ind. Microb.* 24:213-224.
- [4] Keijzer, H., S.E.A.T.M. van der Zee & A. Leijnse 1998. Characteristic regimes for in-situ bioremediation of aquifers by injecting water containing an electron acceptor. *Computational Geosciences* 2:1-22.
- [5] Keijzer, H., M.I.J. van Dijke & S.E.A.T.M. van der Zee 1999. Analytical approximation to characterize the performance of in situ aquifer bioremediation. *Adv. Water Resources* 23:217-228.

- [6] Keijzer, H., R.J. Schotting & S.E.A.T.M. van der Zee 2000. Semi-analytical traveling wave solution of one-dimensional aquifer bioremediation. *Comm. Applied Nonlinear Analysis* 7:1-20.
- [7] Mihelcic, J.R., D.R. Lueking, R.J. Mitzell & J.M. Stapleton 1993. Bioavailability of sorbed- and separate-phase chemicals. *Biodegradation* 4:141-153.
- [8] Monod, J. 1949. The growth of bacterial cultures. *Ann. Rev. of Microb.* 3:371-394.
- [9] Ogram, A.V., R.E. Jessup, L.T. Ou & P.S.C. Rao 1985. Effects of sorption on biological degradation rates of (2,4-dichlorophenoxy)acetic acid in soils. *Appl. Environ. Microb.* 49:582-587.
- [10] Oya, S. & A.J. Valocchi 1997. Characterization of traveling waves and analytical estimation of pollutant removal in one-dimensional subsurface bioremediation modeling. *Water Resources Research* 33:1117-1127.
- [11] Oya, S. 1998. Solute transport and biodegradation characteristics for models of enhanced subsurface bioremediation, Thesis.
- [12] Schäfer, W. & W. Kinzelbach 1991. in: *In Situ Bioreclamation*, Numerical Investigation into the effect of aquifer heterogeneity on in situ bioremediation, eds. R.E. Hinchey and R.F. Olfenbittel, Butterworth-Heinemann, London, p.196.
- [13] Xin, J. & D. Zhang 1998. Stochastic analysis of biodegradation fronts in one-dimensional heterogeneous porous media. *Adv. Water Resources* 22:103-116.

Stochastic analysis of nonlinear biodegradation and transport in heterogeneous aquifers

H. Keijzer and S.E.A.T.M. van der Zee

ABSTRACT

Spatially variable hydraulic properties and biochemical processes influence the field scale transport of reactive solutes in physically heterogeneous aquifers. We consider a biodegradable contaminant and assume that heterogeneous advection, linear sorption and nonlinear biodegradation are the dominant processes. We apply the Lagrangian approach to determine the interaction between physical heterogeneity and nonlinear biodegradation. This approach relates the statistics of the hydraulic conductivity to the statistical moments of the biodegradable contaminant mass flux, e.g. the expected value and the standard deviation of the contaminant mass flux. We determine the changes in the expected contaminant mass flux due to variation of the degree of heterogeneity, the biochemical and the physical parameters. Pore-scale dispersion and molecular diffusion are neglected and we discuss the effect of this assumption on the expected contaminant mass flux. Furthermore, ergodic conditions are considered, the injection and extraction area are large relative to the transverse integral scale. For ergodic conditions, the standard deviation equals zero which yields a lower limit. The upper limit of the standard deviation is found for complete nonergodic conditions and far-field transport.

INTRODUCTION

Theoretical analysis and field test have revealed that spatially variable hydraulic properties (e.g. hydraulic conductivity, porosity) have a profound impact on the transport of solutes. Variation of one of these properties results in spreading of the solute. Additionally to the spatially variable hydraulic properties also biochemical reactions between solute and soil or other solutes may significantly affect the solute transport. For example, if a solute undergoes linear sorption, the solute is retarded, whereas, if it undergoes nonlinear sorption, depending on the initial and boundary conditions, the transport of the solute can be described by either self-sharpening or by self-spreading (rarification) waves [14, 20, 32]. The self-sharpening or traveling waves are also found for solutes that undergo nonlinear biodegradation [23, 27].

To study reactive transport in physically heterogeneous aquifers, one of the hydraulic properties maybe regarded as a random space function (RSF). As a result, the fluid velocity and solute concentration are also RSFs. Dagan et al. [12], Cvetkovic et al. [10] and Cvetkovic and Dagan [7, 8, 14] have developed the Lagrangian approach that relates the statistics of the hydraulic conductivity to the statistical moments of the mass flux. In this approach, the transport of reactive solutes is viewed as taking place along a set of random trajectories where the solute mass is advected and subjected to biochemical processes and pore-scale dispersion and molecular diffusion are neglected. The statistics of the trajectories and the reactive solute distribution are used to determine an expression for the statistical moments of the mass flux of the reactive solute in a heterogeneous aquifer at a specific control plane. The statistics of the trajectories are related to the statistical moments of the hydraulic conductivity via probability density functions (pdf) and the distribution of the reactive solute along one trajectory is determined using the Eulerian mass balance equations. These Eulerian equations are transformed to a Lagrangian form as described by Cvetkovic and Dagan [7] and hold along a trajectory. Hence, the resulting equation are essentially one-dimensional and can be solved either numerically or analytically. Destouni [15] and Destouni and Graham [16] extend the approach such that it is also applicable to heterogeneous soils instead of aquifers only.

The Lagrangian approach is applied to conservative solutes, [10, 12, 30], however, many subsurface solutes undergo biochemical reactions such as sorption and biodegradation. Cvetkovic and Shapiro [9], Selroos and Cvetkovic [28], Dagan and Cvetkovic [13], and Selroos and Cvetkovic [29]

extend the Lagrangian approach to linear sorption kinetics, whereas Simmons et al. [31], and Berglund and Cvetkovic [2] extend it to nonlinear sorption. Both linear sorption kinetics and nonlinear sorption in heterogeneous formations are considered by Cvetkovic and Dagan [7, 8], and Dagan and Cvetkovic [14]. Recently, stochastic approaches were also applied to nonlinear biodegradable solutes [19, 21, 33]. Ginn et al [19] are the first to apply the Lagrangian approach to nonlinear biodegradation with microbial growth. They consider a single limiting substrate and a microorganism population, hence no electron acceptor is necessary to trigger the biodegradation reaction. A numerical method and an approximate analytical method are used to determine the distribution of the substrate over the stream tube. They compare their developed stochastic approach (SCR) and convective-dispersive reaction (CDR) simulations with effective Fickian dispersion coefficient with 2D Monte Carlo calculations in a heterogeneous field. The results show that the CDR significantly overestimates the effect of the reactive sink while the SCR accurately duplicates the ensemble-averaged reactive transport breakthrough. Xin and Zhang [33] use a stochastic approach to study the spatial instead of the temporal moments of a biodegradable solute. They derive analytical solutions for the mean and variance of the solute resident concentration under an explicit condition on the growth and decay rates of biomass and they consider the porosity to be the spatially variable parameter. Kaluarachchi et al. [21] apply the Lagrangian approach to nonlinear biodegradation, taking into account a second electron acceptor, nitrate besides oxygen. They assume that first oxygen is used as electron acceptor. When the oxygen concentration reaches a threshold concentration nitrate takes over. To determine the distribution of the contaminant and electron acceptors, they use a numerical operator splitting technique. In their study, they focus on the influence of the presence of nitrate on the biodegradation of the contaminant. The results show that the presence of nitrate positively influence the remediation.

The work in this paper is closely related to the work of Ginn et al. [19], Xin and Zhang [33], and Kaluarachchi et al. [21]. Whereas Ginn et al. [19] do not consider an electron acceptor, we as well as Xin and Zhang [33] and Kaluarachchi et al. [21] assume that an electron acceptor is needed to trigger the biodegradation. Kaluarachchi et al. [21] even consider a second electron acceptor and use a numerical method to determine the contaminant distribution along a trajectory. Xin and Zhang [33], on the other hand, use an analytical solution, assuming nutrient-deficient conditions and/or a microbial growth rate smaller than the microbial decay rate, to determine

an expression for the averaged solute resident concentration and its variance. In this paper we use the semi-analytical solution of Keijzer et al. [24], assuming a microbial decay rate much smaller than the microbial growth, to determine an expression for the averaged contaminant mass flux in a heterogeneous aquifer. Using this averaged contaminant mass flux, we assess the interaction between heterogeneity and nonlinear biodegradation. Furthermore, we discuss the influence of the assumptions made in the applied Lagrangian approach, e.g. neglecting of pore-scale dispersion and molecular diffusion and considering ergodic conditions.

PROBLEM FORMULATION

Heterogeneous aquifer

We consider fluid flow through a three-dimensional physically heterogeneous aquifer where the hydraulic conductivity is spatially variable. The hydraulic conductivity $\mathbf{K} = \mathbf{K}(\mathbf{x})$ is regarded as a statistically stationary RSF. The Eulerian velocity $\mathbf{V}(V_1, V_2, V_3)$ is related to \mathbf{K} , the porosity and the hydraulic head through Darcy's law, hence, \mathbf{V} is also a RSF. We assume a stationary velocity flow which is parallel to the x_1 coordinate axis and a constant porosity and hydraulic head. Therefore, the fluctuations in \mathbf{V} are the result of the fluctuations in \mathbf{K} only, and the mean velocity given by $\langle \mathbf{V} \rangle = \mathbf{U} = (U, 0, 0)$ with $U = \langle V_1 \rangle$ is parallel to the x_1 coordinate axis.

Field data [11, 18] demonstrated that the hydraulic conductivity can be assumed to be lognormally distributed, $\mathbf{K}(\mathbf{x}) = K_G \exp(Y)$, where K_G is the geometric mean of \mathbf{K} and Y is normally distributed $N(0, \sigma_Y^2)$. Y is assumed to be described by the axisymmetric covariance model with an exponential covariance function,

$$C_Y(\mathbf{r}) = \sigma_Y^2 \exp(-r), \quad (6.1)$$

where $r^2 = (r_1^2 + r_2^2)/I^2 + r_3^2/I_3^2$, I is the integral scale in the horizontal plane and I_3 is the integral scale in the vertical direction.

Transport and Nonlinear biodegradation

We consider a biodegradable contaminant and assume that heterogeneous advection, linear sorption and nonlinear biodegradation are the dominant processes that influence the transport of this contaminant. Thus, pore-scale dispersion and molecular diffusion are neglected, assuming that the effect of the dispersive mechanism, which occurs at scales smaller than those characterizing the hydraulic conductivity variability is of lesser importance than the spreading mechanism caused by large-scale heterogeneity. We discuss the effect of this assumption in the discussion. Moreover, we

assume that the contaminant with concentration g can only be biodegraded by indigenous micro-organisms with concentration m if an electron acceptor or electron donor with concentration c is present. The contaminant is assumed to be a mobile reversible linearly-sorbing compound and the electron acceptor is assumed to be mobile and non-sorbing, e.g. oxygen or nitrate, or reversible linearly-sorbing. The retardation factor of c , R_c , should be smaller than the one for g , R_g otherwise no overlap between the contaminant and electron acceptor takes place, hence no biodegradation occurs [27]. Assuming that the micro-organisms form biofilms around soil particles, they are considered immobile. The microbial growth depends nonlinearly on the contaminant and electron acceptor concentration and is modeled by Monod kinetics [26].

The resulting Eulerian advection-reaction equation for the contaminant and the electron acceptor, and the microbial growth equation are [24]

$$R \frac{\partial g}{\partial t} = -\mathbf{V} \cdot \nabla g - m_g \frac{\partial m}{\partial t}, \quad (6.2)$$

$$\frac{\partial c}{\partial t} = -\mathbf{V} \cdot \nabla c - m_c \frac{\partial m}{\partial t}, \quad (6.3)$$

$$\frac{\partial m}{\partial t} = \mu_m \left(\frac{c}{k_c + c} \right) \left(\frac{g}{k_g + g} \right) m, \quad (6.4)$$

where R denotes the relative retardation factor, R_g/R_c , and m_c [$\text{mg}_c \text{mg}_m^{-1}$] and m_g [$\text{mg}_g \text{mg}_m^{-1}$] denote the stoichiometric parameters which describe, respectively, the ratios of consumed electron acceptor and organic contaminant to newly formed micro-organism. The parameters in equation (6.4) are the maximum specific growth rate, μ_m [day^{-1}], and the dissolved electron acceptor and organic contaminant half saturation constants, k_c [mg l^{-1}] and k_g [mg l^{-1}].

Initially, at $t = 0$, contaminant and microbial mass are homogeneously distributed over the aquifer with contaminant concentration, g_0 [mg l^{-1}], and microbial background mass, m_0 [mg l^{-1}]. The electron acceptor concentration is the limiting factor for biodegradation, and it is initially equal to zero:

$$c = 0, \quad g = g_0, \quad m = m_0 \quad \text{for } x_1 \geq 0 \quad \text{at } t = 0. \quad (6.5)$$

The electron acceptor is injected to enhance biodegradation, hence constant electron acceptor and contaminant concentrations are imposed at the inlet of the domain.

$$c = c_0, \quad g = 0 \quad \text{for } t > 0 \quad \text{at } x_1 = 0. \quad (6.6)$$

At the outlet, purely advective mass fluxes for electron acceptor and contaminant are considered,

$$\frac{\partial c}{\partial x_1} = 0, \quad \frac{\partial g}{\partial x_1} = 0 \quad \text{for } t > 0 \quad \text{at } x_1 = L. \quad (6.7)$$

As pore-scale dispersion and molecular diffusion are neglected, the Lagrangian approach [7, 8, 10, 12, 13] can be applied to determine the averaged contaminant mass flux in a heterogeneous aquifer. In this approach the distribution of the contaminant along a trajectory should be known. To determine this distribution, we transform the above system of equations (6.2)-(6.4) onto a random stream tube centered on $x_2 = \eta$, $x_3 = \zeta$ which yields a system of equations of Lagrangian form, see Cvetkovic and Dagan [7],

$$R \frac{\partial g}{\partial t} = -\frac{\partial g}{\partial \tau} - m_g \frac{\partial m}{\partial t}, \quad (6.8)$$

$$\frac{\partial c}{\partial t} = -\frac{\partial c}{\partial \tau} - m_c \frac{\partial m}{\partial t}, \quad (6.9)$$

$$\frac{\partial m}{\partial t} = \mu_m \left(\frac{c}{k_c + c} \right) \left(\frac{g}{k_g + g} \right) m, \quad (6.10)$$

where now t and the travel time $\tau (= x_1/U)$ are the independent variables, instead of t and x . The initial and boundary conditions change into

$$\begin{aligned} c(\tau, 0) &= 0, & g(\tau, 0) &= g_0, & m(\tau, t) &= m_0, \\ c(0, t) &= c_0, & g(0, t) &= 0, & & \\ \frac{\partial c}{\partial \tau} \left(\frac{L}{U}, t \right) &= 0, & \frac{\partial g}{\partial \tau} \left(\frac{L}{U}, t \right) &= 0. & & \end{aligned} \quad (6.11)$$

In case pore-scale dispersion and molecular diffusion are not neglected, Oya and Valocchi [27] and Keijzer et al. [23] show numerically that in homogeneous aquifers traveling waves may develop for the contaminant, electron acceptor and microbial mass. Assuming that this traveling wave behavior has developed, Keijzer et al. [24] derive semi-analytical solutions that describe the distribution of the contaminant and electron acceptor concentration and the microbial mass. To determine these distributions, they transform the system of equations into a nonlinear second order ordinary differential equation (ODE) system, using two newly defined functions of

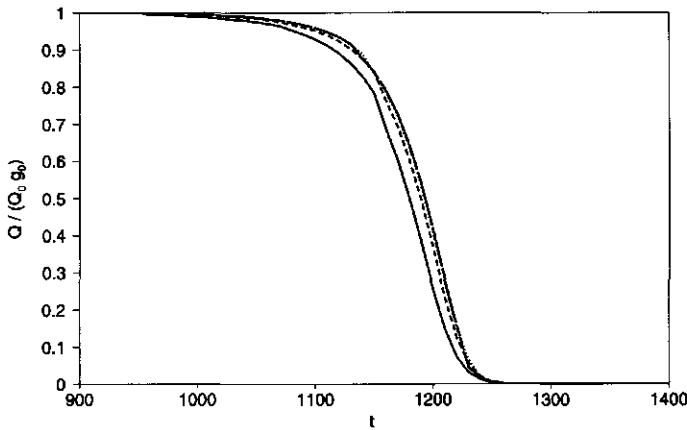


FIGURE 6.1. The breakthrough curves at $x_1 = 100\text{m}$ for different values of α_l . Solid line: $\alpha_l = 0.2\text{m}$, dashed line: $\alpha_l = 0.05\text{m}$, dotted line: $\alpha_l = 5.0 \cdot 10^{-3}\text{m}$, dashed-dotted line: $\alpha_l = 5.0 \cdot 10^{-6}\text{m}$ and long-dashed line: $\alpha_l = 5.0 \cdot 10^{-9}\text{m}$.

c , i.e., u and w [24]

$$u(c) = -\frac{\partial c}{\partial \tau}, \tag{6.12}$$

$$w(c) = \frac{\partial g}{\partial \tau}. \tag{6.13}$$

The nonlinear second order ODE system is solved using an iterative procedure. In each iteration step, u and w are determined by Newton's method. After the iteration, the function u is integrated numerically from a reference point with a designated chosen c . Therefore, the solutions are unique up to a constant translate which is determined by mass balance considerations.

Figure 6.1 shows the semi-analytically determined breakthrough curves (BTC) of the biodegradable contaminant at the CP, $x_1 = 100\text{m}$, for different dispersivities α_l which characterizes the pore-scale dispersion. The other physical and biochemical parameter values used to obtain this figure are given in Table 6.1. For these parameter values, the biodegradation is limited by the microbial growth and the presence of the electron acceptor since, respectively, μ_m is small and k_c is large. Hence, the resulting breakthrough curve is rather spread [25]. It can be seen that decreasing the dispersivity below 0.005 m has no effect on the breakthrough curve. Hence, the semi-analytical solution of Keijzer et al. [24] with $\alpha_l < 0.005$ corresponds excellently with the solution of the system of equations (6.8)-(6.10) with zero pore-scale dispersion and no molecular diffusion.

TABLE 6.1. Parameters values.

Parameter	value	Parameter	value
μ_m	0.05 day ⁻¹	c_0	10.0 mg/l
m_c	1.0 mg/mg	g_0	5.0 mg/l
m_g	5.0 mg/mg	m_0	0.427 mg/l
k_c	1.0 mg/l	U	0.1 m/day
k_g	2.0 mg/l	n	0.4
R	3.0	x_1	100.0 m

Contaminant mass flux

In the following we only determine the averaged contaminant mass flux, observing that the same procedure can be applied for the averaged electron acceptor mass flux. The contaminant mass flux at a point in the CP is defined by Dagan and Cvetkovic [14]

$$q = ng(\tau, t)V_1(x_1; \mathbf{a}) \quad (6.14)$$

where $g(\tau, t)$ results from equation (6.8) and \mathbf{a} is a point in the injection plane (IP) where the solute particle starts from. We use the Eulerian fluid continuity equation $V_1 dA = V_0 dA_0$, where V_0 is the x_1 component of the fluid velocity in the IP with area A_0 , and equation (6.14) to derive the contaminant mass flux Q through the entire CP with area A [14]

$$Q(t; x_1) = \int_A q dA = \int_{A_0} ng(\tau, t)V_0(\mathbf{a})dA_0. \quad (6.15)$$

A deterministic evaluation of Q from (6.15) is feasible if V_0 and τ are known functions of \mathbf{a} for all points within A_0 . Because V_0 and τ are RFSs, Q can not be evaluated in a deterministic manner. Hence, Q is characterized by its statistical moments. The expected contaminant mass flux through the entire CP at x_1 is given by, see Cvetkovic and Dagan [14],

$$\langle Q(t; x_1) \rangle = \langle Q_0 \rangle \int_0^\infty g(\tau, t) \bar{g}_1(\tau; x_1) d\tau, \quad (6.16)$$

where $\langle Q_0 \rangle = nUA_0$ is the mean fluid discharge through A_0 or A , and $\bar{g}_1(\tau; x_1)$ denotes the probability density function of travel time derived by Cvetkovic and Dagan [8], see appendix. Because the reaction along a trajectory does not depend on the spatially variable advection, separate expressions for these processes are used in equation (6.16), i.e. $g(\tau, t)$ and $\bar{g}_1(\tau; x_1)$, respectively. If $g(\tau, t)$ and $\bar{g}_1(\tau; x_1)$ are known, $\langle Q(t; x_1) \rangle$ can be obtained with a single numerical integration.

If the ergodic hypothesis is valid, which is the case if A_0 and A are sufficiently large relative to the transverse integral scale I_3 , then $Q \cong \langle Q \rangle$. If transport is nonergodic, equation (6.16) represents a best estimate of the field-scale contaminant mass flux. Berglund [1] quantifies the uncertainty in $\langle Q \rangle$ as

$$\begin{aligned} \sigma_Q^2(t; x_1) &= (nU)^2 \int \int_{A_0} \int_{\tau} g(\tau, t) g(\tau', t) \bar{g}_2(\tau, \tau'; x_1, \mathbf{a}, \mathbf{a}') d\tau d\tau' da da' \\ &- \langle Q(t; x_1) \rangle^2 \end{aligned} \quad (6.17)$$

where \bar{g}_2 is defined in analogy with \bar{g}_1 . Whereas for \bar{g}_1 an analytical expression is derived [8], an analytical expression for \bar{g}_2 remains to be found. Berglund [1] discusses that $\sigma_Q^2(t; x_1) = 0$ when the ergodic hypothesis is valid and defines an upper limit for $\sigma_Q^2(t; x_1)$ assuming complete nonergodic conditions and far-field transport ($x_1 \gg I$). In the discussion we determine this upper limit for our problem.

RESULTS

If we consider a heterogeneous site contaminated with a specific organic contaminant and we assume that indigenous micro-organism populations are present that can biodegrade the contaminant, some of the physical and biochemical parameters are fixed as we consider that we can not influence their values. We assume that the physical parameter n is fixed. Furthermore, the biochemical parameters k_g , m_g , g_0 , μ_m and m_0 are fixed because the contaminant and micro-organisms present are known. The values of these fixed parameters are given in Table 6.1. The physical parameters x_1 and U can be adapted as, respectively, different observation points and injection velocities can be imposed, and the biochemical parameters k_c , m_c and c_0 can be adapted because different electron acceptors at different injection concentrations can be injected. These physical and biochemical parameters are from now on referred to as control parameters and their values for the reference case are given in Table 6.1. We also consider that the relative retardation factor R is a control parameter because R depends on the chosen injected electron acceptor [25].

The transport and nonlinear biodegradation takes place in heterogeneous aquifers. The degree of heterogeneity depends on the parameters that determine the statistics of the hydraulic conductivity, i.e. σ_Y^2 , I and $e = I_3/I$. The integral scale I and the anisotropy ratio e are kept constant at, respectively, 1 m and 0.2. The variance σ_Y^2 varies from 0.0 to 1.0, to mimic homogeneous to strongly heterogeneous aquifers.

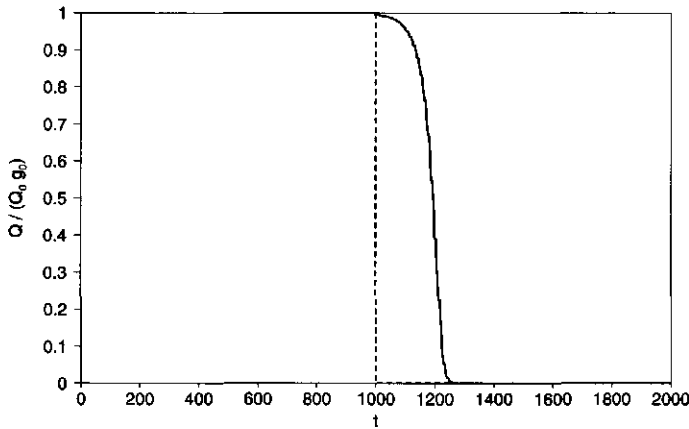


FIGURE 6.2. The breakthrough curve of a conservative solute (dashed line) and a nonlinear biodegradable contaminant (solid line) in a homogeneous aquifer.

To compare results, we scale the expected mass flux, length and time variables to dimensionless variables, using

$$\langle Q' \rangle = \frac{\langle Q \rangle}{\langle Q_0 \rangle g_0}, \quad x'_1 = \frac{x_1}{I}, \quad t' = \frac{t\alpha U}{I},$$

with α the dimensionless traveling wave velocity which is given by [24]

$$\alpha = \left(\frac{1 + \frac{m_c g_0}{m_g c_0}}{1 + R \frac{m_c g_0}{m_g c_0}} \right). \quad (6.18)$$

Effect of nonlinear biodegradation

We briefly show the influence of nonlinear biodegradation on the transport of a biodegradable solute. Figure 6.2 shows the breakthrough curve of a conservative solute and a biodegradable contaminant at $x'_1 = 100$ in a homogeneous aquifer. Comparing these breakthrough curves, we observe that the conservative solute reaches the CP earlier than the biodegradable contaminant. Hence, nonlinear biodegradation causes retardation as is found by Oya and Valocchi [27] and Keijzer et al. [23]. Furthermore, the breakthrough curve of the conservative solute shows a plug flow behavior as pore-scale dispersion and molecular diffusion are neglected and no spreading occurs. The breakthrough curve of the biodegradable contaminant is more gradual and depends on the biochemical parameter values used, see Oya and Valocchi [27] and Keijzer et al. [23].

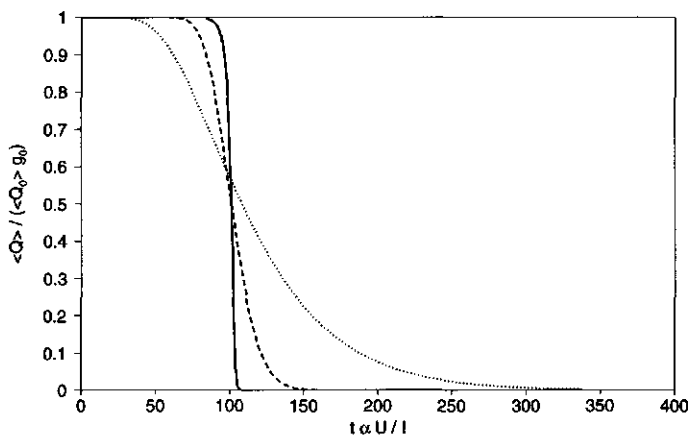


FIGURE 6.3. The expected normalized contaminant mass flux, breakthrough curve, for a homogeneous aquifer (solid line) and two heterogeneous aquifers ($\sigma_Y^2 = 0.1$: dashed line and $\sigma_Y^2 = 1.0$: dotted line).

Effect of heterogeneity and nonlinear biodegradation

To assess the interaction between physical heterogeneity and nonlinear biodegradation, we compare the dimensionless averaged contaminant mass flux $\langle Q' \rangle$ as a function of time under homogeneous and heterogeneous conditions for different values of the physical and biochemical control parameters. Under ergodic conditions $\langle Q' \rangle$ is also referred to as the breakthrough curve [14]. First, we consider the influence of the degree of heterogeneity. Figure 6.3 shows the breakthrough curves of the reference case for a homogeneous aquifer ($\sigma_Y^2 = 0.0$) and two heterogeneous aquifers ($\sigma_Y^2 = 0.1$ and $\sigma_Y^2 = 1.0$). It can be seen that incorporation of heterogeneity leads to a spreading of the breakthrough curve which is also found by Berglund and Cvetkovic [2] for nonlinear sorption, and by Xin and Zhang [33] and Kaluarachchi [21] for nonlinear biodegradation.

Secondly, we vary one of the biochemical control parameters for the same homogeneous and heterogeneous aquifers. Depending on the chosen electron acceptor, k_c , m_c and R have specific values and the injection concentration, c_0 , depends on the solubility of the injected electron acceptor. Figure 6.4.a-d show the breakthrough curves for three different values of k_c , m_c , R and c_0 , respectively. It can be seen that in the homogeneous formation the breakthrough curve is more spread for increasing k_c or R or decreasing m_c or c_0 , which is also found by Oya and Valocchi [27] and Keijzer et al. [25] for the contaminant front. Incorporation of heterogeneity

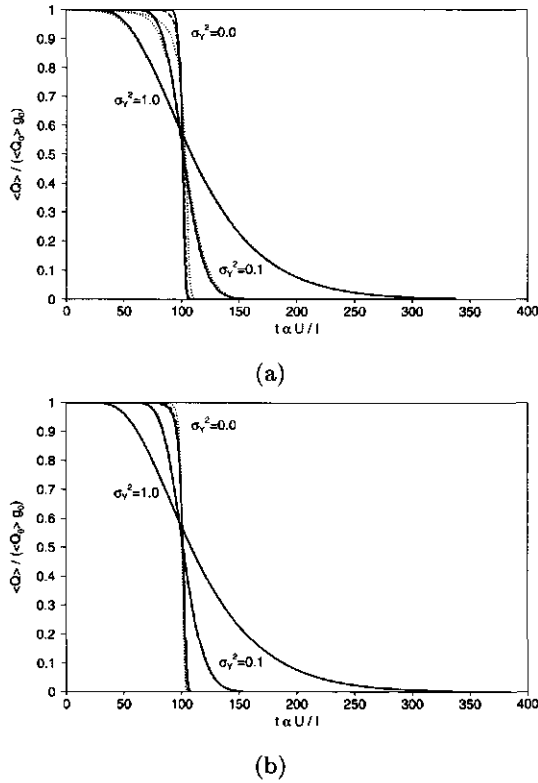
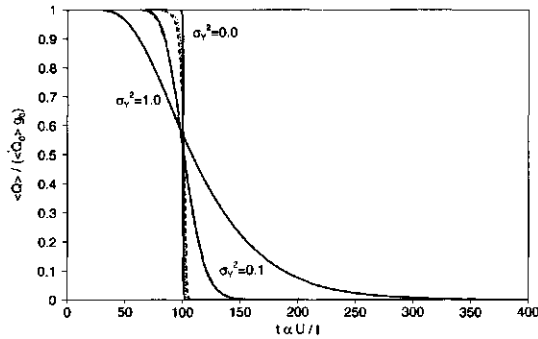


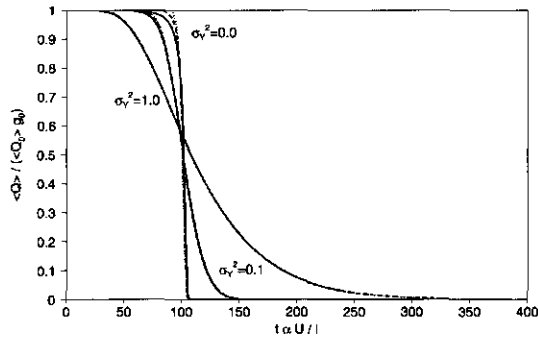
FIGURE 6.4. The expected normalized contaminant mass flux for a homogeneous aquifer $\sigma_Y^2 = 0.0$ and two heterogeneous aquifers ($\sigma_Y^2 = 0.1$ and $\sigma_Y^2 = 1.0$) for different values of the biochemical control parameters. (a) Different values for k_c : $k_c = 0.2$ mg/l (solid line), $k_c = 1.0$ mg/l (dashed line) and $k_c = 5.0$ mg/l (dotted line). (b) Different values for m_c : $m_c = 0.2$ mg/mg (solid line), $m_c = 1.0$ mg/mg (dashed line) and $m_c = 5.0$ mg/mg (dotted line).

results in a smaller difference in breakthrough curves for varying k_c , m_c , R or c_0 separately. For a stronger degree of heterogeneity ($\sigma_Y^2 = 1.0$) there is no significant difference in the breakthrough curves anymore.

If necessary the imposed injection velocity can be increased, although not to an arbitrary value as it is restricted by the soil type. Therefore, we vary V_1 and Figure 6.5 shows the breakthrough curves for three different values of V_1 . For the homogeneous aquifer the breakthrough curve is more spread for decreasing V_1 . Again, this difference diminishes if the degree of heterogeneity increases.



(c)



(d)

FIGURE 6.4. (Continued.) (c) Different values for R : $R = 1.03$ (solid line), $R = 3.0$ (dashed line) and $R = 15.0$ (dotted line). (a) Different values for c_0 : $k_c = 2.0$ mg/l (solid line), $c_0 = 10.0$ mg/l (dashed line) and $c_0 = 50.0$ mg/l (dotted line).

If we compare the breakthrough curves for all the biochemical control parameters and V_1 , see Figure 6.4.a-d and 6.5, we gain a remarkable insight. For strongly heterogeneous aquifers (e.g. $\sigma_Y^2 = 1.0$) there is no difference between the obtained breakthrough curves. So the shape of the breakthrough curve is determined by heterogeneity. Furthermore, we have to be aware that the results in Figure 6.4.a-d and 6.5 are given in dimensionless form. For that reason, time is scaled with the traveling wave velocity (αU). The biochemical control parameters m_c , R and c_0 , and the physical control parameter V_1 influence this traveling wave velocity, see equation (6.18), decreasing m_c or R , or increasing c_0 or V_1 results in an earlier breakthrough.

Finally, the position of the control plane x'_1 may equally be of interest for a contaminated site. To determine the influence of x_1 on the shape of

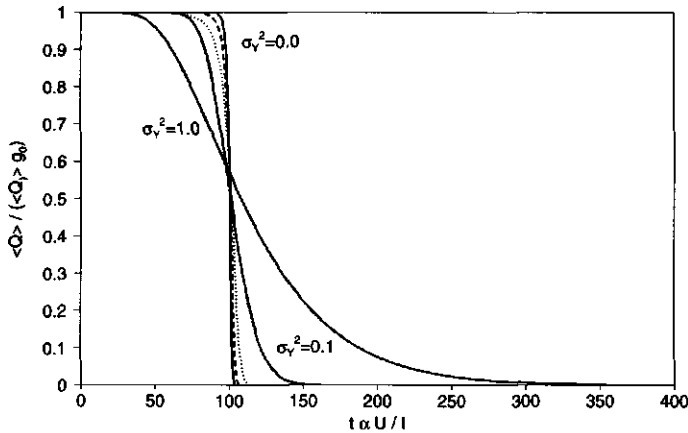


FIGURE 6.5. The expected normalized contaminant mass flux for a homogeneous aquifer $\sigma_Y^2 = 0.0$ and two heterogeneous aquifers ($\sigma_Y^2 = 0.1$ and $\sigma_Y^2 = 1.0$) for three different values of the injection velocity. Solid line: $V_1 = 0.02$ m/day, dashed line: $V_1 = 0.1$ m/day and $V_1 = 0.5$ m/day.

the breakthrough curve developed in the homogeneous and the two heterogeneous aquifers, we derive the temporal moments associated with the breakthrough curve. Dagan and Cvetkovic [14] quantify the mean mass arrival time by the first temporal moment

$$\langle T \rangle = \int_0^\infty t \frac{\partial \langle Q'(t; x_1) \rangle}{\partial t} dt. \quad (6.19)$$

The spreading of the breakthrough curve around $\langle T \rangle$ is quantified by the second central temporal moment [14]

$$\Sigma_T^2 = \int_0^\infty (t - \langle T \rangle)^2 \frac{\partial \langle Q'(t; x_1) \rangle}{\partial t} dt. \quad (6.20)$$

Figure 6.6 shows $\langle T \rangle$ and Σ_T^2 as a function of the CP position x'_1 . As expected, we observe that the mean mass arrival time increases linearly with x'_1 for all formations. The mean mass arrival time is only slightly retarded for the heterogeneous formations. For the homogeneous formation, the spreading of the breakthrough curve is independent of x'_1 since a traveling wave develops [23, 27]. On the other hand, for the heterogeneous formations, the spreading of the breakthrough curve has a linear dependence on x'_1 which is characteristic for a diffusion process, hence, a Fickian behavior is found. Furthermore, Figure 6.6 clearly shows that an increase

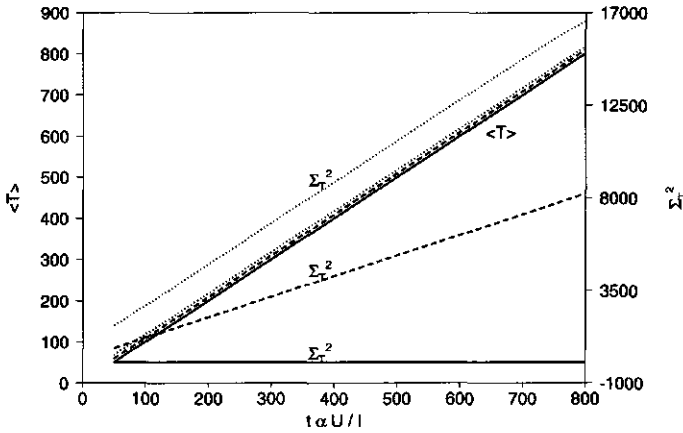


FIGURE 6.6. The mean mass arrival time ($\langle T \rangle$) and the spreading around $\langle T \rangle$ (Σ_T^2) as a function of t' for a homogeneous $\sigma_Y^2 = 0.0$ (solid line) and two heterogeneous aquifers, $\sigma_Y^2 = 0.5$ (dashed line) and $\sigma_Y^2 = 1.0$ (dotted line), respectively.

in the degree in heterogeneity results in a spreading of the breakthrough curve as was also shown in Figure 6.3.

DISCUSSION

Effect of pore-scale dispersion

In the applied Lagrangian approach pore-scale dispersion is neglected. Fiori [17] has shown that for a conservative solute pore-scale dispersion has only a minor impact on the longitudinal macrodispersion for most field situations. Berglund and Fiori [3] perform a temporal moment analysis to show that linear sorption kinetics decrease the effect of pore-scale dispersion on the field-scale transport characteristics (temporal moments) as compared to the nonreactive case. They note that their results are associated with a single linearly sorbing solute, hence more pronounced effects of pore-scale dispersion can be expected in other cases. This is the case, for example, if mixing of interacting compounds occur [22], or if the reaction is controlled by transverse mixing in steady state flow fields [6] as is the case in bioremediation.

Cirpka and Kitanidis [5] determine the influence of pore scale dispersion comparing the temporal moments of the local breakthrough curve to the spatially integrated breakthrough curves. They show that at very large travel distances $x_1 \gg I$ pore-scale dispersion can be neglected. For smaller distances, they develop the advective-dispersive stream tube approach to

include pore-scale dispersion. This approach differs in two aspects from the Lagrangian approach. First, data of a tracer, that undergoes pore-scale dispersion in a heterogeneous aquifer, is used to determine the travel time pdf and an apparent Peclet number of mixing. Secondly, in the derivation of the solute distribution along a stream tube both advection and longitudinal dispersion are accounted for. Cirpka and Kitanidis apply this approach to mixing-controlled reactive transport [4] and show that the Lagrangian approach leads to an underestimation of the reaction rate, whereas the breakthrough curve of the advective-dispersive stream tube approach show an excellent overall agreement with numerical 2D calculations.

In our reference case $x_1 = 100\text{m}$ and $I = 1\text{m}$, i.e., $x_1 \gg I$ and neglecting pore-scale dispersion is justified. If x_1 were small, we could apply the advective-dispersive stream tube approach. The only difficulty would be the determination of the travel time pdf as no analytical expressions are given for the temporal moments of the travel time. Therefore, Cirpka and Kitanidis [4] determine these temporal moments numerically. The inclusion of longitudinal dispersion in the one-dimensional calculations is easily done by including the apparent Peclet number of mixing in the semi-analytical solution of Keijzer et al. [24]. Considering the result of Cirpka and Kitanidis [4], we expect that our results underestimate the biodegradation rate as we neglect pore-scale dispersion, in case x_1 is small.

Effect of nonergodic conditions

If A or A_0 are small relative to the transverse integral scale I_3 then transport is nonergodic. The uncertainty arising in nonergodic transport can be quantified by means of the variance of the contaminant mass flux, see equation (6.17). Since no analytical expression for \bar{g}_2 has been found yet, we determine a lower and upper limit of σ_Q^2 . The σ_Q^2 in ergodic transport equals zero which yields the lower limit. The σ_Q^2 in complete nonergodic transport yields the upper limit [1]. Complete nonergodic conditions imply that the whole contaminant plume is contained within a single stream tube. Hence, the transport domain consists of one stream tube. Moreover, if far-field transport, $x_1 \gg I$ is considered, Berglund [1] shows that the variance of the contaminant mass flux can be simplified to equation (A9) given in the Appendix.

To determine the upper limit of σ_Q^2 , we use the one-particle pdf $\bar{g}(\tau; x_1)$ which is obtained by neglecting the correlation between τ and V_0 , see equation (A12) in the Appendix. Figure 6.7 shows the expected normalized contaminant mass flux and the standard deviation of the normalized contaminant mass flux for two degrees of heterogeneity. The results were

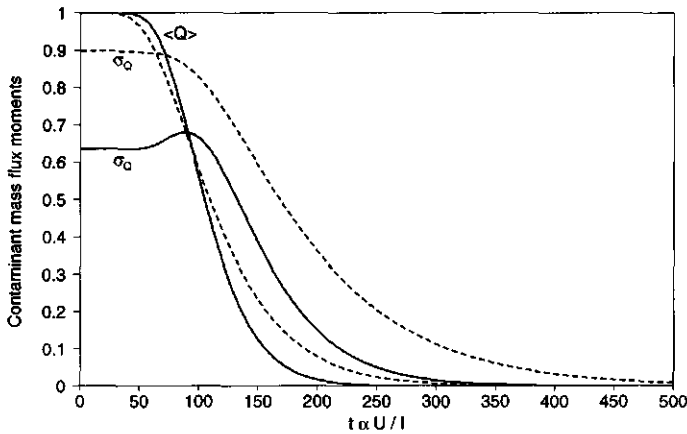


FIGURE 6.7. The expected value and the standard deviation of the normalized contaminant mass flux for two heterogeneous aquifers, $\sigma_Y^2 = 0.5$ (solid lines) and $\sigma_Y^2 = 1.0$ (dashed lines).

obtained by using the reference case parameter values given in Table 6.1. As $x_1 = 100\text{m}$ and $l = 1\text{m}$ the far-field assumption is applicable.

From Figure 6.7, we observe that the standard deviation approaches a constant values when $t \rightarrow 0$. Berglund [1] evaluates this constant as $\sigma'_Q(t \rightarrow 0) = \sigma_Y \sqrt{b(e)}$ which equals 0.62 and 0.88 for $\sigma_Y^2 = 0.5$ and $\sigma_Y^2 = 1.0$, respectively, thus this evaluation is applicable. For $\sigma_Y^2 = 0.5$, σ'_Q increases with time to reach a maximum, which coincides with the largest slope in the curve for $\langle Q' \rangle$. This peak behavior is not found for a higher degree of heterogeneity. Furthermore, the standard deviations show a more distinct tailing than their associate expected values. The difference in tailing between $\langle Q' \rangle$ and σ'_Q is smaller for the smaller degree of heterogeneity. Hence, increasing the degree of heterogeneity results in an increase in uncertainty.

SUMMARY AND CONCLUSIONS

We studied the interaction between flow heterogeneity and nonlinear biodegradation, using the Lagrangian approach to determine the expected normalized contaminant mass flux. In the approach, the semi-analytical solution of Keijzer et al. [24] is used to derive the distribution of the contaminant along a stream tube.

The effect of heterogeneity is illustrated by using reference case values for the biochemical and physical parameters and by considering a homogeneous and two heterogeneous aquifers. The results showed that heterogeneity leads to a spreading in the breakthrough curve. Moreover, if the degree of heterogeneity is high, e.g. $\sigma_Y^2 = 1.0$, variation of the biochemical or physical control parameters has no effect on the resulting breakthrough curves. Hence, for strongly heterogeneous aquifers the shape of the breakthrough curve is controlled by heterogeneity and not by the values of the control parameters.

A key parameter of in situ bioremediation is the 99% remediation time, which is the time at which 99% of the initially present contaminant is either biodegraded or flushed out of the domain of interest. For a homogeneous aquifer, the 99% remediation time depends on the value of the biochemical and physical control parameters as is shown by Keijzer and van der Zee [25]. For strongly heterogeneous aquifers, the shape of the breakthrough curve is determined by the heterogeneity, hence, the 99% remediation time depends on the degree of heterogeneity. Moreover, for the parameters that influence the traveling wave velocity, e.g. m_c , R , c_0 and V_1 , we have to rescale the normalized 99% remediation time to obtain the real 99% remediation time.

We determined the influence of the control plane position on the breakthrough curve, using the temporal first and second central moment, i.e. the mean mass arrival time and the spreading around this time, respectively. The results showed that the constant front velocity developed in the heterogeneous formations is slightly retarded compared to the traveling wave velocity developed in the homogeneous formation. Moreover, the spreading of the breakthrough curve in the heterogeneous formations has a linear dependence on the control plane position, hence a Fickian behavior is found.

In the Lagrangian approach, two important assumptions were made: pore-scale dispersion and molecular diffusion are neglected and ergodic conditions are assumed. Neglecting pore-scale dispersion and molecular diffusion is justified if the length of the domain (x_1) is large relative to the longitudinal integral scale (I). In our reference case $x_1 = 100\text{m}$ and $I = 1\text{m}$, hence, pore-scale dispersion and molecular diffusion may be neglected. If x_1 would be small, we could apply the advective-dispersive stream tube approach of Cirpka and Kitanidis [4]. They applied this approach to mixing-controlled reactive transport and showed an excellent agreement between the results of the advective-dispersive stream tube approach and numerical 2D calculations.

The ergodic hypothesis is valid, if A and A_0 are large relative to the transverse integral scale I_3 . If ergodic conditions hold, the uncertainty of the expected contaminant mass flux, σ_Q^2 , equals zero which can be seen as the lower limit. The upper limit of σ_Q^2 can be found in case complete nonergodic conditions hold, then the whole plume is contained within a single stream tube. In case also far-field transport is assumed, i.e. $x_1 \gg I$, an analytical expression for σ_Q^2 can be found, see the Appendix. The determined standard deviation for the reference case showed that increasing the degree of heterogeneity resulted in a larger σ_Q and a larger difference between $\langle Q \rangle$ and σ_Q .

APPENDIX

For the evaluation of the expected contaminant mass flux, we need to determine the pdf of travel time $\bar{g}_1(\tau; x_1)$ which is defined by

$$\bar{g}_1(\tau; x_1) = \frac{1}{U} \int_{V_0} V_0 g_{v\tau,1}(V_0, \tau; x_1) dV_0. \quad (\text{A1})$$

Cvetkovic and Dagan [8] use a first-order expression to derive the pdf $\bar{g}_1(\tau; x_1)$, which restricts the applicability to low degrees of spatial variability. It is strictly valid for $\sigma_Y^2 \ll 1$. However, a comparison of analytical and numerical results by Selroos and Cvetkovic [29] showed that the first-order results are robust for a variability at least as large as $\sigma_Y^2 = 1$. The expression for $\bar{g}(\tau; x_1)$ given by Cvetkovic and Dagan is

$$\bar{g}_1(\tau; x_1) = \frac{1}{U} \left\{ \frac{\partial}{\partial \tau} \left(\frac{D_0}{\sqrt{X_{II}}} \right) - \left[U + \frac{(x_1 - U\tau)D_0}{X_{II}} \right] \frac{\partial}{\partial \tau} \left(\frac{x_1 - U\tau}{\sqrt{X_{II}}} \right) \right\} \frac{1}{\sqrt{2\pi}} \exp \left(-\frac{(x_1 - U\tau)^2}{2X_{II}} \right), \quad (\text{A2})$$

where the functions X_{II} and D_0 are given by

$$\frac{X_{II}(\tau', e)}{I^2 \sigma_Y^2} = \frac{2}{b} [\tau' b + \exp(-\tau' b) - 1], \quad (\text{A3})$$

$$\frac{D_0(\tau')}{IU \sigma_Y^2} = [1 - \exp(-\tau' b)]. \quad (\text{A4})$$

In these functions, τ' is the dimensionless travel time, $\tau' = \tau U / I$ and e is the anisotropy ratio, $e = I_3 / I$. The function b is given by

$$b(e) = 1 + \frac{19e^2 - 10e^4}{16(e^2 - 1)^2} - \frac{e(13 - 4e^2) \sin^{-1}(\sqrt{1 - e^2})}{16\sqrt{1 - e^2}(e^2 - 1)^2}, \quad 0 \leq e \leq 1. \quad (\text{A5})$$

For the evaluation of the variance of the contaminant mass flux for nonergodic conditions we need to determine the pdf \bar{g}_2 which is defined in analogy with \bar{g}_1

$$\bar{g}_2(\tau, \tau'; x_1, \mathbf{a}, \mathbf{a}') = \frac{1}{U^2} \int \int_{V_0} V_0 V_0' g_{v\tau,2}(V_0, V_0', \tau, \tau'; x_1, \mathbf{a}, \mathbf{a}') dV_0 dV_0'. \quad (\text{A6})$$

Since for complete nonergodic conditions the transport domain consists of one streamtube, the joint pdf of V_0 and τ at two different points in A_0 , $g_{v\tau,2}$ can be written as [1, 10]

$$g_{v\tau,2}(V_0, V_0', \tau, \tau'; x_1, \mathbf{a}, \mathbf{a}') = g_{v\tau,1}(V_0, \tau; x_1) \delta(V_0 - V_0') \delta(\tau - \tau'). \quad (\text{A7})$$

Substitution of equation (A6) and (A7) in equation (6.17) yields

$$\begin{aligned} \sigma_Q^2(t; x_1) &= (nUA_0)^2 \int_{\tau} \int_{V_0} \frac{V_0^2}{U^2} (g(\tau, t))^2 g_{v\tau,1}(V_0, \tau; x_1) dV_0 d\tau \\ &- \langle Q(t; x_1) \rangle^2. \end{aligned} \quad (\text{A8})$$

For far-field transport, $x_1 \gg I$, V_0 and τ are uncorrelated and equation (A8) changes into [1]

$$\sigma_Q^2(t; x_1) = (nUA_0)^2 \frac{\langle V_0^2 \rangle}{U^2} \int_{\tau} (g(\tau, t))^2 \bar{g}(\tau; x_1) d\tau - \langle \bar{Q}(t; x_1) \rangle^2, \quad (\text{A9})$$

where

$$\frac{\langle V_0^2 \rangle}{U^2} = \frac{\sigma_{V_0}^2}{U^2} + 1 = \sigma_Y^2 b(e) + 1, \quad (\text{A10})$$

and $\langle \bar{Q}(t; x_1) \rangle$ is the expected contaminant mass flux obtained with the far-field approximation which yields

$$\langle \bar{Q}(t; x_1) \rangle = \langle Q_0 \rangle \int_0^{\infty} g(\tau, t) \bar{g}(\tau; x_1) d\tau. \quad (\text{A11})$$

Furthermore, $\bar{g}(\tau; x_1)$ results from equation (A2), considering that V_0 and τ are uncorrelated, hence $D_0 = 0$

$$\bar{g}(\tau; x_1) = -\frac{\partial}{\partial \tau} \left(\frac{x_1 - U\tau}{\sqrt{X_{11}}} \right) \frac{1}{\sqrt{2\pi}} \exp \left[-\frac{(x_1 - U\tau)^2}{2X_{11}} \right]. \quad (\text{A12})$$

REFERENCES

- [1] Berglund, S. 1997 *Groundwater Contamination: Significance of hydrochemical processes for remediation and impact evaluation* Ph.D. desertation. Royal Insitute of Technology, Stockholm, Sweden.

- [2] Berglund, S. & V.D. Cvetkovic 1996. Contaminant displacement in aquifers: Coupled effects of flow heterogeneity and nonlinear sorption. *Water Resources Research* 32:23-32.
- [3] Berglund, S. & A. Fiori 1997. Influence of transverse mixing on the breakthrough of sorbing solute in a heterogeneous aquifer. *Water Resources Research* 33:399-405.
- [4] Cirpka, O.A. & P.K. Kitanidis 2000. An advective-dispersive stream tube approach for the transfer of conservative-tracer data to reactive transport. *Water Resources Research* 36:1209-1220.
- [5] Cirpka, O.A. & P.K. Kitanidis 2000. Characterization of mixing and dilution in heterogeneous aquifers by means of local temporal moments. *Water Resources Research* 36:1221-1236.
- [6] Cirpka, O.A., E.O. Frind & R. Helmig 1999. Numerical simulations of biodegradation controlled by transverse mixing. *J. Cont. Hydrology* 40:159-182.
- [7] Cvetkovic, V.D. & G. Dagan 1994. Transport of kinetically sorbing solute by steady random velocity in heterogeneous porous formations. *J. Fluid Mech.* 265:189-215.
- [8] Cvetkovic, V.D. & G. Dagan 1996. Reactive transport and immiscible flow in geological media. II. Applications. *Proc. R. Soc. Lond. A* 452:303-328.
- [9] Cvetkovic, V.D. & A.M. Shapiro 1990. Mass arrival of sorptive solute in heterogeneous porous media. *Water Resources Research* 26:2057-2067.
- [10] Cvetkovic, V.D., A.M. Shapiro & G. Dagan 1992. A solute flux approach to transport in heterogeneous formations 2. Uncertainty analysis. *Water Resources Research* 28:1377-1388.
- [11] Dagan, G. *Flow and transport in heterogeneous formations*, Springer-Verlag, New York, 1989.
- [12] Dagan, G., V.D. Cvetkovic & A.M. Shapiro 1992. A solute flux approach to transport in heterogeneous formations 1. The general framework. *Water Resources Research* 28:1369-1376.
- [13] Dagan, G. & V.D. Cvetkovic 1993. Spatial moments of a kinetically sorbing solute plume in a heterogeneous aquifer. *Water Resources Research* 29:4053-4061.
- [14] Dagan, G. & V.D. Cvetkovic 1996. Reactive transport and immiscible flow in geological media. I. General theory. *Proc. R. Soc. Lond. A* 452: 285-301.
- [15] Destouni, G. 1991. Prediction uncertainty in solute flux through heterogeneous soil. *Water Resources Research* 28:793-801.
- [16] Destouni, G. & W. Graham 1995. Solute transport through an integrated heterogeneous soil-groundwater system. *Water Resources Research* 31:1935-1944.
- [17] Fiori, A. 1996. Finite Peclet extensions of Dagan's solutions to transport in anisotropic heterogeneous formations. *Water Resources Research* 32:193-198.
- [18] Gelhar, L.W. 1986. Stochastic subsurface hydrology from theory to applications. *Water Resources Research* 22:135S-145S.
- [19] Ginn, T.R., C.S. Simmons & B.D. Wood 1995. Stochastic-convective transport with nonlinear reaction: Biodegradation with microbial growth. *Water Resources Research* 31:2689-2700.
- [20] Helfferich, F. 1981. Theory of multicomponent, multiphase displacement in porous media. *Soc. Pet. Eng. J.* 21:51-62.
- [21] Kaluarachchi, J.J., V.D. Cvetkovic & S. Berglund 2000. Stochastic analysis of oxygen- and nitrate-bases biodegradation of hydrocarbons in aquifers. *J. Cont. Hydrology* 41:335-365.

- [22] Kapoor, V., L.W. Gelhar & F. Miralles-Wilhelm 1997. Bimolecular second-order reaction in spatially varying flows: Segregation induced scale-dependent transformation rates. *Water Resources Research* 33:527-536.
- [23] Keijzer, H., M.I.J. van Dijke & S.E.A.T.M. van der Zee 1999. Analytical approximation to characterize the performance of in situ aquifer bioremediation. *Adv. Water Resources* 23:217-228.
- [24] Keijzer, H., R.J. Schotting, & S.E.A.T.M. van der Zee 2000. Semi-analytical traveling wave solution of one-dimensional aquifer bioremediation. *Comm. on Appl. Nonl. Anal.* 7:1-20.
- [25] Keijzer, H. & S.E.A.T.M. van der Zee 2000. Effect of physical, chemical and biochemical processes on the performance of one-dimensional in situ aquifer bioremediation. in prep.
- [26] Monod, J. 1949. The growth of bacterial cultures. *Ann. Rev. of Microb.* 3: 371-394.
- [27] Oya, S. & A.J. Valocchi 1997. Characterization of traveling waves and analytically estimation of pollutant removal in one-dimensional subsurface bioremediation modeling. *Water Resources Research* 33:1117-1127.
- [28] Selroos, J.O. & V.D. Cvetkovic 1992. Modeling solute advection coupled with sorption kinetics in heterogenous formations. *Water Resources Research* 28:1271-1278.
- [29] Selroos, J.O. & V.D. Cvetkovic 1994. Mass flux statistics of kinetically sorbing solute in heterogeneous aquifers: Analytical solution and comparison with simulations. *Water Resources Research* 30:63-69.
- [30] Shapiro, A.M. & V.D. Cvetkovic 1988. Stochastic analysis of solute arrival time in heterogeneous porous media. *Water Resources Research* 24:1711-1718.
- [31] Simmons, C.S., T.R. Ginn & B.D. Wood 1995. Stochastic-convective transport with nonlinear reaction: Mathematical framework. *Water Resources Research* 31:2675-2688.
- [32] van der Zee, S.E.A.T.M. 1990. Analytical traveling wave solution for transport with nonlinear and nonequilibrium adsorption. *Water Resources Research* 26:2563-2578.
- [33] Xin, J. & D. Zhang 1998. Stochastic analysis of biodegradation fronts in one-dimensional heterogeneous porous media. *Adv. Water Resources* 22:103-116.

General conclusions

The numerical simulations show that if an electron acceptor is injected into a domain contaminated with an organic contaminant, three regimes of electron acceptor consumption can be distinguished, e.g. a low electron acceptor consumption regime, an intermediate regime and a fast electron acceptor consumption or traveling wave regime. The results in the first regime can be approximated by first order biodegradation. For the traveling wave regime, semi-analytical expressions are derived that approximate the developed traveling wave velocity and front shapes. With these semi-analytical expressions it is shown that the control parameters m_c , c_0 , v and R influence the traveling wave velocity and k_c , c_0 and v strongly influence the traveling wave front shape. In case a specific electron acceptor is chosen to remediate the aquifer, the only adjustable control parameters are the injection concentration c_0 and the injection velocity v . Results show that by varying these two parameters, the in situ bioremediation performance can be influenced and optimized. If a physically heterogeneous aquifer instead of a homogeneous aquifer is considered, the derived Lagrangian approach can be used to determine the normalized averaged contaminant mass flux which equals the breakthrough curve under ergodic conditions. For a strongly heterogeneous aquifer the developed breakthrough curve shape is controlled by the degree of heterogeneity and not by the value of the control parameters. Hence, the performance of in situ bioremediation in a heterogeneous formation depends on the degree of heterogeneity and the developed traveling wave velocity.

Samenvatting

ACHTERGROND

In de Nederlandse bodem worden regelmatig anorganische en organische verontreinigingen aangetroffen die daar terecht zijn gekomen door toedoen van de mens. Bekende bronnen van anorganische vervuilingen zijn oude gasfabrieken (o.a. cyanide). Organische vervuiling wordt aangetroffen bij o.a. wasserijen (gechloreerde koolwaterstoffen) en benzinepompen (BTEX: benzeen, toluen, etheen en xyleen). Zowel anorganische als organische verontreinigingen kunnen zich in de verschillende fasen van de bodem bevinden: vaste fase, gasfase en waterfase. De verontreinigingen bevinden zich in de vaste fase als ze bijvoorbeeld geadsorbeerd of geprecipiteerd zijn op bodemdeeltjes, in de gasfase als ze vluchtig zijn, en in de waterfase als ze oplosbaar zijn. In de bovenste laag van de bodem, de onverzadigde zone, komen alle drie de fasen voor. Dieper in de bodem verdwijnt de gasfase en vinden we de verzadigde zone. In de verzadigde zone zijn de verontreinigingen het meest mobiel als ze zijn opgelost in de waterfase. Ze worden dan met het grondwater meegevoerd en zullen zich over een groot gebied verspreiden waar ze een risico kunnen vormen voor de volksgezondheid.

Verontreinigingen in de watervoerende laag (aquifer) ondergaan fysische, chemische en biologische processen. Het meevoeren van de verontreiniging met het grondwater is een fysisch proces (advectie). Een ander fysisch proces is dispersie. Dispersie is een vorm van spreiding op microschaal. De stroomsnelheid in de poriën tussen de bodemdeeltjes varieert in grootte en richting en veroorzaakt deze spreiding. Eén van de chemische processen die kunnen optreden, is adsorptie. De opgeloste verontreiniging hecht zich aan bodemdeeltjes en gaat dan deel uitmaken van de vaste fase. Daarnaast kunnen sommige verontreinigingen met behulp van een biologisch proces worden afgebroken. Dit gebeurt door de micro-organismen die van nature in de bodem aanwezig zijn. De verontreiniging wordt dan omgezet in onschadelijke stoffen. Bij deze omzetting is de aanwezigheid van een elektronacceptor of elektron donor essentieel. Zowel adsorptie als biologische afbraak resulteren in een afname van de verontreiniging in de waterfase. Bij adsorptie blijft de verontreiniging echter aanwezig in de vaste

fase van de bodem terwijl bij biologische afbraak de verontreiniging geheel wordt omgezet in andere stoffen.

Behalve de bovengenoemde processen, speelt de ruimtelijke variabiliteit van de fysische bodemeigenschappen een belangrijke rol bij de verspreiding van verontreinigingen. De doorlatendheid en porositeit van de bodem kunnen van plaats tot plaats variëren. Deze variabiliteit wordt veroorzaakt door bodemafzettingen, erosie en morfologische bodemprocessen. Als gevolg van ruimtelijke variabiliteit in de doorlatendheid zijn er gebieden in de bodem waar het grondwater bijna niet doordringt. Wordt het grondwater verrijkt met elektronacceptor of elektrondonor, dan zal het lang duren voordat de elektronacceptor of elektrondonor deze gebieden bereikt. De aanwezige verontreiniging zal hier niet snel worden afgebroken waardoor de verspreiding van een verontreiniging toeneemt.

In de loop der jaren zijn er technieken ontwikkeld voor het reinigen van aquifers. Een oude maar nog steeds bruikbare techniek is oppompen en behandelen (pump and treat). Het grondwater wordt aan de aquifer onttrokken en boven de grond gereinigd met behulp van chemische en / of biologische processen. Bij de nieuwere technieken vindt de reiniging van het grondwater grotendeels plaats in de bodem zelf. Een voorbeeld hiervan is bioremediatie. Bioremediatie is gebaseerd op de pump and treat techniek en richt zich op de stimulatie van biologische afbraak. Hierbij wordt er water, verrijkt met een elektronacceptor of elektrondonor (eventueel met nutriënten aangevuld), in de bodem geïnjecteerd zodat er een gunstig klimaat voor biologische afbraak ontstaat. Is de biologische afbraak in de bodem sterk dan zal het onttrokken grondwater weinig of geen verontreiniging meer bevatten. Reiniging van het grondwater boven de grond is niet meer noodzakelijk.

DOELSTELLING

In dit proefschrift richt ik me op het transport van een organische verontreiniging in een aquifer. Verondersteld wordt dat deze verontreiniging kan adsorberen aan bodemdeeltjes en biologisch afbreekbaar is. Stimulatie van deze afbraak vindt plaats door een elektronacceptor te injecteren. Het doel van dit onderzoek is het beschrijven van het transport gedrag van de organische verontreiniging en van de geïnjecteerde elektronacceptor. Daarbij wordt gekeken welke processen een dominante rol spelen. De resultaten geven een beeld hoe de saneringstechniek bioremediatie geoptimaliseerd kan worden. Daarnaast wordt aandacht besteed aan het effect van fysische heterogeniteit op de verspreiding van de verontreiniging, waarbij de doorlatendheid de ruimtelijke variabele is.

RESULTATEN

Om het gedrag van biologisch afbreekbare verontreinigingen te onderzoeken, is er een numeriek model ontwikkeld (Hoofdstuk 2). In dit numerieke model wordt de biologische afbraak beschreven met Monod-kinetiek. In de bestaande literatuur wordt biologische afbraak in veel gevallen beschreven met een lineaire relatie tussen de concentratie van de verontreiniging in oplossing en de hoeveelheid afgebroken verontreiniging. Er wordt geen rekening gehouden met het feit dat de aanwezigheid van micro-organismen en elektronacceptoren noodzakelijk is voor de biologische afbraak van de verontreiniging. Het is realistischer de biologische afbraak te beschrijven met behulp van Monod-kinetiek. Monod-kinetiek relateert de groei van de micro-organismen niet-lineair aan de beschikbare concentraties van verontreiniging en elektronacceptor. Tegelijkertijd relateert Monod-kinetiek de groei van micro-organismen lineair aan de grootte van de micro-organismenpopulatie. De afbraak van de verontreiniging en de consumptie van de elektronacceptor zijn op hun beurt weer gerelateerd aan de groei van de micro-organismen. Daarnaast wordt er in het numerieke model vanuit gegaan dat de verontreiniging vast zit tussen bodemdeeltjes. Dat wil zeggen dat de verontreiniging residueel aanwezig is en immobiel is. Verder wordt er verondersteld dat de micro-organismenpopulatie klein is, dat er in beginsel geen elektronacceptor in de bodem aanwezig is, en dat de doorlatendheid constant is (niet ruimtelijk variabel). Om de biologische afbraak op gang te brengen wordt er een elektronacceptor geïnjecteerd.

Op het moment dat de elektronacceptor wordt geïnjecteerd, is de micro-organismenpopulatie nog klein en is er minimale afbraak. De indringing van de elektronacceptor in de verontreinigde aquifer, hetgeen inzichtelijk wordt gemaakt aan de hand van een concentratiefront, is dan te benaderen met behulp van eerste orde afbraak. Na verloop van tijd is de micro-organismenpopulatie sterk gegroeid zodat er maximale afbraak plaatsvindt. De verspreiding van de elektronacceptor in de aquifer als gevolg van dispersie wordt tegengewerkt door de consumptie van de elektronacceptor gedurende de biologische afbraak van de verontreiniging. Deze tegengestelde effecten komen in balans waardoor zich concentratiefronten voor de elektronacceptor, de verontreiniging en de micro-organismen ontwikkelen die met constante front snelheid en niet-veranderende frontvormen door de aquifer reizen. Deze fronten noemen we lopende golven.

Aangezien het uitvoeren van numerieke simulaties tijdrovend is, is er gezocht naar een analytische beschrijving die de numerieke resultaten goed

benadert (Hoofdstuk 3). Op het moment dat de lopende golven zich ontwikkelen kunnen we de wiskundige vergelijkingen, die de verschillende processen beschrijven, transformeren naar een meebewegend coördinatenstelsel. Met behulp van deze transformatie en de massabalans voor de verontreiniging en elektronacceptor wordt er een semi-analytische oplossing afgeleid. De semi-analytische oplossing wordt gebruikt om na te gaan wat voor effect de verschillende processen hebben op de ontwikkelde frontvormen. Een toename in de dispersie zorgt voor een spreiding in het front terwijl een toename in de biologische afbraak er juist voor zorgt dat het front steiler wordt. De semi-analytische oplossing geeft tevens een indicatie van de prestatie van de saneringstechniek bioremediatie, en deze te verbeteren is.

In hoofdstuk 4 t/m 6 wordt de veronderstelling aangaande de mobiliteit van de verontreiniging versoepeld. Er wordt aangenomen dat de verontreiniging mobiel is en kan adsorberen aan bodemdeeltjes. De adsorptie wordt beschreven met een lineaire relatie tussen de concentratie van verontreiniging in oplossing en de hoeveelheid stof geadsorbeerd aan de vaste fase. Ook nu is er een semi-analytische oplossing af te leiden die de numeriek verkregen concentratiefronten goed benadert. Met behulp van deze oplossing wordt de verhouding tussen de hoeveelheid afgebroken en onttrokken verontreiniging bepaald en de 99% remediatietijd berekend (Hoofdstuk 5). De remediatietijd geeft de tijd weer die nodig is om 99% van de initieel aanwezige verontreiniging af te breken dan wel te onttrekken. Er wordt verondersteld dat de bioremediatie een goede prestatie levert wanneer de 99% remediatietijd klein is en wanneer er meer verontreiniging wordt afgebroken dan onttrokken. Dit omdat afbraak resulteert in de omzetting van verontreiniging naar onschadelijke stoffen terwijl na onttrekking altijd nog een reinigingsstap nodig is.

Op het moment dat bioremediatie wordt toegepast op een bepaalde verontreinigde locatie, kunnen alleen de injectiesnelheid en de injectieconcentratie van de elektronacceptor gevarieerd worden. De verontreiniging staat vast, dus kan er vastgesteld worden welke elektronacceptor noodzakelijk is om de biologische afbraak te stimuleren. Een toename in de injectieconcentratie resulteert in een grotere afbraak. Hierdoor zal de 99% remediatietijd afnemen en de verhouding tussen de hoeveelheid afgebroken en onttrokken verontreiniging toenemen. Een toename in de injectiesnelheid zal de hoeveelheid afgebroken verontreiniging niet beïnvloeden. Het resulteert alleen in een grotere onttrekking van de verontreiniging. Hierdoor zullen de 99% remediatietijd en de verhouding tussen hoeveelheid afgebroken en onttrokken verontreiniging afnemen. In dit laatste geval gaat de bioremediatie op de pump and treat techniek lijken.

Tenslotte wordt aandacht besteed aan de invloed van de fysische heterogeniteit op de verspreiding van de biologische afbreekbare verontreiniging (Hoofdstuk 6). De veronderstelling aangaande een constante doorlatendheid is losgelaten. Er wordt gebruik gemaakt van een stochastische methode om de ruimtelijke variabiliteit van de doorlatendheid te beschrijven. Verondersteld wordt dat de ergodische hypothese geldig is wanneer de injectielengte groot is ten opzichte van de transversale correlatielengte. De transversale correlatielengte geeft de afstand in verticale richting weer waarover de doorlatendheden aan elkaar gecorreleerd zijn. Is de ergodische hypothese geldig dan kan de gemiddelde doorbraakcurve van de verontreiniging bepaald worden. De resultaten laten zien dat in een relatief heterogeen aquifer de vorm van de doorbraakcurve bepaald wordt door de heterogeniteit en niet door de balans tussen dispersie en niet-lineaire biologische afbraak. De gemiddelde doorbraaktijd daarentegen wordt niet beïnvloed door de fysische heterogeniteit.

CONCLUSIES

Uit dit onderzoek kan geconcludeerd worden dat niet-lineaire biologische afbraak grote invloed heeft op de verspreiding van de verontreiniging in een aquifer. Het zorgt er voor dat de verontreiniging zich met een lagere snelheid door de aquifer beweegt en dat het concentratiefront een constante vorm houdt. Dit wordt veroorzaakt door de balans tussen dispersie en niet-lineaire biologische afbraak. Daarnaast blijkt dat met behulp van de afgeleide semi-analytische oplossing de bioremediatie geoptimaliseerd kan worden. Aangezien biologische afbraak te prefereren is boven onttrekking van verontreiniging, levert een toename in de injectieconcentratie een betere bioremediatieprestatie dan een toename in de injectiesnelheid. Verder heeft het onderzoek aangetoond dat fysische heterogeniteit een spreiding in de doorbraakcurve van de verontreiniging veroorzaakt.

Nawoord

Ik had dit proefschrift nooit kunnen afronden zonder de hulp en aanmoediging van vele mensen. Een aantal wil ik hier in het bijzonder bedanken.

In de eerste plaats Sjoerd van der Zee, mijn promotor en begeleider. Sjoerd, bedankt voor je ondersteuning en voor het corrigeren van mijn artikelen. Jij hield overzicht tijdens mijn onderzoek en voorkwam dat ik te veel in de details bleef hangen. In de tweede plaats Toon Leijnse. Toon, jij hebt mij wegwijs gemaakt in verschillende numerieke transport modellen. Dit resulteerde tot het gebruik van een van deze modellen in mijn verdere onderzoek. Ik heb het erg op prijs gesteld dat ik bij jou terecht kon met vragen aangaande modelleerwerk, numerieke wiskunde en stoftransport.

Tijdens de ontwikkeling van de semi-analytische oplossing heb ik veel gehad aan de discussies met Rink van Dijke. Wij hebben laten zien dat e-mail een goede vervanging van de telefoon kan zijn. Bij Ruud Schotting kon ik terecht toen bleek dat er problemen waren bij het oplossen van het verkregen ODE systeem. Ruud, ik was af en toe ten einde raad maar jij bleef me motiveren.

De afgelopen 5 jaar heb ik één dag in de week thuis gewerkt, de rest van de week werkte ik in Wageningen. Daar was ik over het algemeen te vinden achter mijn computer. Sommige mensen van de vakgroep zullen gedacht hebben dat ik vergroeid was met deze computer. De laatste twee jaar heeft Chris mij gezelschap gehouden. Chris, bedankt voor de gezelligheid en natuurlijk voor je hulp bij het "L^AT_EX-en", mooi boekje vind je niet?

Om diverse redenen overnachtte ik regelmatig in Wageningen. Verscheidene collega's boden mij een slaappleats aan. Vaak logeerde ik bij Mari of Jacqueline. Mari en Jacqueline, bedankt voor de slaappleats en de gezellige gesprekken voor het slapen gaan. Verder wil ik al mijn collega's in de kelder bedanken voor de prettige sfeer die daar heerst. In de tijd dat het reizen van Rotterdam naar Wageningen mij de neus uitkwam was het deze sfeer die er voor zorgde dat ik toch weer in de auto stapte.

Als laatste wil ik Jacqueline, Aenea en Thijs bedanken voor hun hulp bij het schrijven van de introductie en de Nederlandse samenvatting en René Nieuwenburg voor het ontwerpen van de kaft en natuurlijk Perry voor zijn enorme steun.

Henriëtte

Curriculum Vitae

Henriëtte Keijzer werd op 16 juni 1969 geboren te Sassenheim. Zij behaalde in 1985 het MAVO-diploma aan de RK IVO Scholengemeenschap Duinzicht te Oegstgeest en in 1988 het VWO-diploma aan de Scholengemeenschap Rijnlands Sassenheim te Sassenheim. In september 1988 begon ze aan de studie Technische Wiskunde aan de Technische Universiteit Delft. Tijdens haar afstuderen deed zij onderzoek naar oceaanstromingen bij het RIVM en in 1994 studeerde zij af bij de vakgroep Numerieke Wiskunde.

Van 1995 tot en met 2000 werkte zij als assistent in opleiding bij de vakgroep Bodemkunde en Plantenvoeding van de Landbouwuniversiteit Wageningen. Gedurende deze periode heeft zij onderzoek gedaan naar het transport gedrag van organische verontreinigingen die biologisch afbreekbaar zijn. De belangrijkste resultaten zijn in dit proefschrift beschreven. Sinds september 2000 is zij als toegevoegd onderzoeker werkzaam bij Wageningen Universiteit. Waar zij werkt aan het verificatieonderzoek Krimpenerwaard, dat wordt uitgevoerd in samenwerking met IWACO, adviesbureau voor water en milieu, te Rotterdam.